16 F11121
17 RF11121810
DTIC ELECTE OCT 6 1980 S D C
B.S. LEVEL
AD A090108

6

THE COHERENCE OF ACOUSTIC SIGNALS IN THE OCEAN AND APPLICATION TO THE DESIGN OF VERY LARGE ARRAYS.

10 William John Graham

A DISSERTATION

in

Electrical Engineering and Science

The Ruth H. Hooker Technical Library
JUN 04 1980
Naval Research Laboratory

APPROVED FOR PUBLIC RELEASE
DISTRIBUTION UNLIMITED

11 . 1979

12 180

Presented to the Graduate Faculty of the University of Pennsylvania in Partial Fulfillment of the Requirements for the Degree of Doctor of Philosophy.

9 Doctoral thesis

The Ruth H. Hooker Technical Library
JUN 01 1980
Naval Research Laboratory

Supervisor of Dissertation

Graduate Group Chairman

15 N00014-77-C-0252

DDC FILE COPY
237000 JM
80 9 12 019

ACKNOWLEDGMENTS

The idea of coherently combining underwater acoustic subarrays into a very large array was originated by my advisor and dissertation supervisor Professor Bernard D. Steinberg of the Valley Forge Research Center. I wish to acknowledge his great effort in creating interest in this research and in obtaining the necessary support. I also express my thanks for the guidance and motivation which he gave me throughout the period of this research.

I wish to thank Professor Fred Haber and Dr. Tong L. Lim for their collaboration during the initial stages of this research, and to Dharam Kaushal for many helpful discussions on wave propagation.

Credit for typing the manuscript is due to Shirley Levy. I wish to express my thanks for her perseverance and excellent cooperation throughout the preparation of the text. I also wish to thank Barbara Nordeen for her efforts in scheduling the work.

I wish to acknowledge the support of the Department of the Navy, Office of Naval Research, Contract N00014-77-C-0252 for this research project.

Accession For
NTIS GRA&I
DTIC TAB
Unannounced
Justification
By
Distribution/
Availability Codes
Dist | Avail and/or Special
A

TABLE OF CONTENTS

ACKNOWLEDGMENTS ii

LIST OF ILLUSTRATIONS v

LIST OF SYMBOLS viii

CHAPTER 1 - INTRODUCTION 1
1.1 THE PROBLEM OF COHERING WIDELY SPACED RECEIVERS 2
1.2 THE COHERENCE FUNCTION APPROACH TO THE SOLUTION 5
1.3 SUMMARY OF RESULTS 6
1.4 SUMMARY OF PREVIOUS WORK 7
1.5 ORGANIZATION AND CONTENTS 11
REFERENCES 15

CHAPTER 2 - UNDERWATER ACOUSTIC PROPAGATION AND ARRAY PROCESSING 17
2.1 THE WAVE EQUATION AND RAY SOLUTION 17
2.2 EFFECT OF RANDOM FLUCTUATIONS 23
2.3 SIGNAL AND NOISE CHARACTERISTICS 28
2.4 THE COHERENCE FUNCTION 28
2.5 ARRAY PROCESSING 33
2.5.1 CONVENTIONAL ARRAY 36
2.5.2 VERY LARGE ARRAY (VLA) 39
2.5.2.1 VLA OF SUBARRAYS 43
REFERENCES 46

CHAPTER 3 - OCEANOGRAPHIC FLUCTUATIONS AND THEIR EFFECTS ON PROPAGATION 47
3.1 CHARACTERISTICS OF OCEANOGRAPHIC FLUCTUATIONS 47
3.2 TYPES OF OCEANOGRAPHIC FLUCTUATIONS 51
3.2.1 SPATIAL VARIATIONS DUE TO MULTIPATH INTERFERENCE 53
3.2.2 INTERNAL WAVES 56
3.2.3 INTERNAL TIDES 59
3.2.4 FREQUENCY SELECTIVE MULTIPATH INTERFERENCE 62
3.3 SUMMARY 63
REFERENCES 64

CHAPTER 4 - THE MULTIPATH COHERENCE FUNCTION FOR UNCORRELATED UNDERWATER CHANNELS 66
4.1 INTRODUCTION 66
4.2 DERIVATION OF THE MULTIPATH COHERENCE FUNCTION 68
4.3 EXTENSION TO SOURCES SEPARATED IN SPACE/TIME 74
4.3.1 DISCUSSION OF SCANNING CHANNEL 78

TABLE OF CONTENTS
(Continued)

	4.3.2 DERIVATION OF THE COHERENCE FUNCTION	82
4.4	SUMMARY	90
	REFERENCES	92
CHAPTER 5 - THE COHERENCE FUNCTION IN TERMS OF THE OCEANOGRAPHIC FLUCTUATIONS		94
5.1	INTRODUCTION	94
5.2	EFFECT ON COHERENCE OF OCEANOGRAPHIC FLUCTUATIONS	95
	5.2.1 INTERNAL WAVES	96
	5.2.2 SPATIAL VARIATIONS DUE TO MULTIPATH INTERFERENCE	97
	5.2.3 INTERNAL TIDES	104
	5.2.4 FREQUENCY SELECTIVE MULTIPATH INTERFERENCE	111
5.3	THE COMPLETE MULTIPATH COHERENCE FUNCTION	115
	5.3.1 COMBINED EFFECTS ON COHERENCE	115
	5.3.2 COMPUTATION OF THE COHERENCE FUNCTION	123
5.4	SUMMARY	124
	REFERENCES	127
CHAPTER 6 - APPLICATION TO A SUPERARRAY SYSTEM DESIGN		128
6.1	SYSTEM DESIGN APPROACH	128
6.2	SYSTEM DESIGN PROCEDURE	131
6.3	CONSIDERATIONS IN SYSTEM IMPLEMENTATION	136
6.4	SUMMARY	144
	REFERENCES	145
CHAPTER 7 - SUMMARY AND RECOMMENDATIONS FOR FURTHER STUDY		147
7.1	SUMMARY OF RESULTS	147
7.2	ANALYSIS OF RESULTS	149
	7.2.1 CONCLUSIONS	149
	7.2.2 LIMITATIONS	154
7.3	RECOMMENDATIONS FOR FURTHER STUDY	156
APPENDIX		158
INDEX		161
BIBLIOGRAPHY		164

LIST OF ILLUSTRATIONS

Figure		Page
1.1	Organization of dissertation.	12
2.1	Underwater sound speed profile.	19
2.2	Ray paths and sound channel.	19
2.3	Ray travel times, pressure amplitudes, and arrival angles.	21
2.4	Frequency selective multipath interference.	24
2.5	Perturbation of ray paths.	24
2.6	Λ-Φ diagram for internal waves.	29
2.7	Signal processing for random channels.	29
2.8	Configuration of conventional array.	40
2.9	Configuration of VLA.	40
2.10	Comparison of conventional array gain with VLA gain.	44
3.1	Spatial and temporal phase fluctuations.	48
3.2	Distribution of ray arrival angles.	61
3.3	Acoustic propagation geometry for internal tide fluctuations.	61
4.1	Random channel representation.	75
4.2	Source-receiver configuration for scanning.	75
4.3	Scanning geometry.	79
5.1	Scan distance and scan time for uncorrelated internal wave fluctuations.	98

LIST OF ILLUSTRATIONS
(Continued)

Figure		Page
5.2	Characteristic function for internal wave fluctuations.	98
5.3	RMS travel time fluctuation due to internal waves.	99
5.4	Range variation of internal wave auto-coherence.	99
5.5	Frequency variation of internal wave auto-coherence.	101
5.6	Characteristic function for spatial multipath interference.	101
5.7	Average phase variation due to spatial multipath interference.	103
5.8	Range variation of auto-coherence due to spatial multipath interference.	103
5.9	Frequency variation of auto-coherence due to spatial multipath interference.	105
5.10	Source-receiver configuration for internal tide fluctuations.	105
5.11	Coherence due to internal tides.	112
5.12	Travel time fluctuation due to 4m amplitude internal tide.	112
5.13	Temporal multipath configuration for 4 ray arrivals.	116
5.14	Auto-coherence due to frequency selective multipath interference.	116
5.15	General form of auto-coherence.	121
5.16	Comparison of auto-coherences -- scanning direction $\theta=+90°$.	121

LIST OF ILLUSTRATIONS
(Continued)

Figure		Page
5.17	Comparison of auto-coherences -- scanning direction $\theta=0°$.	122
5.18	Comparison of auto-coherences -- scanning direction $\theta=-90°$.	122
6.1	VLA beamforming and scanning.	130
6.2	Required value of MCF for specified VLA gain.	135
6.3	VLA configuration for design example.	135
6.4	VLA coverage area for design example.	137
6.5	Beacon configuration and coverage areas for design example.	137
6.6	Exact beacon coverage area and resolution cell for design example.	138

LIST OF SYMBOLS

∇^2	Laplacian
$p(x,y,z,t)$	acoustic pressure
c'	sound speed including random fluctuations
$c(z)$	deterministic sound speed at depth z
c_0	nominal sound speed (1500 m/sec)
ω	acoustic frequency in radians
A	pressure amplitude
$\phi(x,y,z,t)$	pressure phase
∇	gradient operator
λ	acoustic wavelength
g; Δg	sound speed gradient; change in gradient
f	acoustic frequency
θ	vertical ray angle; bearing angle; scan angle
θ_0	initial ray angle
T	ray travel time
R	range
T_0	bulk time delay; deterministic ray travel time; correlation time for internal wave fluctuations (1.6 hr)
T_S	time spread
$\delta c(x,y,z,t)$	random fluctuation of sound speed
ℓ_0	smallest correlation length of fluctuations
τ_0	smallest correlation time of fluctuations
Λ	diffraction parameter

LIST OF SYMBOLS
(Continued)

R_F	Fresnel zone radius
$\tilde{\Phi}$	rms phase fluctuation
t_k	ray travel time fluctuation
K	number of rays; ray parameter
μ	fractional sound speed fluctuation
$\tilde{D}(S,\tau)$	phase structure function
$\rho(S,\tau)$	phase correlation function
$\gamma_S(\omega)$	signal coherence function
$\gamma_N(\omega)$	noise coherence function
S_A	average array signal power received
S_0	average sensor signal power received
N_A	average array noise power received
N_0	average sensor noise power received
G	array gain
G_S	subarray gain
G_V	VLA gain
Re	real part of
Φ	rms travel time fluctuation
Γ_S	signal coherence matrix
Γ_N	noise coherence matrix
w	complex array sensor weight
W	weight matrix

LIST OF SYMBOLS
(Continued)

$\dagger$	conjugate transpose
d	receiver separation
L	array length
L_S	subarray length
L_V	VLA length; vertical correlation length of internal waves
k, k_0	acoustic wavenumber
u	array pattern variable
Δu_B	beamwidth of conventional array
Δu_M	spacing between primary maxima of conventional array
$\Delta \rho_B$	range beamwidth of VLA
ΔS_B	cross-range beamwidth of VLA
$\Delta \rho_M$	range spacing between primary maxima of VLA
ΔS_M	cross-range spacing between primary maxima of VLA
N	number of sensors
N_S	number of sensors in subarray
N_V	number of subarrays in VLA
$\mathcal{L}_0$	characteristic length of large scale fluctuations
$\mathcal{T}_0$	characteristic time of large scale fluctuations
L_0	correlation length for internal wave fluctuations (6.4 km)
x	range increment in scanning
σ	rms ray arrival angle

LIST OF SYMBOLS
(Continued)

t_S	travel time fluctuation due to spatial multipath interference
L_H	horizontal correlation length of internal waves
ω_W	radian frequency of internal waves
$D(S,\tau)$	structure function of travel time fluctuations
S	scan distance
τ	scan time
Δc_0	sound speed fluctuation due to internal tide
ω_T	radian frequency of internal tide
k_T	wavenumber of internal tide
λ_T	wavelength of internal tide
ϕ	acoustic propagation angle from internal tide normal
Δ	fractional travel time fluctuation due to internal tide
$\delta(\cdot)$	Dirac delta function
$h(t)$	random impulse response
$H(\omega)$	random transfer function for single channel
$\mathcal{H}(\omega)$	random transfer function for cophasing and scanning
$H_0(\omega)$	deterministic transfer function
γ_m, γ_n	auto-coherences for channels m, n.
t_W	travel time fluctuation due to internal waves
t_T	travel time fluctuation due to internal tides
γ_W	auto-coherence due to internal waves
γ_T	auto-coherence due to internal tides

LIST OF SYMBOLS
(Continued)

γ_M	auto-coherence due to frequency selective multipath interference
$\gamma'_{W,S}$	auto-coherence due to internal waves and spatial multipath interference
c_W	characteristic function for t_W
c_S	characteristic function for t_S
ϕ_S	average phase in scanning
Δt_T	total travel time fluctuation due to internal tide
ΔR	change in source range
R_0	beacon range
$\tilde{r}_S$	sensor separation
Δf	coherence bandwidth
$\Delta\theta_S$	subarray beamwidth
A_B	beacon coverage area
S_x	scan distance parallel to VLA baseline
S_y	scan distance perpendicular to VLA baseline
N_B	number of beacons
A_T	total coverage area
τ_S	upper limit on scan time
T_B	beacon lifetime
σ_S	common coverage area of subarray beams
N_R	number of resolution cells
σ_V	VLA resolution cell

CHAPTER 1

INTRODUCTION

A problem of great interest and importance in underwater acoustic signal detection is the coherent combination of the outputs of widely spaced receivers to form a very large array. The description "widely spaced" means that the receivers are separated by distances much larger than both the acoustic wavelength of interest, and the correlation distance of the random fluctuations in the medium. The implication is that the signals received by the individual sensors are stochastically independent, so that totally new methods of array processing are required.

There are two aspects of this problem, which involve entirely separate methods of investigation. The first is pre-detection coherent combination, by which the receivers use a priori information about the state of the medium to search coherently for a signal source; the objective is to improve signal detectability, and performance is quantitatively measured by the array gain. The second aspect is post-detection coherent combination, in which the receivers independently detect a signal source, measure the signal phase in real time, and then form a coherently focused array by correctly phase shifting the signals. This is essentially a problem in signal processing. The former aspect, however, is primarily a problem in underwater acoustic wave propagation in a random medium, and requires a complete analysis of the space and time varying characteristics of the ocean environment. This is the problem to which this research has been devoted, and which is the

subject of this dissertation.

1.1 THE PROBLEM OF COHERING WIDELY SPACED RECEIVERS

As an acoustic propagation medium, the ocean presents many difficult problems to signal reception. The speed of sound underwater varies in space and time, and these fluctuations are both random and deterministic. Deterministic spatial variations include a gradual change in the sound speed with depth, causing refraction of acoustic rays and a multipath signal at the receiver. In addition, there are oceanographic phenomena which are space/time random processes, resulting in unpredictable variations in the sound speed. Some of these fluctuations are internal waves, tidal phenomena, currents, eddies, and surface waves. The combined effect of these sound speed changes is a received signal with random amplitude and phase varying spatially and temporally. Another important cause of spatial phase variations is the effect of ray paths which change with range and the resulting spatial change of multipath interference. Additive noise further degrades signal reception; the primary sources are ambient noise, which is random and spatially continuous, and discrete noise sources such as shipping traffic whose characteristics may often resemble signals of interest.

To overcome some of these obstacles, acoustic sensors are combined into an array. An amplification and a phase shift are applied to the received output of each sensor and the results are summed. If each phase shift is proportional to the time of arrival of the signal at that sensor, then the array is phased for that particular signal source direction. For other directions, the reception will be partially

incoherent, which helps in rejection of noise. In a conventional array, the spacing between sensors is on the order of a wavelength. Since the correlation distance of most random phase and amplitude fluctuations is much greater than this, each sensor sees nearly identical fluctuations and the signal outputs of the sensors can still be summed coherently. Therefore the primary cause of degradation of signal reception for a conventional array is the interfering noise. Many techniques have been developed for noise rejection and can be found in the literature.

Another important function of an array is localization of a signal source. A measure of localization ability is the beamwidth, which is inversely proportional to the size of the array in wavelengths. The disadvantage of a conventional array is that since most signal sources are in the far field, the array can only scan in angle; range information must be estimated from the intensity of the received signal. The localization is then limited by the array beamwidth. However, if the receivers are separated by large distances, i.e., distances very much greater than a wavelength, and on the same order of magnitude as the range of interest for signal detection, then, in principle some of these limitations may be overcome. The array could then scan in both range and angle, since signal sources would be in the near field of the huge aperture. Also, since the effective beam of the array is then a very small two dimensional focal spot, resolution ability would be greatly enhanced.

But the use of a very large array also introduces many additional problems. The greatest obstacle is that of localization ambiguity.

If the number of component sensors is small and they have omnidirectional reception, then there are numerous locations at which a signal source may be coherent at the array, and localization would be impossible. For this reason, the topic considered here will be limited to the case in which each receiver itself is an array (henceforth, reference to a sensor will imply a subarray receiver). This limits the ambiguity problem to the area of overlap of the beams of the subarrays, before coherent combination. Another problem is the fact that, since the sensors are now spaced at distances much greater than the correlation lengths of random oceanographic fluctuations, the randomness in the signal is independent among the receivers. The correct phase shift to apply to each receiver to search coherently for a signal source is now a completely unknown quantity. What, if anything, can be done to coherently combine these receivers to form a superarray aperture, and thereby improve signal detection capability? This is the question which will be addressed and answered in the dissertation.

The basic approach to the problem is as follows. A beacon signal source is placed in the ocean, and radiates a known waveform to each sensor. Each sensor measures the travel time of the signal in propagating through the random ocean channel. This information yields the correct phase shifts for the superarray to focus on the beacon. The objective is to scan the superarray focal spot away from the beacon in search of a signal. But since the ocean is fluctuating both spatially and temporally, the distance and time for which this can be done is limited due to loss of coherence. More beacons will be required so

that the superarray may scan from beacon to beacon to maintain an acceptable level of coherence; the sensors must also refocus on the same beacon as often as is determined by the stability time of the fluctuations. The results to be presented in this dissertation will be utilized to determine these required beacon spacings and refocusing times, for specified system performance parameters.

1.2 THE COHERENCE FUNCTION APPROACH TO THE SOLUTION

The underwater propagation path between the source and each sensor is modeled as a random channel whose stochastic parameters depend upon the oceanographic fluctuations. Since the random variations in the received signal are uncorrelated among all sensors, the ability to coherently combine the distorted signals depends upon the degree of similarity of their waveforms. In the frequency domain, this is viewed as a measure of how well each spectral component of the signal pairs can be combined in phase, despite the randomness.

A quantitative measure of this pairwise coherence is given by the spectral coherence function. Its magnitude, varying between zero and unity, is the gain in received signal power achieved by combining a pair of random signals with partial coherence; a value of unity indicates 100% gain in signal power. The argument of the coherence function is the average phase difference between the signals necessary to coherently combine them. By considering all possible pairs of sensors in an array, the coherence function defines an important array performance parameter, the array gain. The coherence function is therefore the key to the relationship of array performance to oceanographic

fluctuations. The bulk of this research has been devoted to developing a parametric form for the coherence function, which can be used to predict array system performance. The general theory of the coherence function is presented in Section 2.4, and its solution for the random multipath ocean channel, called the multipath coherence function, is developed in Chapters 4 and 5.

1.3 SUMMARY OF RESULTS

By means of the model of uncorrelated random propagation channels, an expression for the coherence function has been derived in terms of the parameters of real oceanographic fluctuations. The model is generalized to include scanning distances and times. Although the results include the most recent information available on ocean phenomena such as internal waves and tides, the structure of the model itself is independent of these data and can easily accommodate future changes or new theoretical developments in oceanographic fluctuations.

The results of the analysis demonstrate a simplification that allows numerical results to be computed with no more than a hand calculator. The derived expression for the multipath coherence function is a composite of three factors which affect signal coherence: deterministic multipath interference, random fluctuations which are incoherent among the rays of a multipath set, and fluctuations which are completely coherent among rays. The actual multipath configuration can be obtained from a ray tracing computer program or from experimental measurements of an ocean channel's impulse response. The second factor is dominated by internal waves and the spatial variations due to

ray paths which change with range. The last factor is a fluctuation due to internal tides. The value of this mathematical factorization is that it permits each source of coherence degradation to be analyzed separately and the relative effects of each to be compared.

In the coherence function, system design parameters such as scan distance and scan time have been related to the parameters of the ocean fluctuations. This enables a determination of required beacon spacings and beacon refocusing times for the design of a superarray system. These results are then applied to a superarray system design to demonstrate practicality.

Numerical results of the analysis show that widely spaced receivers can be combined with partial coherence to cover large ocean areas, and with significant realizable array gain. In addition, it is shown that such a system design is practical with respect to required density of beacons and refocusing times. Methods of implementation of such a system are proposed, which require only system components and procedures well within the limits of current capabilities, both technically and economically.

1.4 SUMMARY OF PREVIOUS WORK

The primary application of this work is to an adaptive array technique known as self-cohering. When the array element locations are not known accurately, or when the medium has a randomly varying index of refraction, then array beamforming and scanning must be performed not by a priori phasing based only on array geometry but also by measurement of signal phase from a direction near the desired source location.

Self-cohering techniques applied to retrodirective antenna arrays were first discussed in [1]. A survey of current and previous work in self-cohering techniques, and an analysis of beamforming and scanning of self-cohering microwave arrays, is given by Steinberg [2]. Most of the current research in self-cohering techniques for very large HF and microwave arrays is being done at the Valley Forge Research Center [3].

Self-cohering techniques for arrays were first introduced into the field of optics in the early 1970's. A description of some of this work can be found in [4]. In principle, the techniques are identical to those used for antenna arrays.

Although adaptive techniques have been used in underwater acoustic array processing for some years [5], a common assumption has been perfect signal coherence across the array aperture. A discussion of signal processing for very large arrays can be found in [6]; however, the unlikely assumption of perfect signal coherence is also made in that report.

The most important aspect of this work is the analysis of signal coherence in random ocean channels. There are two different definitions of coherence in common use. In the field of electromagnetic wave propagation, particularly in optics, the measure of coherence most commonly used is simply the normalized time-domain cross-correlation function. A thorough theoretical analysis of the significance and application of this coherence function is given by Beran and Parrent [7], and they also give a survey of previous researches. It is surprising, however, that all of these researchers were unaware of the other

definition of coherence until its rediscovery by Mandel and Wolf [8] in 1976. First introduced in time series analysis by Wiener [9] in 1930, it is defined as the cross-power spectral density of two time functions, normalized by their auto-power spectral densities. Probably the best description and explanation of the physical significance of this spectral coherence function is given by Koopmans [10], who also presents a complete history of its development. Other analyses of this coherence function and its use can be found in Bendat and Piersol [11], and Jenkins and Watts [12].

The spectral coherence function is the measure which is used in this work. Its advantage is that it gives an unambiguous quantitative measure of the ability, at each frequency, to coherently combine randomly distorted signals. A good discussion of the difference between the two measures of coherence, and the advantages of the spectral coherence function, is given by Roth [13]. In the field of underwater acoustic array processing, both definitions of coherence have been used. Use of the cross-correlation coefficient in the definition of array gain was demonstrated in [14]. Some applications of the spectral coherence function to underwater acoustic processing are given in [15].

There has been a number of studies, both experimental and theoretical, of coherence of acoustic signals in a random ocean environment and its effect on array performance. Smith [16] has presented an analysis of spatial coherence in random multipath channels due to the effects of variations of multipath interference with range. However his results are limited to separations for which the received signal is a plane wave, and the random variations are completely correlated.

Jobst and Zabalgogeazcoa [17, 18] have analyzed the effects of a moving source on signal coherence in a multipath channel. Here again the signal is assumed to be a plane wave across the array and the phase fluctuations are also assumed to be completely correlated among sensors. Munk et al [19] have determined limits on coherent processing due to phase fluctuations caused by internal waves. Their analysis is also limited to small sensor separations and large phase fluctuations.

The major difference between all previous work and the work to be performed here is that the former has been limited to sensor separations that are <u>within the correlation distance of the random fluctuations</u>. Degradation of coherence, then, essentially becomes just a matter of lack of correlation between the randomness in signals. But this gives no insight into the ability to combine signals with partial coherence when the receivers are far beyond this correlation distance. If the random fluctuations in signals received by widely separated sensors are small enough, then the possibility exists for achieving some gain by properly phase-shifting one signal with respect to the other. Another difference from previous work is that plane wave phase shifts are generally used for conventional beamforming and scanning. However, these do not take into account the phase bias due to multipath and oceanographic fluctuations. By using the true average phase difference between signals as predicted by the coherence function in terms of oceanographic fluctuations a further increase in gain may be realized. The spectral coherence function is a suitable measure of this potential, and it is toward this end that most of this research has been directed.

1.5 ORGANIZATION AND CONTENTS

The chapters of this dissertation are organized into five interrelated levels of material as indicated in Fig. 1.1. The first level consists of this introductory chapter which lays the groundwork for the dissertation by stating the problem, the approach to the solution, and giving a summary of results and previous work. The second level is composed of Chapters 2 and 3 and presents essential background information. Chapter 2, "Underwater Acoustic Propagation and Array Processing", discusses the wave equation and ray solution, and variations in the sound speed as causes of phase and amplitude fluctuations. Some characteristics of underwater acoustic signals and noise are presented and the general theory of the coherence function is developed. Basic array processing theory in the space and time domains is discussed including the general effect of the randomness of the medium. Array gain and its relationship to the coherence function is presented and methods of beamforming are discussed. Conventional arrays are considered with respect to their characteristics of size, directivity, resolution, and correlation of random fluctuations. The characteristics of very large arrays are presented, including near field focusing and scanning, resolution, uncorrelated channels and uncorrelated noise, and the array pattern. A comparison is then made between conventional arrays and very large arrays (VLA). Finally, the topic of a VLA composed of conventional subarrays is discussed.

Chapter 3, "Oceanographic Fluctuations and Their Effects on Propagation", presents the characteristics of oceanographic fluctuations determined from experimental observations, and classifies them according to

LEVELS OF ORGANIZATION

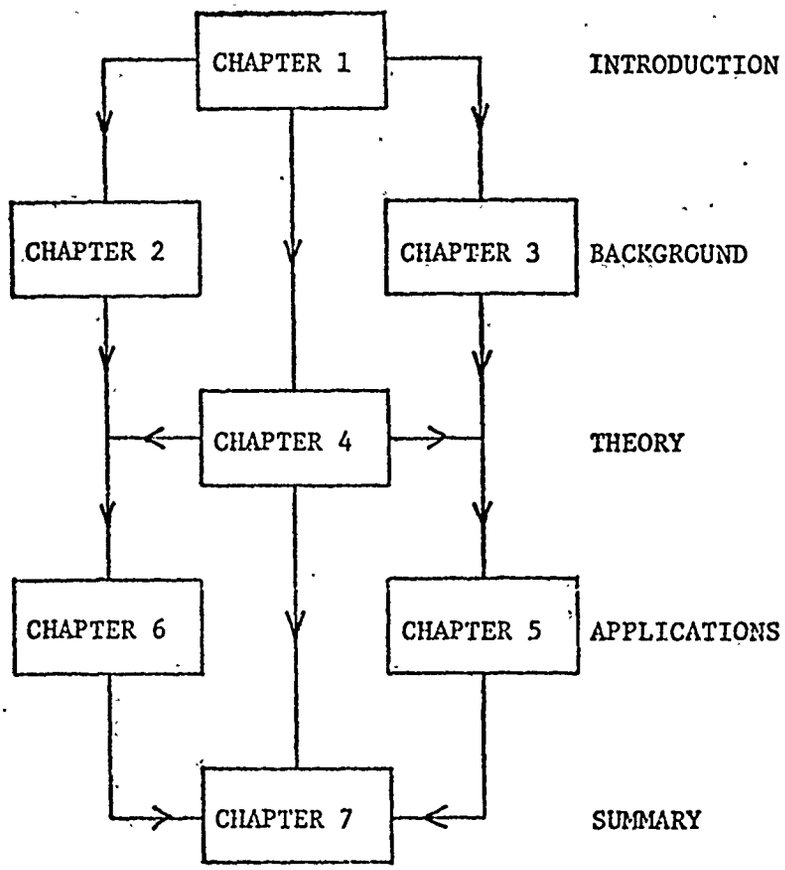

Fig. 1.1 Organization of dissertation.

their effect on array processing. Types of fluctuations are then discussed and the theory of those fluctuations which are relevant to the design of a VLA is developed. The chapter concludes with a summary of the relative importance of these fluctuations according to the latest experimental and theoretical results.

The third level of organization consists of the central theory of the dissertation, presented in Chapter 4, "The Multipath Coherence Function for Uncorrelated Underwater Channels". This level makes the transition from background material to the subject of the thesis and, with few exceptions, follows directly from the first chapter for one thoroughly familiar with the background presented in Chapters 2 and 3. The MCF is presented as a new measure of array performance, and its physical significance is explained. The MCF is derived using the stochastic time-varying channel representation of multipath propagation for general oceanographic fluctuations. The theory is then extended to include the effects of VLA scanning in space and time. The results of the analysis are discussed in detail, and the summary presents a prelude to the development of the MCF in terms of real oceanographic fluctuations in Chapter 5.

The fourth level of organization, composed of Chapters 5 and 6, is an application of the central theory of Chapter 4 to the background material presented in Chapters 3 and 2, respectively. Chapter 5, "The Coherence Function in Terms of the Oceanographic Fluctuations", incorporates the parameters of the predominant fluctuations into the MCF and analyzes the effects of each on coherence. In particular, new theories are developed for the effects of spatially varying multipath

interference and internal tides. Complete numerical results are given which show the effects of source range, frequency, multipath characteristics, and scanning on coherence, due to each individual source of fluctuation. Physical interpretations of the results are also given.

Chapter 6, "Application to a Superarray System Design", is concerned with a practical application of the previous developments to the design of a large underwater aperture of coherently combined subarrays. An approach to a complete VLA system design is outlined, including such considerations as beacon placement, beacon waveforms, and required beacon spacings. A system design procedure is then given which proposes a methodology for implementation of system specifications. Finally, other important considerations are mentioned, such as localization and source tracking.

The last level of organization is comprised of Chapter 7, "Summary and Recommendations for Further Study". This chapter concludes the work with an interpretation of results and a statement of all limitations. Recommendations are then made for future studies of relevant topics not considered here.

As illustrated in Fig. 1.1, the essence of this dissertation can be obtained from Chapters 1, 4, and 7 which contain a statement of the problem, the method of solution, and results, respectively. Chapters 2 and 3 provide a basis for the development of Chapters 5 and 6, which latter are necessary for a full understanding of how the conclusions of Chapter 7 follow from the theory developed in Chapter 4.

REFERENCES

[1] Special issue on Active and Adaptive Antennas, IEEE Trans. Antennas Prop., Vol. AP-12, No. 2, March 1964.

[2] B. D. Steinberg, Principles of Aperture and Array System Design, John Wiley and Sons, New York, 1976.

[3] Valley Forge Research Center Quarterly Progress Reports Nos. 1-29, May 1972 to May 1979, Moore School of Electrical Engineering, University of Pennsylvania, Philadelphia, Pennsylvania.

[4] Special issue on Adaptive Optics, J. Opt. Soc. Am., Vol. 67, No. 3, March 1977.

[5] A. M. Vural, "An Overview of Adaptive Array Processing for Sonar Applications," Proceedings Eascon '75.

[6] P. M. Schultheiss, S. Chow, "Signal Processing for Very Large Arrays," Final Report, Yale University, Dept. of Engineering and Applied Science, June 1976.

[7] M. J. Beran and G. B. Parrent, Jr., Theory of Partial Coherence, Prentice-Hall, Inc., Englewood Cliffs, N.J., 1964.

[8] L. Mandel, E. Wolf, "Spectral Coherence and the Concept of Cross-Spectral Purity," J. Opt. Soc. Am., Vol. 66, No. 6, June 1976.

[9] N. Wiener, "Generalized Harmonic Analysis," Acta Math. 55. Reprinted in Selected Papers of Norbert Wiener, MIT Press, Cambridge, Massachusetts, 1964.

[10] L. H. Koopmans, The Spectral Analysis of Time Series, Academic Press, New York, 1974.

[11] J. S. Bendat and A. G. Piersol, Measurement and Analysis of Random Data, John Wiley and Sons, New York, 1966.

[12] G. M. Jenkins, D. G. Watts, Spectral Analysis and its Applications, Holden-Day, San Francisco, California, 1968.

[13] P. R. Roth, "Effective Measurements Using Digital Signal Analysis," IEEE Spectrum, April 1971.

[14] R. J. Urick, Principles of Underwater Sound, McGraw-Hill, New York, 1975.

[15] G. C. Carter, C. H. Knapp, "Coherence and its Estimation via the Partitioned Modified Chirp-Z Transform," IEEE Trans. Acous., Speech, Sig. Proc., Vol. ASSP-23, No. 3, June 1975.

[16] P. W. Smith, Jr., "Spatial Coherence in Multipath or Multimodal Channels," J. Acoust. Soc. Am., Vol. 60, No. 2, August 1976.

[17] W. J. Jobst, "An Application of Poisson Process Models to Multipath Sound Propagation of Sinusoidal Signals," J. Acoust. Soc. Am., Vol. 57, No. 6, Part II, June 1975.

[18] W. Jobst and X. Zabalgogeazcoa, "Coherence Estimates for Signals Propagated Through Acoustic Channels with Multiple Paths," J. Acoust. Soc. Am., Vol. 65, No. 3, March 1979.

[19] R. F. Dashen, S. M. Flatte, W. H. Munk and F. Zachariasen, "Limits on Coherent Processing Due to Internal Waves," JASON Report JSR-76-14, Stanford Research Institute, California, June 1977.

CHAPTER 2

UNDERWATER ACOUSTIC PROPAGATION AND ARRAY PROCESSING

2.1 THE WAVE EQUATION AND RAY SOLUTION

The propagation of an underwater acoustic wave obeys the wave equation for the pressure

$$\nabla^2 p = \frac{1}{c^2}\frac{\partial^2 p}{\partial t^2} \tag{2.1}$$

in which $p = p(x,y,z,t)$ and $c = c(z)$.

Assuming a time dependence $e^{j\omega t}$, the wave equation becomes

$$\left(\nabla^2 + \frac{\omega^2}{c^2}\right) p = 0. \tag{2.2}$$

By making a substitution of the form

$$p = Ae^{-j\phi} \tag{2.3}$$

the Eikonal equation for the phase is obtained:

$$|\nabla\phi|^2 = \frac{\omega^2}{c^2} \quad . \tag{2.4}$$

The speed of sound, $c(z)$, has a variation with ocean depth determined

primarily by variations in temperature and pressure. The sound speed increases as temperature and pressure increase, resulting in a sound speed profile as shown in Fig. 2.1. The sound speed usually has its maximum at the surface where the temperature is the highest. The sound speed decreases as depth increases due to the decreasing temperature until the effect of increasing pressure causes it to again increase. The depth of the minimum sound speed is known as the sound channel axis. Maximum variations of c(z) are from about 1480 m/sec to 1550 m/sec and depend on climate, season and time of day.

The Eikonal equation is valid if

$$\lambda \frac{\Delta g}{c} << 1 \qquad (2.5)$$

i.e., if the fractional change in the sound speed gradient, $g = dc/dz$, over the distance of a wavelength is very small compared to $f = c/\lambda$. The surfaces $\phi(x,y,z)$ = constant define the wavefronts and the ray paths perpendicular to these wavefronts can be found once c(z) has been specified. An example of ray tracing for a specific sound speed profile is given in Fig. 2.2. From the Eikonal equation comes the underwater acoustic equivalent of Snell's law, written as

$$c(z) = c(z_v)\cos\theta \qquad (2.6)$$

in terms of the sound speeds at a depth z and at the vertex depth z_v, and the angle θ which a ray makes with the horizontal at a depth z. When the gradient g is positive, a ray is concave upward, and when g is negative, it is concave downward. For a ray which leaves a source at

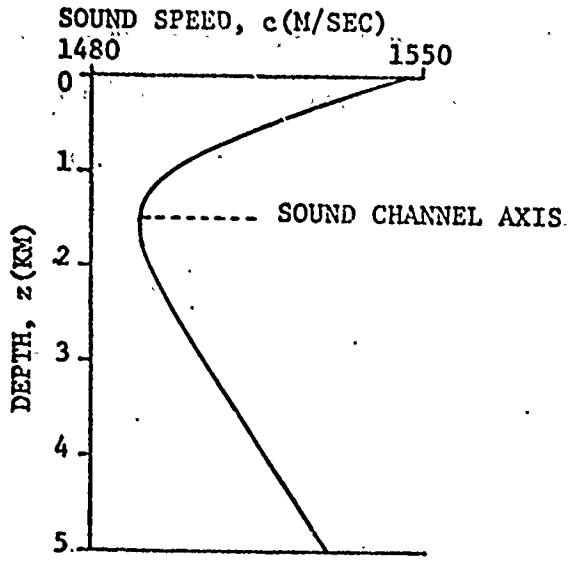

Fig. 2.1 Underwater sound speed profile.

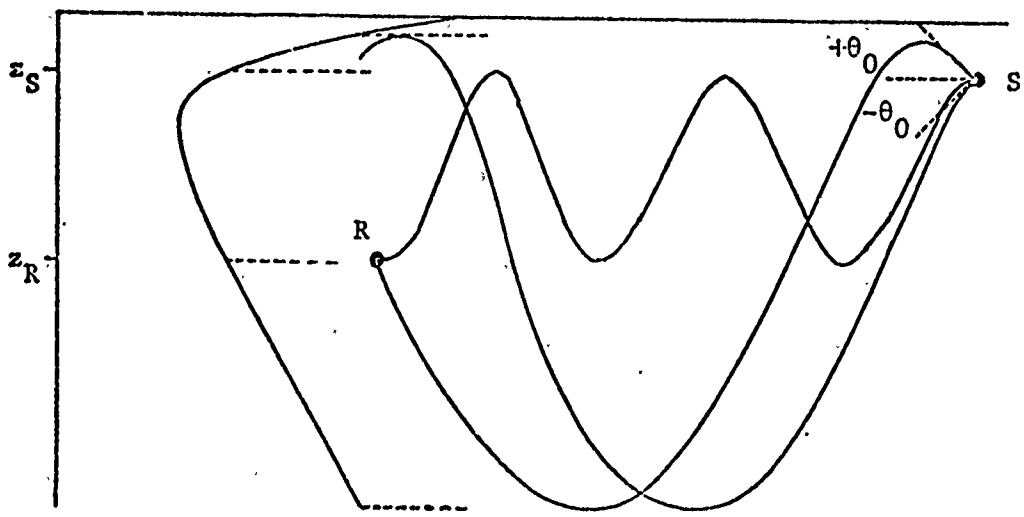

Fig. 2.2 Ray paths and sound channel.

depth z_s at an initial angle θ_0, the sound speed at the vertex can be found from (2.6). The ray is within a sound channel when it has both an upper and a lower vertex and all rays which leave the source at angles smaller than θ_0 will stay within this sound channel. Certain rays which leave the source will reach a receiver at a depth z_R. The underwater sound channel is therefore characterized by multipath propagation between source and receiver.

The total phase of a ray in propagating from source to receiver is $\phi = \omega T$, and total travel time is found directly from (2.4) as

$$T = \int_{\text{ray path}} \frac{dS}{c(z)} . \tag{2.7}$$

The travel times, pressure amplitudes, and arrival angles of all rays which reach a receiver are usually obtained from a ray tracing computer program. For a specified sound speed profile, source range, frequency, source depth and receiver depth, the program will compute the above quantities for all possible ray paths between source and receiver.

An example of the characteristics of multipath propagation is shown in Fig. 2.3. The source and receiver are separated by a range R = 500 km. The figure shows the travel times and relative amplitudes of the rays reaching the receiver, all of which are bottom reflected. The nominal or average travel time for the channel is seen to be on the order of $T_0 = R/c = 500/1.5 = 333$ sec and is called the bulk time delay. The rays arrive in pairs with approximately the same amplitude,

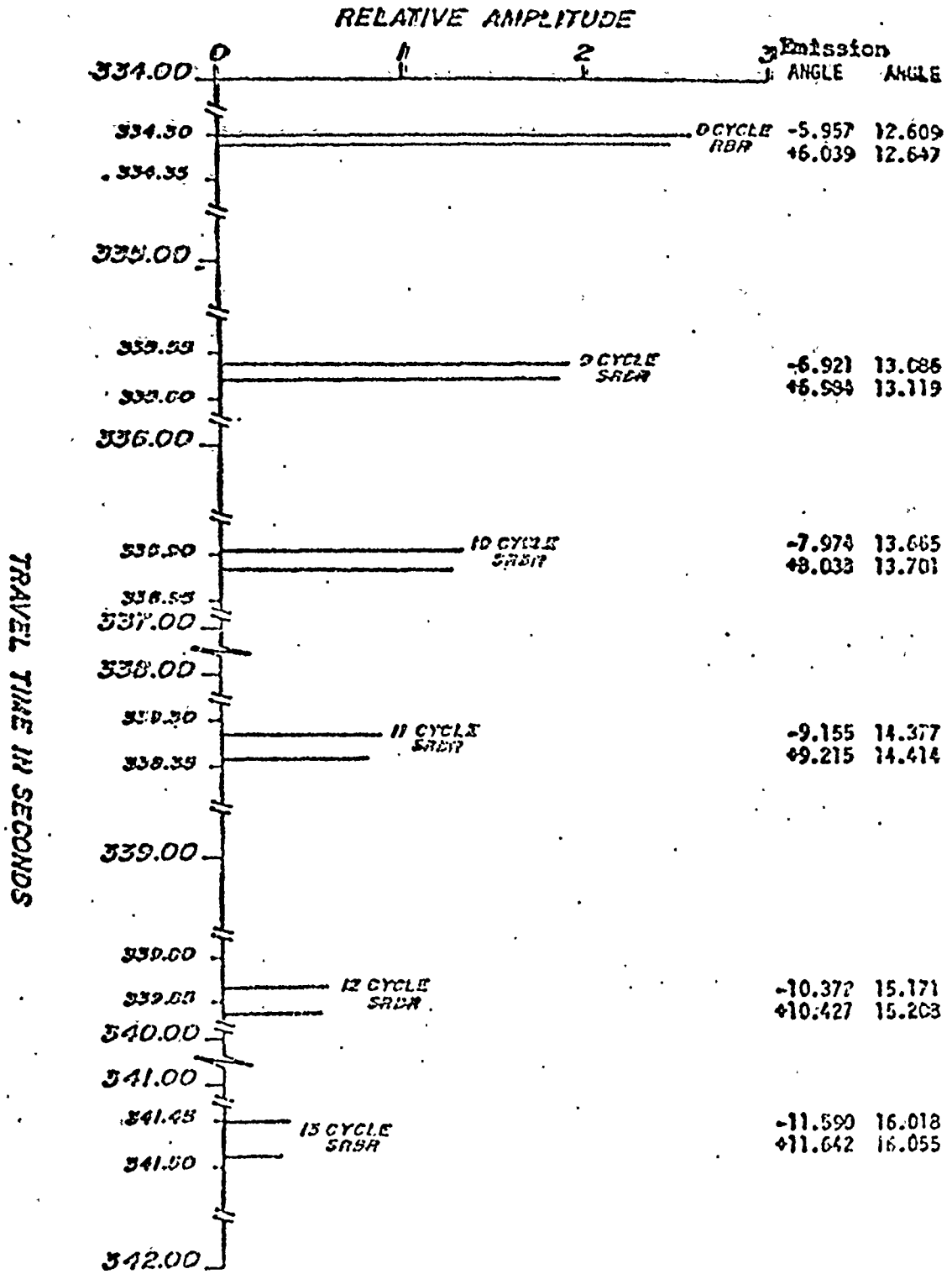

Fig. 2.3 Ray travel times, pressure amplitudes, and arrival angles (from reference 9, Chapter 3).

one ray arriving at an upward angle and the other at the same angle in a downward direction. The initial angles of these rays at the source are also equal about the horizontal. Rays which leave the source at small angles have larger amplitudes due to shorter path lengths and fewer bottom reflections. As the initial angle of each ray pair increases, its path length and number of bottom reflections increase, and the relative amplitude decreases. Due to the attenuation of high angle rays over long ranges, ray arrivals with significant amplitudes are usually limited to small arrival angles. The time between the first ray arrival and the last ray arrival is called the time spread of the channel, T_S. The time spread usually increases with increasing range and, for the figure shown, $T_S = 7$ sec.

The received pressure field for a multipath channel is the superposition of K individual ray arrivals given by

$$H(\omega) = \sum_{k=1}^{K} p_k = e^{j\omega t} \sum_{k=1}^{K} A_k e^{-j\omega T_k} , \qquad (2.8)$$

This field exhibits interference among the component rays resulting in frequency selective fading. Depending upon the arrival times and amplitudes of the rays, the received field will demonstrate constructive or destructive interference at different acoustic frequencies as depicted in Fig. 2.4. The received field will be at a maximum at frequencies for which the rays are all in phase, while for other frequencies it may fade due to total destructive interference. Frequency selective fading demonstrates the importance of a frequency domain analysis of multipath channels.

2.2 EFFECT OF RANDOM FLUCTUATIONS

Besides the deterministic variation of sound speed with depth, there are oceanographic fluctuations which are random processes in space and time and cause fluctuations in the ocean temperature, resulting in random fluctuations in the sound speed. Among these fluctuations are internal waves, which are predominant, internal tides, currents, and eddies. The sound speed is now given by

$$c' = c(z) + \delta c(x,y,z,t) \tag{2.9}$$

where $\delta c/c$ is typically on the order of 10^{-4}. In the presence of this random sound speed fluctuation, the rays will be slightly perturbed from their deterministic paths as shown in Fig. 2.5.

The effect of the fluctuations must be found by solving the wave equation using the sound speed given by (2.9). The method of solution depends upon the acoustic wavelength, range from source to receiver, and the correlation lengths and times of the random fluctuations. In this work, the solution for the pressure in the presence of ray perturbations will be restricted to the geometrical optics region where diffraction effects are negligible so that amplitude fluctuations are much smaller than the phase fluctuations. The conditions which must be satisfied for this solution to be valid are:

1. The wavelength is much smaller than the smallest correlation length of the fluctuations,

$$\lambda \ll \ell_0 \quad . \tag{2.10}$$

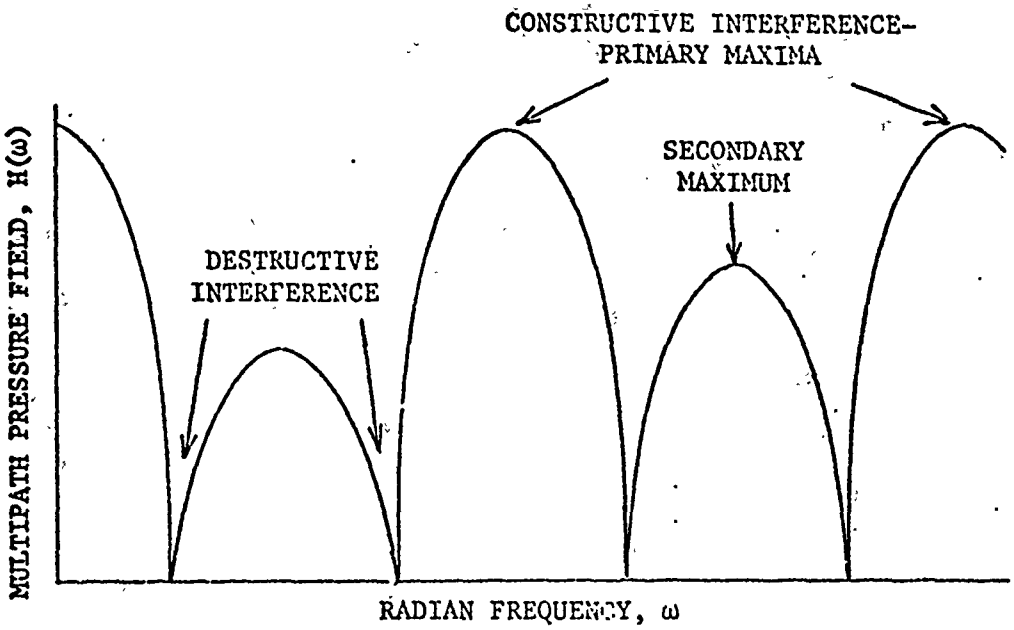

Fig. 2.4 Frequency selective multipath interference.

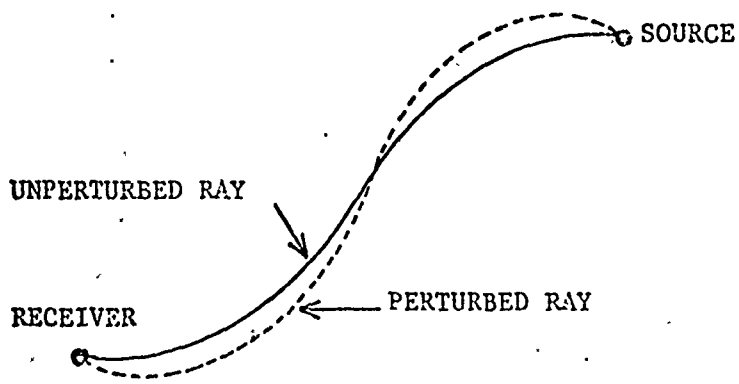

Fig. 2.5 Perturbation of ray paths.

2. The travel time is much smaller than the smallest correlation time of the fluctuations,

$$T \ll \tau_0. \tag{2.11}$$

3. Diffraction effects (and therefore ray amplitude fluctuations) are negligible, which requires that the size of a Fresnel zone be smaller than the smallest correlation length of the fluctuations,

$$\Lambda = \frac{R_F^2}{\ell_0^2} \lesssim 1. \tag{2.12}$$

For homogeneous, isotropic fluctuations, the condition is

$$\Lambda = \frac{\lambda R}{\ell_0^2} \lesssim 1. \tag{2.13}$$

For inhomogeneous, anisotropic fluctuations such as internal waves, the diffraction parameter Λ is obtained by an average over a ray path,

$$\Lambda = \left\langle \frac{R_F^2}{\ell_0^2} \right\rangle_{\text{ray path}} . \tag{2.14}$$

For internal waves [1]

$$\Lambda = (50\ \text{Hz}/f)(R/300\ \text{km}). \tag{2.15}$$

4. The total mean square phase fluctuation for an individual ray, $\tilde{\Phi}^2$, satisfies

$$\Lambda\tilde{\Phi}^2 \lesssim 1. \tag{2.16}$$

For internal waves [1]

$$\tilde{\Phi}^2 = (f/50\ \text{Hz})^2 (R/300\ \text{km}). \tag{2.17}$$

The region $\Lambda \gtrsim 1$, $\tilde{\Phi} \lesssim 1$ corresponds to the Rytov solution of the wave equation (the method of smooth perturbations) in which amplitude variations are no longer negligible. The combination of this region and the geometrical optics regime comprises the unsaturated region, in which a propagating wave can still be represented by an amplitude and a phase. This is no longer true, however, in the saturated regions in which there are very strong perturbations in the ray paths. A diagram of these regions for internal wave fluctuations is given in Fig. 2.6.

With the restriction to the geometrical optics region, the total phase of the kth ray is

$$\phi_k = \omega \int_{k^{th}\ \text{ray path}} \frac{dS}{c(z)+\delta c(x,y,z,t)} = \omega \int \frac{dS}{c} - \frac{\omega}{c_0} \int \frac{\delta c}{c}\, dS = \omega(T_k - t_k). \tag{2.18}$$

The received random multipath field now becomes

$$H(\omega) = e^{j\omega t} \sum_{k=1}^{K} e^{-j\omega T_k} e^{j\omega t_k} \tag{2.19}$$

where t_k is the travel time variation caused by perturbations in the ray path. The mean square phase fluctuation is

$$\tilde{\Phi}_k^{\,2} = \omega^2 \left\langle t_k^{\,2} \right\rangle = \left(\frac{\omega}{c_0}\right)^2 \left\langle \left(\int \frac{\delta c}{c}\, dS \right)^2 \right\rangle . \tag{2.20}$$

Another important parameter in determining the effects of phase fluctuations is the phase structure function [2], defined as the mean square difference in the phase fluctuations between two rays. In terms of the fractional sound speed fluctuation along rays 1 and 2, $\mu_1 = (\delta c/c)_1$ and $\mu_2 = (\delta c/c)_2$, it is given by

$$\tilde{D}_{12} = \left\langle (\omega t_1 - \omega t_2)^2 \right\rangle = \left\langle \left[\frac{\omega}{c_0} \int_{\text{ray } 1} \mu_1 dS - \frac{\omega}{c_0} \int_{\text{ray } 2} \mu_2 dS \right]^2 \right\rangle$$

$$= \tilde{\Phi}_1^2 - 2\tilde{\Phi}_1\tilde{\Phi}_2\rho_{12} + \tilde{\Phi}_2^{\,2} \tag{2.21}$$

where the total phase correlation between the two rays is

$$\rho_{12} = \frac{1}{\tilde{\Phi}_1\tilde{\Phi}_2} \left(\frac{\omega}{c_0}\right)^2 \int_1\int_2 \left\langle \mu_1\mu_2 \right\rangle dS_1 dS_2 \quad . \tag{2.22}$$

The phase structure function thus depends upon the total mean square phase fluctuation for each ray, and on the correlation between the sound speed fluctuations at all points along the ray paths, given by $\left\langle \mu_1\mu_2 \right\rangle$.

2.3 SIGNAL AND NOISE CHARACTERISTICS

The definition of signals and noise is somewhat subjective in that it depends upon what type of acoustic reception is of primary interest, and which others cause interference in the attempt to detect it. A signal may be a partially coherent narrow band acoustic wave such as a discrete frequency line from a surface ship, while the noise may be incoherent and broadband, such as ambient noise arising from a superposition of numerous long range sources. On the other hand, a signal might be a broadband random source, while interfering noise could be narrow band and highly coherent such as from surface ships. In this study, a signal is defined as any acoustic wave, either random or deterministic, narrow band or broadband, which originates at a single point source, and therefore is partially coherent at separated sensors. Also the noise will be limited to random broadband ambient noise which is incoherent at separated receivers.

2.4 THE COHERENCE FUNCTION

Consider an acoustic point source radiating a waveform s(t) which has a spectrum $S(\omega)$*. Assume that the wave propagates without attenuation along single paths to two separated receivers. In each channel, the signal incurs a time delay equal to its travel time, a random travel time fluctuation, and an additive noise. The travel time fluctuation is slowly varying compared to duration time of the signal. The received outputs are then spectrum analyzed and summed as depicted in Fig. 2.7.

*In this discussion waveforms are truncated at some finite time. Fourier transforms are taken over this finite time interval.

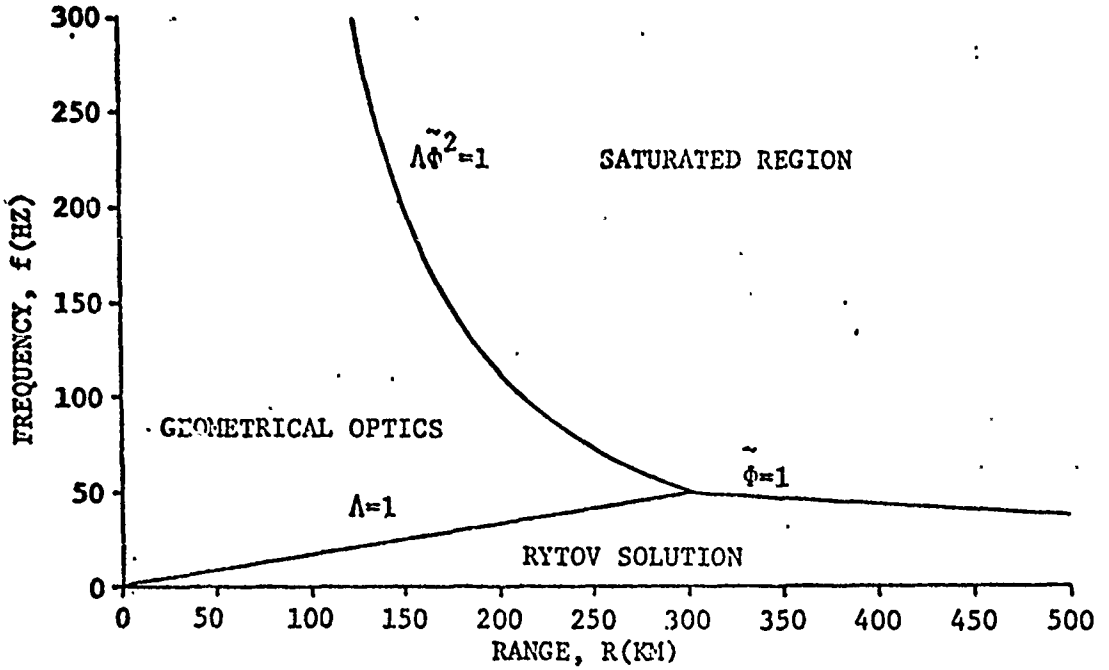

Fig. 2.6 Λ-Φ diagram for internal waves.

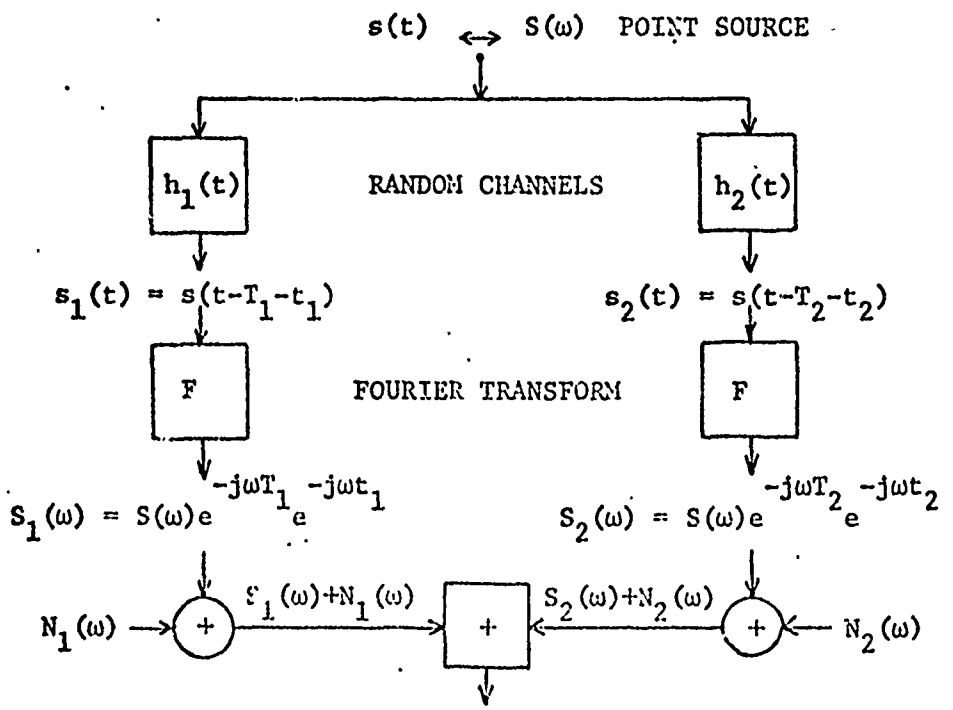

Fig. 2.7 Signal processing for random channels.

The ensemble average power output of this resulting two element array is proportional to

$$P_T = \left\langle |S_1(\omega)+N_1(\omega)+S_2(\omega)+N_2(\omega)|^2 \right\rangle$$
$$= \left\langle |S_1(\omega)|^2 \right\rangle + \left\langle |S_2(\omega)|^2 \right\rangle + 2\mathrm{Re}\left\langle S_1(\omega)S_2^*(\omega) \right\rangle$$
$$+ \left\langle |N_1(\omega)|^2 \right\rangle + \left\langle |N_2(\omega)|^2 \right\rangle + 2\mathrm{Re}\left\langle N_1(\omega)N_2^*(\omega) \right\rangle \quad . \qquad (2.23)$$

Assuming equal noise power

$$N_0(\omega) = \left\langle |N_1(\omega)|^2 \right\rangle = \left\langle |N_2(\omega)|^2 \right\rangle , \qquad (2.24)$$

and equal signal power,

$$S_0(\omega) = \left\langle |S_1(\omega)|^2 \right\rangle = \left\langle |S_2(\omega)|^2 \right\rangle , \qquad (2.25)$$

then

$$P_T = 2S_0(\omega)+2S_0(\omega)\mathrm{Re}\gamma_S(\omega)+2N_0(\omega)+2N_0(\omega)\mathrm{Re}\gamma_N(\omega) \quad . \qquad (2.26)$$

The quantities $\gamma_S(\omega)$ and $\gamma_N(\omega)$ are the signal and noise coherence functions, respectively, defined as

$$\gamma_S(\omega) = \frac{\left\langle S_1(\omega)S_2^*(\omega) \right\rangle}{\left\langle |S_1(\omega)|^2 \right\rangle^{1/2} \left\langle |S_2^*(\omega)|^2 \right\rangle^{1/2}} \quad , \; 0 \le |\gamma_S(\omega)| \le 1 \qquad (2.27)$$

and

$$\gamma_N(\omega) = \frac{\left\langle N_1(\omega)N_2^*(\omega) \right\rangle}{\left\langle |N_1(\omega)|^2 \right\rangle^{1/2} \left\langle |N_2^*(\omega)|^2 \right\rangle^{1/2}} \quad , \; 0 \le |\gamma_N(\omega)| \le 1 \quad . \qquad (2.28)$$

The significance of these functions is more apparent in their relationship to array gain. The array gain is defined as the signal to noise power ratio of the array divided by the signal to noise power ratio of the individual receiver,

$$G \equiv \frac{S_A/N_A}{S_0/N_0} \tag{2.29}$$

or, equivalently, as the signal power gain of the array divided by the noise power gain of the array

$$G \equiv \frac{S_A/S_0}{N_A/N_0} \ . \tag{2.30}$$

Since for the two receiver array,

$$S_A = 2S_0 + 2S_0 \mathrm{Re}\gamma_S \tag{2.31}$$

and

$$N_A = 2N_0 + 2N_0 \mathrm{Re}\gamma_N \ , \tag{2.32}$$

then

$$G = \frac{1+\mathrm{Re}\gamma_S}{1+\mathrm{Re}\gamma_N} \ . \tag{2.33}$$

It can be seen from (2.33) that $\gamma_S(\omega)$ is a quantitative measure of the gain in average signal power achieved by combining a pair of sensors with partial coherence; a value of unity indicates 100% gain in

signal power.

In order to make the significance of the coherence function more clear, it will be assumed that the random travel time fluctuations, t_1 and t_2, are temporally stationary Gaussian random processes which have zero mean, variance σ^2, and spatial correlation coefficient ρ with largest correlation distance L_0, so that for receivers with separations greater than L_0, $\rho = 0$. From (2.27), the coherence function is

$$\gamma_s(\omega) = \left\langle e^{-j\omega(t_1-t_2)} \right\rangle e^{-j\omega(T_1-T_2)} = e^{-\omega^2\sigma^2(1-\rho)} e^{-j\omega(T_1-T_2)} . \quad (2.34)$$

It can now be clearly seen that the coherence depends upon both the correlation of the fluctuations and their size. The most important conclusion to be made is that if $\rho = 0$, the coherence $\gamma_s(\omega)$ is not necessarily zero, and in fact can attain values very close to unity if σ^2 is small enough. The major premise of this dissertation is that the random fluctuations are stochastically independent due to the large receiver separations, so that the major effort is directed toward determining the size of the random fluctuations. The above expression also hints at the fact that the argument of the coherence function is the average phase difference between the signals necessary to coherently combine them.

For arbitrary signals, the coherence function is formally defined as [3, 4, 5]

$$\gamma_s(\omega) = \frac{G_{12}(\omega)}{\sqrt{G_1(\omega)G_2(\omega)}} \tag{2.35}$$

where $G_{12}(\omega)$ is the cross power spectral density of the received signals, and $G_1(\omega)$, $G_2(\omega)$ are the auto power spectral densities. Its two most important properties are

1 - its magnitude, varying between zero and unity, is a quantitative measure of the ability to combine random signals by giving the gain in average signal power.

2 - its argument is the average phase difference between the signals necessary to coherently combine them [4].

It should be noted that the coherence function is not simply the frequency domain analog of the normalized time cross-correlation function. The correlation function is normalized only to the mean of the total power in each channel, but the coherence function is normalized at each frequency separately [6]. Another major difference is that the correlation function includes the entire spectrum of frequencies present in the signal waveform; there may be a high degree of coherence at certain discrete frequencies, but this information will be lost if coherence is low over the major portion of the signal spectrum. This again demonstrates the importance of frequency domain analysis.

2.5 ARRAY PROCESSING

It was stated in the previous section that the argument of the signal coherence function is the average phase difference between

the two received signals. In practice, then, each sensor pair would phase shift the received signal by this amount before adding the receiver outputs. The degradation of coherence would then be determined by the magnitude of the coherence function which is a measure of the random phase fluctuation about the average.

The generalization of array gain to an array of N sensors with amplifications and phase shifts applied to their received signals before combination is [7]

$$G = \frac{\sum_{m=1}^{N} \sum_{n=1}^{N} w_m w_n^* \gamma_{Smn}(\omega)}{\sum_{m=1}^{N} \sum_{n=1}^{N} w_m w_n^* \gamma_{Nmn}(\omega)} \tag{2.36}$$

$$= \frac{W^\dagger \Gamma_S W}{W^\dagger \Gamma_N W}$$

in which the w_m are the complex weights for the amplifications and phase shifts, and the signal coherence between receivers m and n is $\gamma_{Smn}(\omega)$, with $\gamma_{Snm}(\omega) = \gamma_{Smn}^*(\omega)$ and $\gamma_{Smm}(\omega) = 1$, and likewise for $\gamma_{Nmn}(\omega)$. Conventional beamforming is the choice of the w_m to co-phase for the average signal phase difference given by $\gamma_{Smn}(\omega)$. This does not consider the effects of the noise on array gain. Adaptive beamforming [8] however, consists of choosing the weight matrix W to optimize the quantity (2.36), which does take the noise coherence matrix, Γ_N, into account. For the case of incoherent noise, Γ_N becomes the unit matrix, and the two methods are then equivalent.

Assume that the signal coherence has the same magnitude between all pairs of sensors so that $|\gamma_{Smn}| = \gamma_S$ for $m \neq n$, and that the weights have unit magnitudes, with their phases chosen to cophase perfectly for the average phase difference between each pair of signals given by the argument of γ_{Smn}. If the pairwise noise coherences are also equal so $|\gamma_{Nmn}| = \gamma_N$ for $m \neq n$, and if the noise has zero mean, then

$$G = \frac{1+(N-1)\gamma_S}{1+(N-1)\gamma_N} \tag{2.37}$$

This expression will be valuable in comparing conventional arrays with very large arrays.

Another important performance parameter in array processing is the directional power response of the array, called the array pattern. When an array is cophased for a particular source direction, a signal arriving from a different direction will cause a different array response due to the different relative path lengths among sensors to the new source direction. The direction for which the array is cophased is the primary maximum of the pattern and is called the main beam. For some other directions the relative path lengths will cause a partially destructive interference resulting in a region of lower power response called the sidelobe region. Besides the direction of the main beam, constructive interference will occur in other directions causing additional primary maxima in the pattern. Since an array cannot distinguish which primary maximum is receiving a signal source, this results in source location ambiguities sometimes

called grating lobes. The quantities of relevance in this study are the main beam width and the distance between primary maxima. The order of magnitude of these quantities can be estimated independent of noise and random fluctuations.

Consider a single path channel with constant, non-random sound speed, and a source at a range R_n. The signal received at the nth sensor is proportional to $s(t-T_n)$ which has a spectrum $S_n(\omega) = S(\omega)e^{-j\omega T_n}$, where $T_n = R_n/c$. The response of an array of N sensors to this signal is

$$\begin{aligned} P_A &= \sum_{m=1}^{N} \sum_{n=1}^{N} w_m w_n^* S_m(\omega) S_n^*(\omega) \\ &= |S(\omega)|^2 \sum\sum w_m w_n^* e^{-j\omega(T_m - T_n)} . \end{aligned} \tag{2.38}$$

To cophase for a signal at a different range, R_{n0}, the complex weights are chosen so that $w_n = |w_n| e^{j\omega T_{n0}}$, with $T_{n0} = R_{n0}/c$. Eq. (2.38) then gives the response to a source at an arbitrary range R_n; when $R_n = R_{n0}$, the array response is at its maximum.

2.5.1. CONVENTIONAL ARRAY

Consider a linear array of length L, whose N receivers are located at distances d_n from the origin, which receives a signal from a source at range R_0, as depicted in Fig. 2.8. A conventional array is characterized by

1 - receiver separations which are on the order of wavelengths,

and therefore much smaller than the smallest correlation distance of the fluctuations, i.e.

$$d_n \sim \lambda << \ell_0. \tag{2.39}$$

2 - Fraunhofer diffraction, so that the source is in the far field, and the array receives a plane wave, i.e.

$$R_0 > \frac{L^2}{\lambda} . \tag{2.40}$$

It therefore follows that the total phase to receiver n is

$$\omega\tau_n = \omega\tau_0 + kd_n \sin\theta \tag{2.41}$$

and from (2.38) the array pattern is

$$P_A = \sum_{m=1}^{N} \sum_{n=1}^{N} w_m w_n^* e^{jk(d_m - d_n)\sin\theta} . \tag{2.42}$$

If the weights are chosen to form a beam in the direction θ_0, then

$$w_n = |w_n| e^{-jkd_n \sin\theta_0} \tag{2.43}$$

so the pattern is

$$P_A = \sum_{m=1}^{N} \sum_{n=1}^{N} |w_m||w_n^*| e^{jk(d_m - d_n)u} \tag{2.44}$$

in which the pattern variable in sine space has been introduced,

$$u = \sin\theta - \sin\theta_0 \ . \tag{2.45}$$

The width of the main beam of the conventional array is approximately

$$\Delta u_B \sim \frac{\lambda}{L} \tag{2.46}$$

and the spacing between primary maxima when the receivers are nearly equally spaced is on the order of

$$\Delta u_M \sim \frac{N\lambda}{L} \ . \tag{2.47}$$

Since (2.45) shows that the maximum range of u is 2, there will be no ambiguities if

$$L \lesssim \frac{N\lambda}{2} \ . \tag{2.48}$$

Eq. (2.39) implies that $\rho = 1$ between all receiver pairs, so that the coherence from (2.34) becomes

$$\gamma_{Smn} = e^{-jk(d_m - d_n)\sin\theta} \tag{2.49}$$

which shows that the average phase difference between the received signals is

$$\phi_m - \phi_n = -k(d_m - d_n)\sin\theta \ . \tag{2.50}$$

After cophasing, the gain of (2.37) for unit weights is

$$G = \frac{N}{1+(N-1)\gamma_N} \tag{2.51}$$

in which the noise may be partially coherent due to the close sensor spacings. For $\gamma_N \to 0$, $G \to N$, which is the maximum attainable value. For $\gamma_N \to 1$, $G \to 1$, and for large N, the gain can be no greater than $1/\gamma_N$, and does not depend on N. This implies that for very small values of γ_N, it is worthwhile increasing N to increase G, but for medium values of γ_N, say $\gamma_N = .5$, the gain can be no more than G = 2, i.e., 3 dB, no matter how large N is.

2.5.2 VERY LARGE ARRAY (VLA)

Consider now the configuration of a VLA depicted in Fig. 2.9. In contrast to the conventional array, it has the following characteristics:

1 - receiver separations which are greater than the larges correlation distance of the fluctuations, and therefore much greater than a wavelength,

$$d_n \gg L_0 \gg \lambda \ . \tag{2.52}$$

2 - Fresnel diffraction, which implies that the source is in the near field, and the signal is not a plane wave, i.e.

$$R_0 < \frac{L^2}{\lambda} \ . \tag{2.53}$$

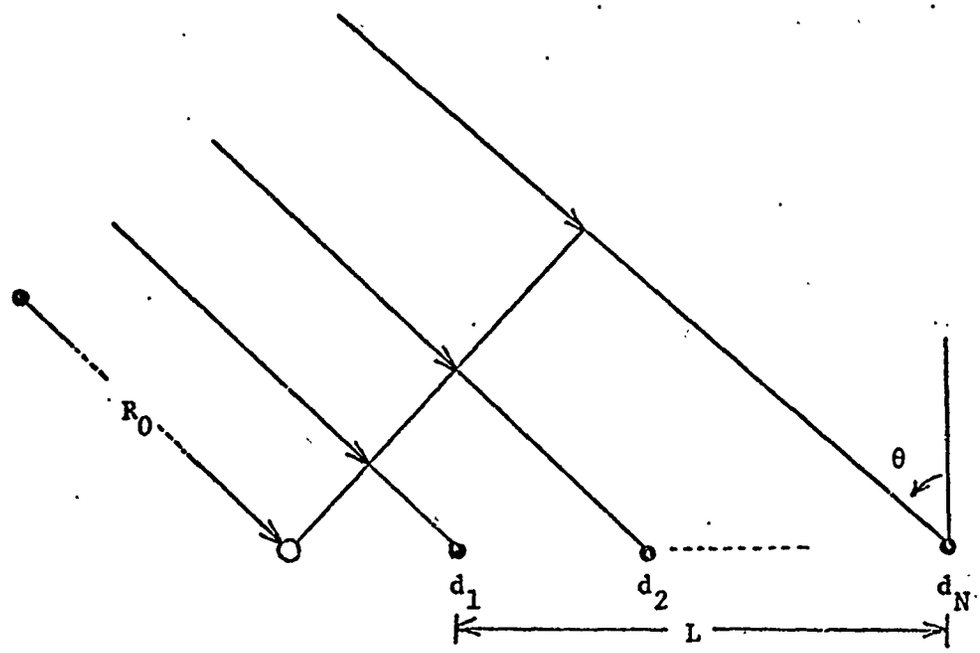

Fig. 2.8 Configuration of conventional array.

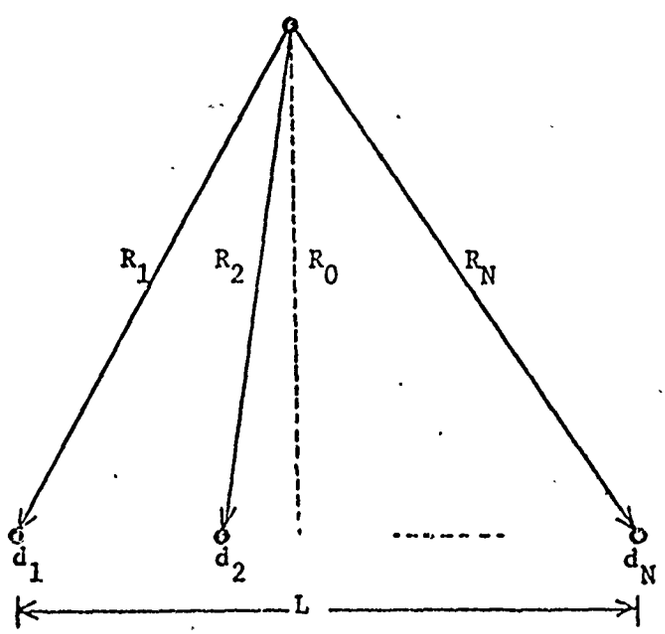

Fig. 2.9 Configuration of VLA.

For a single path, non-random medium, $T_n = R_n/c$, and the array pattern from (2.38) is

$$P_A = \sum\sum w_m w_n^* e^{jk(R_m - R_n)} \tag{2.54}$$

in which the weights should be chosen to cophase for the desired source location. Unlike the conventional array, a VLA can discriminate in range. It is therefore convenient to give the pattern characteristics in units of length in both range and azimuth.* The radial width of the main beam, called the depth of field, is on the order of

$$\Delta\rho_B \sim \lambda \left(\frac{R_0}{L}\right)^2 \tag{2.55}$$

and the corresponding width of the main beam in azimuth or cross-range is

$$\Delta S_B \sim \lambda \left(\frac{R_0}{L}\right) . \tag{2.56}$$

The spacing between primary maxima when the receivers are nearly equally spaced is

$$\Delta\rho_M \sim N^2\lambda \left(\frac{R_0}{L}\right)^2 \tag{2.57}$$

in range and

*These results were obtained from computations using a linear VLA of equally spaced receivers.

$$\Delta S_M \sim N\lambda\left(\frac{R_0}{L}\right) \tag{2.58}$$

in cross range.

It is apparent that, since L is large for the VLA (on the order of R_0), there are numerous ambiguities in both range and azimuth, with spacings on the order of wavelengths. For the same reason, the VLA beamwidth is much smaller than that of a conventional array.

The characteristic of large spacings from (2.52) implies that the random fluctuations are uncorrelated between receivers, so that $\rho = 0$. From the simple example of (2.34) the coherence is then

$$\gamma_{Smn} = e^{-\omega^2\sigma^2} e^{-j\omega(T_m - T_n)} . \tag{2.59}$$

The coherence now depends only on the size of the fluctuations determined by σ. The average phase difference is

$$\phi_m - \phi_n = -\omega(T_m - T_n) . \tag{2.60}$$

In general, this phase difference cannot be predetermined due to the random fluctuations, so that some method of measurement must be used.

Due to the large receiver spacings, the ambient noise will be incoherent, so that $\gamma_N = 0$. The idealized gain from (2.37) then becomes

$$G = 1+(N-1)\gamma_S . \tag{2.61}$$

For $\gamma_S \to 0$, $G \to 1$, and for $\gamma_S \to 1$, $G \to N$, its maximum. However, in contrast with the conventional array, there is now no limit to the attainable gain as N increases. For intermediate values of γ_S, and for large values of N, $G \to N\gamma_S$. A comparison of the idealized gain as a function of the number of receivers, N, is given in Fig. 2.10 for the VLA and the conventional array.

2.5.2.1 VLA OF SUBARRAYS

Consider a situation in which there are N individual omnidirectional receivers with which to design an array. If N is small then it is not practical to design a VLA with these receivers by separating them all by large distances. There is no increase in localization due to directional ambiguities, and gain is lost due to decrease of signal coherence because of the large receiver spacings. However it is practical to subdivide the N available receivers into coherently combined conventional subarrays. There will be an increase in localization ability over that of a single conventional array of N receivers since each subarray has a beam which can intersect those of the other subarrays, and the ambiguities of the VLA are limited to this region of intersection.

Consider a system of N_V subarrays, each containing N_S receivers. The subarray gain is

$$G_S = \frac{N_S}{1+(N_S-1)\gamma_N} \tag{2.62}$$

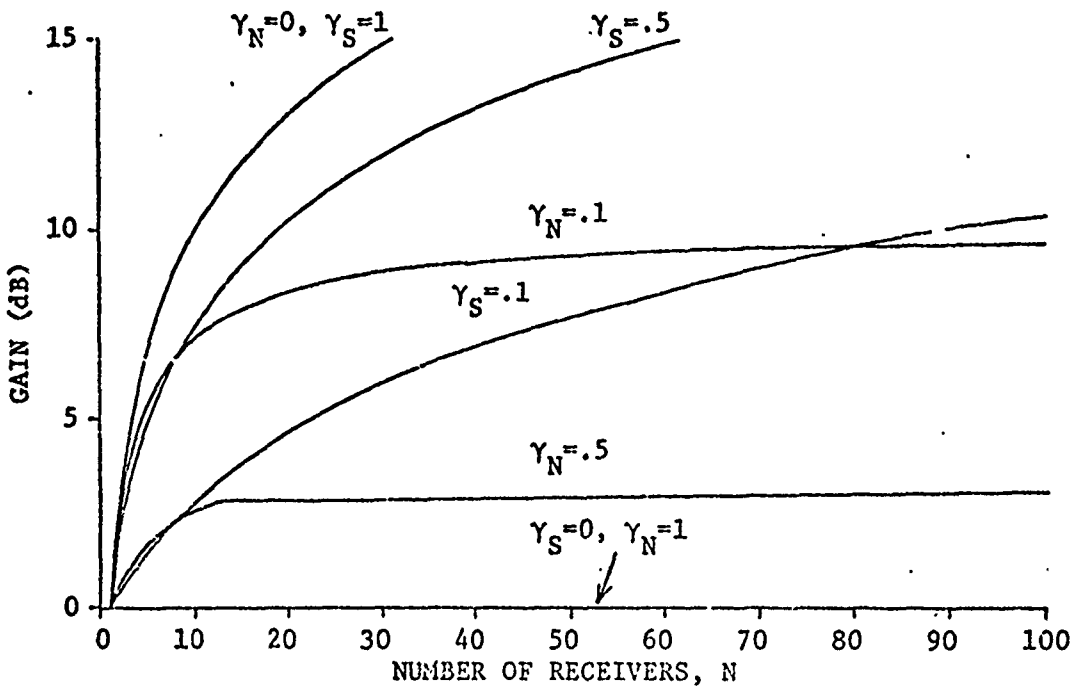

Fig. 2.10 Comparison of conventional array gain with VLA gain.

and the gain of a VLA of omnidirectional sensors is

$$G_V = 1+(N_V-1)\gamma_S \tag{2.63}$$

so that the gain of a VLA of subarrays is

$$\begin{aligned} G &= G_V G_S \\ &= 1+(N_V-1)\gamma_S \cdot \frac{N_S}{1+(N_S-1)\gamma_N} . \end{aligned} \tag{2.64}$$

For $\gamma_N = 0$,

$$G = N_S[1+(N_V-1)\gamma_S]. \tag{2.65}$$

It can be seen from this expression that even small values of VLA gain, G_V, can be very significant. For example, with $N_S = 20$, $N_V = 2$, and $\gamma_S = .5$, from (2.65), $G = 30$. By combining only 2 subarrays with a coherence of only 50% the effective number of elements in each subarray when they are used incoherently has been increased from 20 to 30. The expense of an individual subarray system including its deployment, operations personnel, signal processing, etc., may be huge. The coherent combination of such subarrays requires only some additional signal processing procedures and algorithms. Therefore, from a cost effectiveness viewpoint, a VLA gain of only 1.5 will increase the value of such a large system by this same factor, with minimal additional expense.

The subarrays may still be used incoherently to increase

localization ability due to the intersection of their beams. When they are combined coherently, the localization is no better than the incoherent system, but the value of the increase in gain achieved may be outstanding.

Due to the VLA ambiguity problem, application of the theory presented here will be limited to a VLA of subarrays. Further analysis of this subject will be presented in Chapter 6.

REFERENCES

[1] R. F. Dashen, S. M. Flatte, W. H. Munk and F. Zachariasen, "Sound Transmission Through a Fluctuating Ocean," JASON Report JSR-76-39, Stanford Research Institute, California, May 1977.

[2] V. I. Tatarskii, Wave Propagation in a Turbulent Medium (Translated from the Russian), McGraw-Hill, New York, 1961.

[3] N. Wiener, "Generalized Harmonic Analysis," Acta Math. 55. Reprinted in Selected Papers of Norbert Wiener, MIT Press, Cambridge, Massachusetts, 1964.

[4] L. H. Koopmans, The Spectral Analysis of Time Series, Academic Press, New York, 1974.

[5] J. S. Bendat and A. G. Piersol, Measurement and Analysis of Random Data, John Wiley and Sons, New York, 1966.

[6] P. R. Roth, "Effective Measurements Using Digital Signal Analysis," IEEE Spectrum, April 1971.

[7] R. J. Urick, Principles of Underwater Sound, McGraw-Hill, New York, 1975.

[8] D. J. Edelblutte, J. M. Fisk and G. L. Kinnison, "Criteria for Optimum-Signal-Detection Theory for Arrays." J. Acoust. Soc. Am., Vol. 41, No. 1, January 1967.

CHAPTER 3

OCEANOGRAPHIC FLUCTUATIONS AND THEIR EFFECTS ON PROPAGATION

3.1 CHARACTERISTICS OF OCEANOGRAPHIC FLUCTUATIONS

Oceanographic fluctuations cause variations in the amplitude and phase of a multipath acoustic signal. Some of these fluctuations are environmental, in that they are due to variations in the ocean medium itself, such as internal wave fluctuations, independent of the presence of an acoustic signal.

The other fluctuations are classified as acoustic, since they depend upon the presence of an acoustic signal and its propagation characteristics. Examples of this type are spatial multipath variations due to changing source or receiver location, and frequency selective fading caused by multipath arrivals with different travel times. In addition, the environmental fluctuations cause acoustic fluctuations, since signal characteristics are influenced by the medium.

Acoustic fluctuations may be spatial and temporal. At a fixed location, the amplitude and phase of a signal will vary with time, and at any given time, they will vary for different source or receiver locations. A good example of environmentally induced acoustic phase fluctuations, which demonstrates their spatial and temporal variability, is given in Fig. 3.1. This shows the results of a 13 month time series of acoustic phase taken in the Straits of Florida,

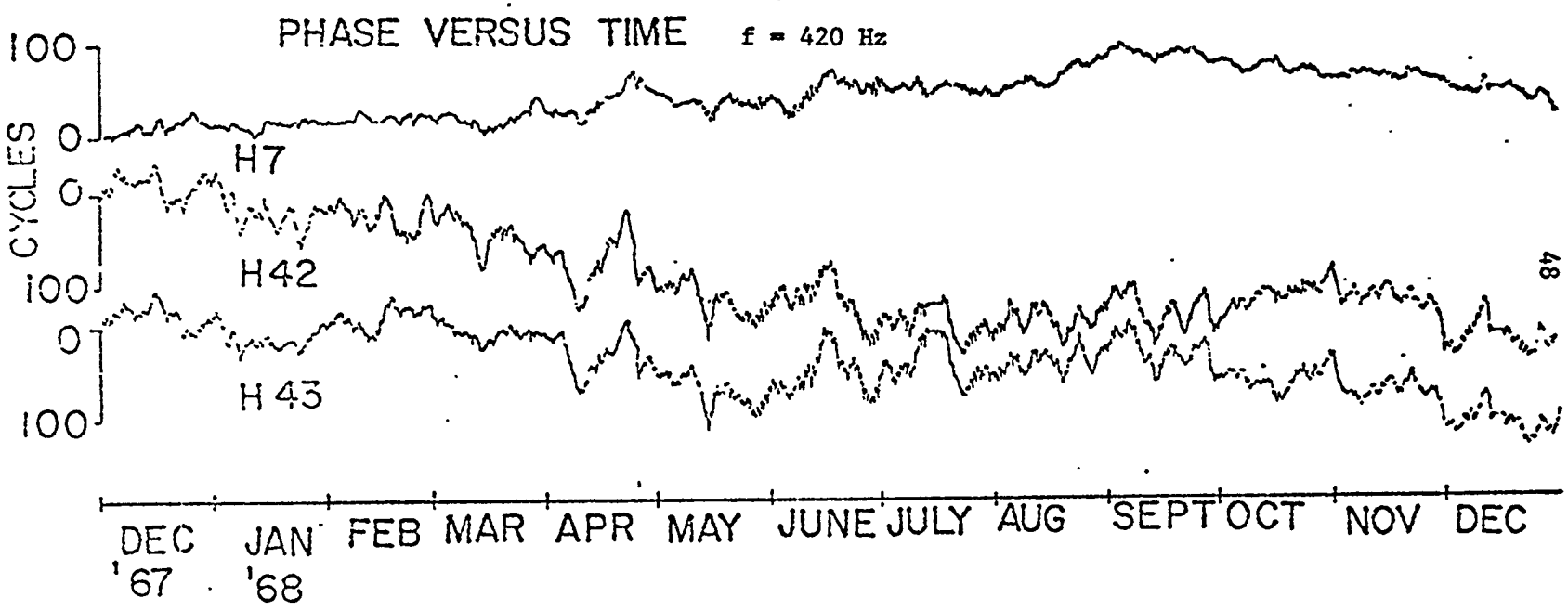

Fig. 3.1 Spatial and temporal phase fluctuations (from reference 1).

and reported by Steinberg, et al [1]. The measurements were made at three fixed colinear hydrophones at ranges of 7, 42, and 43 miles from a fixed source. Besides the obvious temporal phase variation, it can be seen how the phase varies with receiver separation at a given time.

Environmental fluctuations are also characterized by a temporal spectrum with different correlation lengths and correlation times. Periods of the spectral components vary from minutes to months, and characteristic lengths of the fluctuations have a scale ranging from meters to thousands of kilometers. It can be stated as a general rule, that the lower the frequency of the fluctuation, the larger are its energy content, correlation length, and correlation time. In Fig. 3.1, note the high degree of correlation between the entire time series of H42 and H43 due to their small separation, while they have a high correlation with H7 only at the longer period, larger amplitude fluctuations.

Environmental fluctuations can also be classified as geographic and non-geographic. Non-geographic fluctuations are those which occur in all areas of all oceans of the world, such as interval waves and internal tides. Currents and eddies are examples of the latter, and occur only in certain areas of the ocean under certain conditions.

An excellent report on current knowledge of environmental and acoustic fluctuations in the sea and measurement techniques is presented by Sykes [2]. This report summarizes the results of measurements done over the last decade of all types of oceanographic

fluctuations and their effects on propagation, and gives a complete bibliography. Any reader who desires further information concerning oceanographic fluctuations should consult this report.

Further analysis here will be limited to only those fluctuations which are relevant to this study. In order to determine this limitation, a further description of the VLA system is necessary.

As described in Section 1.1, a VLA focuses its widely spaced receivers on a beacon source at time t. Using average phase shifts determined by the pairwise coherences among all receivers, the VLA then scans a distance S at time $t + \tau$. The statistics of coherence are determined by considering an ensemble of identical such systems over which the environmental random processes of interest are stationary in space and time. The requirement of stationarity first implies that each member of the ensemble must have the same climate, meteorological conditions, and season, all of which affect the nominal multipath structure. Secondly, the requirement that

$$\tau \ll T_0 \tag{3.1}$$

and

$$S \ll \mathcal{L}_0 \tag{3.2}$$

where T_0 and $\mathcal{L}_0$ are characteristic time and length of some portion of the spectrum in time and space of all environmental fluctuations places a limit on the fluctuations which must be considered in order to maintain stationarity. For τ on the order of hours and S on the order

of 100 km the environmental fluctuations can be limited to

1 - Internal waves, which have correlation time of an hour, and correlation length of several kilometers.

2 - Internal tides, with a correlation time of hours, and correlation distance of tens of kilometers.

Larger scale fluctuations with T_0 on the order of days or longer, and $\mathcal{L}_0$ of hundreds of kilometers or larger, can then be omitted and stationarity will still be maintained.

In order to maintain a uniformity in the analysis and results, this study will also be limited to those types of fluctuations which are not geographic in nature, and therefore apply to all oceans of the world. The analysis thus ignores geographic anomalies such as currents and eddies which may further degrade coherence.

3.2 TYPES OF OCEANOGRAPHIC FLUCTUATIONS

There are many known types of oceanographic fluctuations, and some have only been analyzed experimentally. Sykes [2] lists the primary causes of acoustical fluctuations as

1. Surface waves which cause frequency spreading of the signal spectrum due to the Doppler effect. Their effect is negligible compared to other fluctuations.
2. Internal waves, which occur due to varying density of the ocean, and which cause variations in the sound speed. They are one of the predominant causes of acoustic phase fluctuations.

3. Tidal phenomena, diurnal and semi-diurnal, cause changes in water depth which are negligible effects for deep ocean propagation, tidal streaming causing currents which are a geographic effect, and internal tides which are one of the primary causes of non-geographic phase fluctuations.
4. Rossby waves which cause long term large space scale fluctuations.
5. Solar heating which causes daily changes in water temperature and acoustic phase. Its effect is less than internal tides.
6. Changes in lunar declination cause large phase fluctuations with a period of 27 days and a large space scale.
7. Wind influences acoustic phase by changing the water temperature.
8. Source motion causes spatial variations in multipath interference, as well as frequency shifting and spreading due to a different Doppler shift for each ray path.

In addition to these from reference [2], a very important cause of acoustic phase and amplitude fluctuations is

9. Frequency selective fading due to variations in multipath interference as frequency varies. This effect was explained in Section 2.1. The four types of fluctuations to be considered in this analysis will be discussed in the following sections in their order of importance.

3.2.1 SPATIAL VARIATIONS DUE TO MULTIPATH INTERFERENCE

As source-to-receiver range varies, the travel time of each ray changes at a different rate. This causes a variation of the amplitude and phase of the resultant multipath field described in Section 2.1. For large changes in range, the number and types of rays which reach the receiver may also vary due to changing propagation geometry. However, for smaller range variations, the ray types and number of arrivals will remain constant. This latter situation will be considered here for simplicity; in any event, the region over which the ray characteristics do not change must be computed from a ray tracing program.

Clark, et al [3], have analyzed, through a ray tracing program, the variations in resultant phase and amplitude for a source moving from 500 km to 520 km at various speeds. The results of interest to this study are the purely spatial variations without regard to the complicated variations due to the Doppler effect. In the frequency domain analysis, the effect of Doppler shift can be overcome by shifting the filter frequency of the receiver by the proper amount.

Some interesting conclusions can be drawn from the results of [3]. First, there is a linear phase trend given by ωT where $T = R/c$. When this effect is subtracted out, there is still a fluctuation of the resultant amplitude and phase. This fluctuation increases as the range increases from the reference point. Secondly, as the reference range increases, the spread of arrival angles generally decreases, since higher angle rays are attenuated by an increasing number of

bottom reflections. This implies that the variation in resultant phase will be less, since there is less of a phase difference among rays with closely spaced arrival angles.

The importance of these variations is that they might severely affect scanning ability of a VLA, since average phase shifts will be used to scan, and there may be large variations about the average due to the spatial multipath interference. Due to the impracticality of computing actual variations with a ray tracing program for each situation, the following analysis will take a stochastic approach to the solution.

Theory

Consider the expression for a multipath field presented in Section 2.1,

$$H(\omega) = \sum_{k=1}^{K} p_k = e^{j\omega t} \sum_{k=1}^{K} A_k e^{-j\omega T_k} \quad . \qquad (2.8)$$

Each of the K rays has an angle of arrival θ_k. Some characteristics of the spread of angular arrivals are symmetry about the horizontal, and a rapidly decreasing density of arrivals as angle increases from the horizontal. If (2.8) represents the field received from a source at range R, then for a range R + x, where x is small compared to R, the received field is proportional to

$$H(\omega) = \sum_{k=1}^{K} A_k e^{-j\omega T_k} e^{-j\omega \frac{x}{c} \cos\theta_k}$$

$$= \sum_{k=1}^{K} A_k e^{-j\omega T_k} e^{-j\omega t_{Sk}} \quad . \tag{3.3}$$

The quantity t_{Sk} is the travel time variation due to the spatial changes in multipath interference.

It is desired to determine how the amplitude and phase of $H(\omega)$ vary with x for different characteristics of the arrival angles, θ_k. First, assume that each θ_k is an independent random sample from some distribution which approximates the characteristics of the deterministic spread of θ_k. Although T_k is also a function of θ_k, the quantity of interest is the deviation of the phase and amplitude of $H(\omega)$ from its value at range R, regardless of the values of T_k, so that the T_k will be considered to be non-random. In accordance with the arrival angle characteristics stated above, the ray arrivals will be approximated by a zero mean Gaussian distribution, as shown in Fig.3.2. Since θ_k is small, the exponential in (3.3) can be expanded as

$$e^{-j\omega \frac{x}{c} \cos\theta_k} = e^{-j\omega \frac{x}{c}} e^{j\omega \frac{x}{c} \frac{\theta_k^2}{2}} \quad . \tag{3.4}$$

The expected value of the received field is then

$$\langle H(\omega) \rangle = c_S(\omega) \sum_{k=1}^{K} A_k e^{-j\omega T_k} \tag{3.5}$$

where $c_S(\omega)$ is the characteristic function of t_{Sk},

$$c_S(\omega) = \left\langle e^{-j\omega t_{Sk}} \right\rangle = [1+(2\alpha\sigma^2)^2]^{-1/4} \exp j\left[-2\alpha + \frac{1}{2}\tan^{-1}(2\alpha\sigma^2)\right] \tag{3.6}$$

where $\alpha = \omega x/2c$ and the variance is $\sigma^2 = \left\langle \theta_k^2 \right\rangle$. This result shows that the average field is attenuated as its resultant phase and amplitude fluctuations increase due to increases in source range variation, frequency, and angular ray spread, σ. In addition, the resultant average phase is a composite of two terms. The first is the nominal phase change due to a change in range and the second is due to the spread in arrival angles. The characteristic function, $c_S(\omega)$, will be utilized in Chapter 5 to determine the effects of these spatial variations on coherence.

3.2.2 INTERNAL WAVES

The greatest contribution to the knowledge of internal waves and their effect on acoustic signals has been made by oceanographers. Reference [2] gives an extensive bibliography concerning work in internal waves.

Internal waves are generated in regions of varying density in the

ocean. Propagation of the waves causes random variations of the density, and hence the sound speed. The scale sizes of internal wave fluctuations vary from meters to kilometers, with correlation distances in the horizontal much greater than the vertical, i.e. $L_H >> L_V$, implying that the ocean is anisotropic. In addition, the sound speed fluctuations caused by internal waves are much greater at the surface than at greater depths, so that the ocean is also inhomogeneous. Internal waves are also characterized by a dispersive spectrum; roughly speaking, the spectrum of the phase fluctuations varies as ω_W^{-3} for periods ranging from 1 hr. to 24 hr. [4].

The theory of internal waves used here will be based largely on references [5] and [6]. This theory has been verified by comparison with experiment [4], and by computer simulation [7]. Conclusions have also been made that show that internal waves play a much larger part in causing acoustic fluctuations than internal tides [8].

There are three important quantities which characterize the effects of internal waves on acoustic propagation:

1. The strength parameter, $\tilde{\Phi}$, discussed in S. 2.2, which is the r.m.s. value of the phase fluctuation for a single ray in the geometrical optics region. Depending on the angle at which the ray crosses the sound channel axis, it has the values [5]

$$\tilde{\Phi}^2 = \left(\frac{f}{50\ \text{Hz}}\right)^2\left(\frac{R}{300\ \text{km}}\right), \text{ steep ray;} \qquad (2.17)$$

$$\tilde{\Phi}^2 = 2\left(\frac{f}{50\ \text{Hz}}\right)^2\left(\frac{R}{300\ \text{km}}\right), \text{ axis ray.} \qquad (3.7)$$

In order to make the frequency dependence explicit, the r.m.s. travel time fluctuation is introduced as

$$\Phi = \tilde{\Phi}/\omega \ . \qquad (3.8)$$

It has corresponding values given by

$$\Phi^2 = (3.4\text{x}10^{-8}\text{sec}^2\text{km}^{-1})R, \text{ steep ray;} \qquad (3.9)$$

$$\Phi^2 = (6.8\text{x}10^{-8}\text{sec}^2\text{km}^{-1})R, \text{ axis ray.} \qquad (3.10)$$

2. The diffraction parameter, Λ, defined in Section 2.2.
3. The phase structure function defined in (2.21).

   For a horizontal separation, S, at constant range, R, and a temporal separation, τ, the phase structure function for internal waves is [6]

$$\tilde{D}(S,\tau) = 2\tilde{\Phi}^2\left[\frac{1}{2}\left(\frac{S}{6.4\ \text{km}}\right)^2 + \frac{1}{2}\left(\frac{\tau}{1.6\ \text{hr}}\right)^2\right]. \qquad (3.11)$$

   From (2.21) and (3.11), the phase correlation coefficient for internal waves can be deduced as

$$\rho(S,\tau) = 1 - \frac{1}{2}\left[\left(\frac{S}{6.4\ \text{km}}\right)^2 + \left(\frac{\tau}{1.6\ \text{hr}}\right)^2\right]. \qquad (3.12)$$

The structure function for the travel time fluctuations is then written as

$$D(S,\tau) = \tilde{D}(S,\tau)/\omega^2$$

$$= 2\Phi^2[1-\rho(S,\tau)] \ . \qquad (3.13)$$

Internal wave fluctuations are such that they cause phase fluctuations which are uncorrelated among the individual rays of a multipath field [6]. Also as in [6], it will be assumed that the strength parameter and the phase structure function are the same for each ray.

3.2.3 INTERNAL TIDES

Internal tides are due to periodic lunar motion and cause corresponding periodic variations in the sound speed. There are two predominant internal tides, the semi-diurnal and the diurnal. In the deep ocean, the dominant cause of tidally induced phase fluctuations is the first mode M2 component internal tide, which has a period of 12.42 hr and a wavelength of 100 km. The internal tide propagates outward and inward from a continental shelf, causing a sinusoidal sound speed perturbation with the same wavelength and frequency as the tide.

An acoustic propagation model incorporated in a ray tracing program by Weinberg, et al [9], has been used to numerically calculate phase variations due to internal tides based upon sound speed perturbations derived by Mooers [10]. The model considers an acoustic path which is perpendicular to the direction of propagation of the internal tide.

The results confirm that there are no marked differences in the phase behavior for different ray paths, and that phase fluctuations due to internal tides can therefore be considered as coherent among the individual rays. Since the phase behavior is independent of the ray considered, it is sufficient to restrict the analysis to a ray on the sound channel axis, and to assume that it yields a good description of the bulk time delay variations.

Fig. 3.3 depicts the geometry of an axis ray propagating from a range R at an angle ϕ with respect to the wave normal of the internal tide. The axis sound speed at some range R from the receiver varies according to the tidal propagation as

$$c(r,t) = c_0+\Delta c_0 \sin(\omega_T t - k_T r\cos\phi) \tag{3.14}$$

where c_0 is the unperturbed axis sound speed, Δc_0 is a small perturbation due to the internal tide, and

$$\omega_T = 2\pi/(12.42 \text{ hr.}), \tag{3.15}$$

$$k_T = 2\pi/(100 \text{ km.}) \tag{3.16}$$

are the radian frequency and wavenumber, respectively, of the M2 tide. The travel time of the ray is given by

$$T = \int_0^R \frac{dr}{c(r,t)} . \tag{3.17}$$

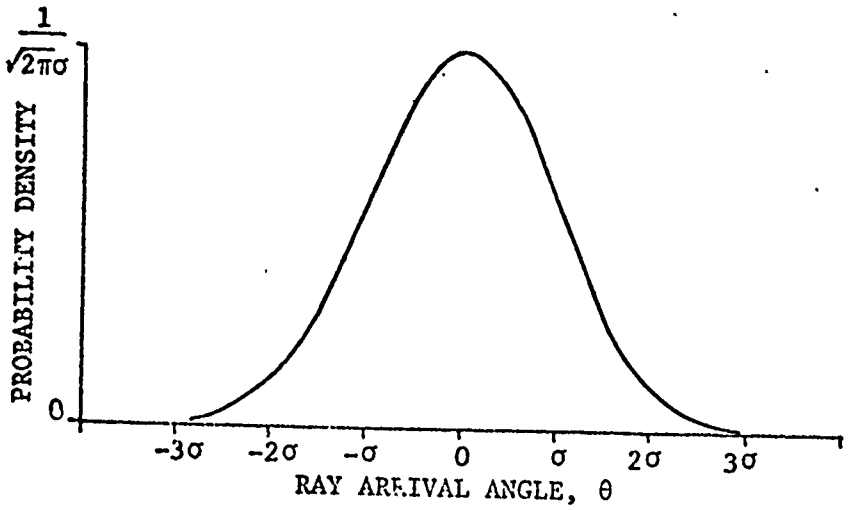

Fig. 3.2 Distribution of ray arrival angles.

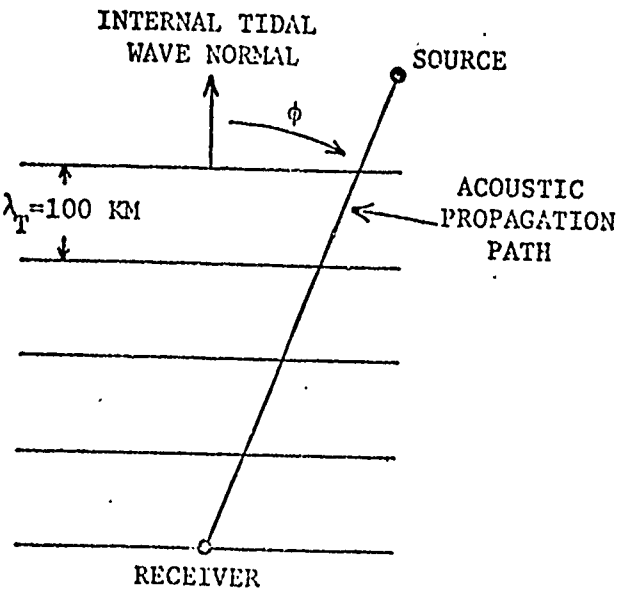

Fig. 3.3 Acoustic propagation geometry for internal tide fluctuations.

Since $\Delta c_0 << c_0$, the result of integration simplifies to

$$T = T_0\left[1 - \frac{2\Delta c_0}{c_0}\sin(\omega_T t - k_T R\cos\phi/2)\frac{\sin(k_T R\cos\phi/2)}{(k_T R\cos\phi/2)}\right]$$

where $T_0 = R/c_0$ is the travel time in the absence of the internal tide.

Some important observations concerning the travel time fluctuations can now be made, based upon the above expression. The maximum variation occurs when the acoustic path is perpendicular to the direction of the internal tide propagation, i.e., when the acoustic signal propagates parallel to a continental shelf; the minimum variation is when the acoustic path is in the same direction as the internal tide ($\phi = 0$). This is the opposite of the claim made in reference [9]*. Secondly, it can be seen that, for very long source ranges, the fractional variation in sound speed decreases.

The model shows excellent agreement with experiment [9].

3.2.4 FREQUENCY SELECTIVE MULTIPATH INTERFERENCE

The interference of multipath arrivals with different travel times causes an acoustic fluctuation in the frequency domain called frequency selective fading which was briefly described in Section 2.1. This is listed as the least important acoustic fluctuation to be considered

*There were no computations done in this reference for the case of acoustic propagation in the same direction as internal tide propagation, which would require a range dependent sound speed profile.

because it is a semi-periodic function of frequency, while the other fluctuations increase monotonically with frequency. However, it plays an important role in the analysis of coherent frequencies and coherent bandwidths which will be discussed in Chapter 5.

3.3 SUMMARY

A survey and classification of oceanographic fluctuations has been presented. In order to maintain a uniformity in applications of the results, consideration of environmental fluctuations has been limited to those which are not geographic. However this does not preclude the later inclusion of anomalous fluctuations, since the multipath coherence function developed in Chapter 4 will have general applicability because of a classification of fluctuations according to those which are completely correlated among rays (e.g. internal tides), and those which are uncorrelated (e.g. internal waves and spatial variations).

The justification for considering only internal waves and tides as the predominant types of environmental fluctuations is due to the very large scale sizes and correlation times of other fluctuations relative to VLA scan distances and scan times. In principle the theory could be extended to larger systems which must consider these fluctuations if more was known about their characteristics. However the much larger amplitude of these fluctuations would make the design of a larger system impractical, so that the size of a VLA system would still be determined by the smaller fluctuations considered here. In addition, the combined effect of the smaller fluctuations on coherence is large

enough to preclude consideration of larger fluctuations.

There has been some controversy between the oceanographic and acoustic communities concerning the relative importance of internal waves and internal tides. A paper describing a recent experiment claims that 70% of the energy in phase fluctuations of periods less than one day is due to the semi-diurnal internal tide [11]. However, the large frequency bandwidth used in making that conclusion includes a large portion of energy due to high amplitude internal wave fluctuations, while the internal tide itself has an extremely narrow bandwidth. An analysis using uniformly accepted values for sound speed fluctuations due to both internal waves and internal tides has shown that 90% of the total energy in the phase fluctuations is due to internal waves [8]. Internal waves therefore have the larger effect on phase fluctuations and it will be shown in Chapter 5 that internal tides have a negligible effect on coherence compared to internal waves and spatial fluctuations.

REFERENCES

[1] J. C. Steinberg, J. G. Clark, H. A. DeFerrari, M. Kronengold, and K. Yacoub, "Fixed-System Studies of Underwater Acoustic Propagation," J. Acoust. Soc. Am., Vol. 52, No. 5 (Pt.2), 1972.

[2] A. O. Sykes, "Environmental and Acoustic Fluctuations in the Sea," ONR, Arlington, Virginia, June 1977.

[3] J. G. Clark, R. P. Flanagan, and N. L. Weinberg, "Multipath Acoustic Propagation with a Moving Source in a Bounded Deep Ocean Channel," J. Acoust. Soc. Am., Vol. 60, No. 6, December 1976.

[4] W. H. Munk and F. Zachariasen, "Sound Propagation Through a Fluctuating Stratified Ocean: Theory and Observation," J. Acoust. Soc. Am., Vol. 59, No. 4, April 1976.

[5] R. F. Dashen, S. M. Flatte, W. H. Munk, and F. Zachariasen, "Sound Transmission Through a Fluctuating Ocean," JASON Report JSR-76-39, Stanford Research Institute, California, May 1977.

[6] R. F. Dashen, S. M. Flatte, W. H. Munk, and F. Zachariasen, "Limits on Coherent Processing Due to Internal Waves," JASON Report JSR-76-14, Stanford Research Institute, California, June 1977.

[7] S. M. Flatte and F. D. Tappert, "Calculation of the Effect of Internal Waves on Oceanic Sound Transmission," J. Acoust. Soc. Am., Vol. 58, No. 6, December 1975.

[8] F. Dyson, W. Munk, and B. Zetler, "Interpretation of Multipath Scintillations Eleuthera to Bermuda in Terms of Internal Waves and Tides," J. Acoust. Soc. Am., Vol. 59, No. 5, May 1976.

[9] N. L. Weinberg, J. G. Clark, and R. P. Flanagan, "Internal Tidal Influence on Deep-Ocean Acoustic-Ray Propagation," J. Acoust. Soc. Am., Vol. 56, No. 2, August 1974.

[10] C. N. K. Mooers, "Sound Speed Perturbations Due to Internal Tides," J. Acoust. Soc. Am., Vol. 53, p. 333(A), 1973.

[11] W. Jobst and L. Dominijanni, "Measurements of the Temporal, Spatial, and Frequency Stability of an Underwater Acoustic Channel," J. Acoust. Soc. Am., Vol. 65, No. 1, January 1979.

CHAPTER 4

THE MULTIPATH COHERENCE FUNCTION FOR UNCORRELATED UNDERWATER CHANNELS

4.1 INTRODUCTION

This chapter introduces a new measure for determining the coherence of acoustic signals in multipath channels which have random fluctuations that are uncorrelated between channels. This multipath coherence function (MCF) is based upon a formulation of the spectral coherence function in terms of the random multipath transfer functions. The MCF allows each channel to be analyzed individually, and separates the effects of random fluctuations from the effects of deterministic multipath interference (frequency selective fading).

The physical significance of coherence was explained in Section 2.4. Coherence is a quantitative measure of the extent to which it is possible to combine randomly distorted signals in phase, at each frequency in the signal spectrum. The coherence is quantitatively related to the array gain in that it is a measure of the increase in received signal power achieved by combining signals with partial coherence relative to combining them incoherently (i.e., adding intensities).

All previous analyses of coherence have been limited to the situation in which the receivers are located within the correlation distance or "patch size" of the random fluctuations. Most of these investigations have used this correlation length as the limiting sensor separation for which coherent processing can be performed. Smith [1] has presented an analysis of spatial coherence in random multipath

channels due to the effects of spatial variations in multipath interference. However, his results are limited to separations for which the received signal is a plane wave, and he assumes that random variations are large, and completely correlated between sensors. Jobst [2] has analyzed the effects of a moving source on signal coherence in a multipath channel by assuming the number of ray arrivals to be a random variable. Here again, the signal is assumed to be a plane wave across the array, and phase fluctuations are assumed to be completely correlated between sensors. Munk, et al [3] have determined limits on coherent processing due to phase fluctuations caused by internal waves whose characteristics they have thoroughly analyzed [4, 5]. Their analysis also is limited to small sensor separations, and their criterion for degradation of coherence is not quantitatively related to array gain. Beran and McCoy [6,7] have done analyses of coherence in ocean channels using the mutual coherence function. Again their work is limited to plane wave propagation within the correlation distance of the fluctuations.

There are two major differences between all known previous work and the results to be presented here; the former have all been limited to the case in which the sensor separations are small enough that they are within the correlation distance of the random fluctuations, and each ray defines a plane wave arrival across the sensors. The results in this dissertation apply when the receivers have uncorrelated fluctuations, and each may even receive an entirely different multipath field.

4.2 DERIVATION OF THE MULTIPATH COHERENCE FUNCTION

Quantitatively, the coherence function can be defined in terms of the power spectral densities of the received signals, using the stochastic time varying channel approach [8, 9, 10]. Consider a point source* radiating a signal s(t) with spectrum $S(\omega)$ which propagates through two linear, random multipath channels as shown in Fig. 4.1. Since the channels are time dispersive, the impulse response is of the form†

$$h(t) = \sum_{k=1}^{K} A_k \delta(t-T_k) \tag{4.1}$$

in which K is the number of ray arrivals, A_k is the amplitude of a ray, and T_k is its travel time including random fluctuations which are slowly varying compared to signal duration time and travel time. The transfer function is proportional to

$$H(\omega) = \sum_{k=1}^{K} A_k e^{-j\omega T_k} \quad . \tag{4.2}$$

The resulting output spectra at sensors m and n are

$$S_m(\omega) = H_m(\omega) S(\omega) \tag{4.3}$$

and

$$S_n(\omega) = H_n(\omega) S(\omega), \tag{4.4}$$

---

*This insures that the source is coherent.

†Reflection phase shifts have been omitted. They will only affect the exact locations of coherent frequencies (Section 5.2.4) which must be found by measurement.

in which $H_m(\omega)$ and $H_n(\omega)$ may be different.

It is desired to coherently combine the received signals $S_m(\omega)$ and $S_n(\omega)$. A measure of the ability to do so is given by the spectral coherence defined in Section 2.4 as

$$\gamma_{Smn}(\omega) = \frac{G_{mn}(\omega)}{\sqrt{G_m(\omega)G_n(\omega)}} \quad . \tag{2.35}$$

Since the complex transfer functions of the channels are random, it can easily be shown that

$$G_{mn}(\omega) = \left\langle H_m(\omega)H_n^*(\omega)\right\rangle G(\omega) \tag{4.5}$$

and

$$G_m(\omega) = \left\langle |H_m(\omega)|^2\right\rangle G(\omega) \tag{4.6}$$

where $\langle\cdot\rangle$ denotes an average over an ensemble of random processes as described in Section 3.1, and $G(\omega)$ is the power spectral density of the input signal, $s(t)$. The coherence can then be written as

$$\gamma_{Smn}(\omega) = \frac{\left\langle H_m(\omega)H_n^*(\omega)\right\rangle G(\omega)}{\left\langle |H_m(\omega)|^2\right\rangle^{\frac{1}{2}} \left\langle |H_n^*(\omega)|^2\right\rangle^{\frac{1}{2}} G(\omega)} \quad . \tag{4.7}$$

The coherence therefore is independent of the input signal and depends only on the properties of the channel. If the random transfer functions of the channels are independent, the multipath coherence function can be written as

$$\gamma_{Smn}(\omega) = \frac{\left\langle H_m(\omega)\right\rangle}{\left\langle |H_m(\omega)|^2\right\rangle^{\frac{1}{2}}} \cdot \frac{\left\langle H_n^*(\omega)\right\rangle}{\left\langle |H_m^*(\omega)|^2\right\rangle^{\frac{1}{2}}} = \gamma_m(\omega)\gamma_n^*(\omega) \tag{4.8}$$

where $\gamma_m(\omega)$ and $\gamma_n(\omega)$ will be called the auto-coherences.

The significance of this result is very important. First, it demonstrates the existence of partial coherence when the channels are uncorrelated. Second, the convenient factorization into two auto-coherences allows each channel to be analyzed independently of all the others. This implies that, for an array of N receivers, only N auto-coherences must be computed to completely determine array gain. This can represent a great savings compared to the computation of $\frac{N(N-1)}{2}$ much more complicated pairwise coherences if the channels are not independent. Although the most important oceanographic fluctuations, i.e. internal waves, are independent among receivers of a VLA, the MCF can easily be generalized to include an additional type of fluctuation which may have some degree of correlation between channels e.g. internal tides. The effect of this generalization will be the addition of a third factor to the MCF which is the coherence due to the correlated fluctuations alone.

The random travel time of a ray will now be written in terms of its components as

$$T_k = T_{k0} + t_{Wk} + t_T, \quad \text{ray } k \tag{4.9}$$

identified as:

T_{k0} - the nominal travel time of the ray in the absence of any fluctuations.

t_{Wk} - a zero-mean fluctuation which is independent and identically distributed among the rays of a channel and uncorrelated between channels.

t_T - a fluctuation which is completely correlated among rays of a channel, having the same value for each ray; there may be some degree of correlation between channels, and it is independent of the fluctuation t_{Wk}

The transfer functions of the two channels are therefore

$$H_m(\omega) = \sum_{k=1}^{K_m} A_{km} e^{-j\omega(T_{k0m}+t_{Wkm}+t_{Tm})} \tag{4.10}$$

$$H_n(\omega) = \sum_{k=1}^{K_n} A_{kn} e^{-j\omega(T_{k0n}+t_{Wkn}+t_{Tn})}. \tag{4.11}$$

The numerator of the MCF is then

$$\left\langle H_m(\omega) H_n^*(\omega) \right\rangle = \sum_{k}\sum_{\ell} A_{km} A_{\ell n} e^{-j\omega T_{k0m}} e^{j\omega T_{\ell 0n}} \left\langle e^{-j\omega t_{Wkm}} \right\rangle \left\langle e^{j\omega t_{W\ell n}} \right\rangle \cdot$$

$$\left\langle e^{-j\omega(t_{Tm}-t_{Tn})} \right\rangle = \left[c_{Wm}(\omega) (\sum_k A_{km}) H_{m0}(\omega) \right] \left[c_{Wn}(\omega) (\sum_k A_{kn}) H_{n0}(\omega) \right] \cdot$$

$$\left\langle e^{-j\omega(t_{Tm}-t_{Tn})} \right\rangle \tag{4.12}$$

where $H_{m0}(\omega)$ and $H_{n0}(\omega)$ are the normalized transfer functions in the absence of fluctuations, and $c_{Wm}(\omega)$ is the characteristic function of t_{Wkm}. Similarly,

$$\left\langle |H_m(\omega)|^2 \right\rangle = \sum_k \sum_\ell A_{km} A_{\ell m} e^{-j\omega(T_{k0m}-T_{\ell 0m})} \left\langle e^{-j\omega(t_{Wkm}-t_{W\ell n})} \right\rangle$$

$$= \sum_k A_{km}^2 + \left[(\sum_k A_{km})^2 |H_{m0}(\omega)|^2 - \sum_k A_{km}^2 \right] c_{Wm}^2(\omega) \tag{4.13}$$

with an analogous expression for channel n. The ratio of coherent field intensity to incoherent field intensity is the quantity $(\sum_k A_{km})^2/(\sum_k A_{km}^2)$. When the ray amplitudes are equal, this ratio is equal to K_m, the number of rays in channel m. Henceforth, the parameter K_m will be substituted, with the understanding that it designates this ratio when the amplitudes are unequal. The square magnitude of the MCF can then be written as

$$|\gamma_{Smn}(\omega)|^2 = \frac{K_m c_{Wm}^2(\omega) |H_{m0}(\omega)|^2}{1+[K_m |H_{m0}(\omega)|^2 - 1] c_{Wm}^2(\omega)} \cdot \frac{K_n c_{Wn}^2(\omega) |H_{n0}(\omega)|^2}{1+[K_n |H_{n0}(\omega)|^2 - 1] c_{Wn}^2(\omega)}$$

$$= |\gamma_m(\omega)|^2 |\gamma_n(\omega)|^2 \tag{4.14}$$

where $\gamma_m(\omega)$, $\gamma_n(\omega)$ are the auto-coherences. It is shown in the appendix that each of these factors has an envelope given by

$$\text{env}|\gamma_m(\omega)|^2 = \frac{K_m c_{Wm}^2(\omega)}{1+(K_m-1) c_{Wm}^2(\omega)} \quad . \tag{4.15}$$

The complete MCF is therefore

$$\gamma_{Smn}(\omega) = \left[\frac{K_m c_{Wm}^2(\omega)}{1+(K_m-1)c_{Wm}^2(\omega)}\right]^{\frac{1}{2}} H_{m0}(\omega) \left[\frac{K_n c_{Wn}^2(\omega)}{1+(K_n-1)c_{Wn}^2(\omega)}\right]^{\frac{1}{2}} H_{n0}^*(\omega) \cdot$$

$$\left\langle e^{-j\omega(t_{Tm}-t_{Tn})} \right\rangle$$

$$= \gamma_m(\omega)\gamma_n^*(\omega)\gamma_{Tmn}(\omega) \tag{4.16}$$

$$= \gamma_{Wm}(\omega)\gamma_{Mm}(\omega)\gamma_{Wn}(\omega)\gamma_{Mn}^*(\omega)\gamma_{Tmn}(\omega) \quad .$$

The MCF has conveniently factored into five terms that permit the effects of the random fluctuations to be analyzed independently of the effects of multipath interference as can be seen by writing

$$\gamma_{Smn} = \gamma_W \gamma_T \gamma_M \tag{4.17}$$

in which the effect of uncorrelated ray fluctuations is

$$\gamma_W = \gamma_{Wm}\gamma_{Wn} \quad , \tag{4.18}$$

that of correlated ray fluctuations is

$$\gamma_T = \gamma_{Tmn} \quad , \tag{4.19}$$

and the effect of deterministic multipath interference is

$$\gamma_M = \gamma_{Mm}\gamma_{Mn}^* \quad . \tag{4.20}$$

The argument of the MCF, which is the average phase difference between two received signals, is given by the phase of γ_T added to that of

γ_M. The characteristics of the individual coherence factors will be analyzed in Chapter 5.

4.3 EXTENSION TO SOURCES SEPARATED IN SPACE/TIME

The preceding section has derived the MCF for a fixed source location. An extension of the analysis to include scanning to a different location at a later time will introduce additional coherence factors due to the effects of randomness in the scanning channel. The VLA system design procedure discussed in Sections 1.1 and 3.1 requires the use of a known beacon source upon which the array can initially focus due to the unknown multipath structure and unknown phase of each ray due to the initial state of random fluctuations.

The source-receiver configuration for scanning is illustrated in Fig. 4.2. From a beacon source at location $\bar{y}$ and time t, the sensor at $\bar{x}$ receives a signal proportional to the transfer function of the channel, denoted by

$$H(\omega,\bar{x},\bar{y},t) = A(\omega,\bar{x},\bar{y},t)e^{j\phi(\omega,\bar{x},\bar{y},t)} , \tag{4.21}$$

and the sensor at $\bar{x} + \bar{\xi}$ receives

$$H(\omega,\bar{x}+\bar{\xi},\bar{y},t) = A(\omega,\bar{x}+\bar{\xi},\bar{y},t)e^{j\phi(\omega,\bar{x}+\bar{\xi},\bar{y},t)} . \tag{4.22}$$

It is desired to form a VLA by focusing the receivers on the known source at $\bar{y}$, t, and then scanning for an unknown source at $\bar{y}+\bar{\eta}$, $t+\tau$. Each receiver cophases for the beacon source by using a matched

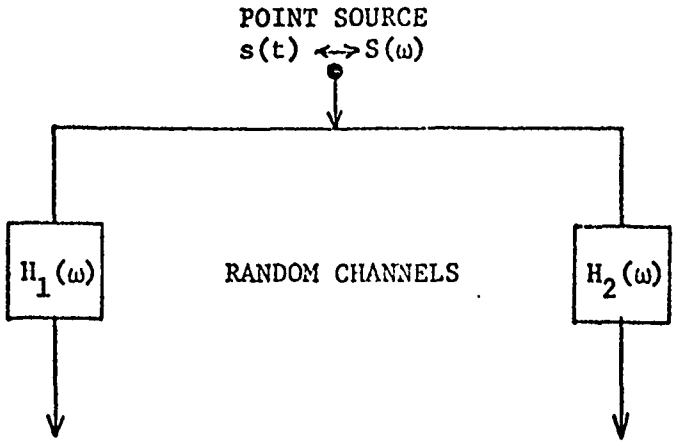

Fig. 4.1 Random channel representation.

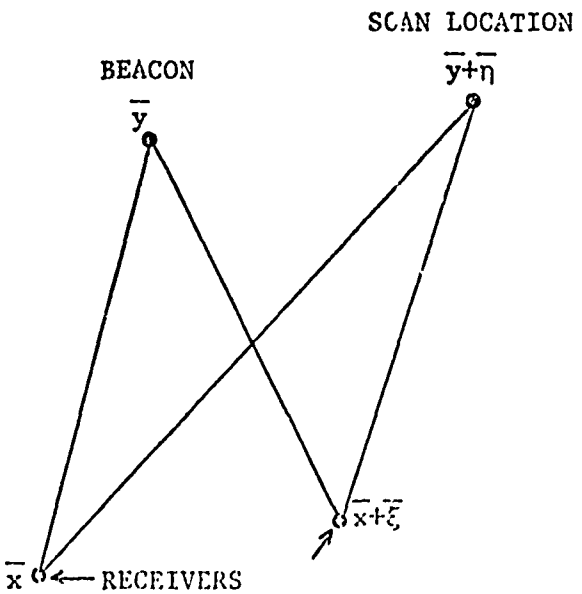

Fig. 4.2 Source-receiver configuration for scanning.

filter, so that the received signals are then proportional to

$$H(\omega,\bar{x},\bar{y},t)H^{*}(\omega,\bar{x},\bar{y},t) \tag{4.23}$$

and

$$H(\omega,\bar{x}+\bar{\xi},\bar{y},t)H^{*}(\omega,\bar{x}+\bar{\xi},\bar{y},t) \quad . \tag{4.24}$$

The signals from the unknown source at $\bar{y}+\bar{\eta}$ at time $t+\tau$, are

$$H(\omega,\bar{x},\bar{y}+\bar{\eta},t+\tau) = A(\omega,\bar{x},\bar{y}+\bar{\eta},t+\tau)e^{j\phi(\omega,\bar{x},\bar{y}+\bar{\eta},t+\tau)} \tag{4.25}$$

and

$$H(\omega,\bar{x}+\bar{\xi},\bar{y}+\bar{\eta},t+\tau) = A(\omega,\bar{x}+\bar{\xi},\bar{y}+\bar{\eta},t+\tau)e^{j\phi(\omega,\bar{x}+\bar{\xi},\bar{y}+\bar{\eta},t+\tau)} \quad . \tag{4.26}$$

After cophasing for the source at $\bar{y}$ and applying phase shifts to scan to $\bar{y}+\bar{\eta}$, $t+\tau$, the signals received from the unknown source are

$$H(\omega,\bar{x},\bar{y}+\bar{\eta},t+\tau)H^{*}(\omega,\bar{x},\bar{y},t)e^{j\phi'(\omega,\bar{x},\bar{y}+\bar{\eta},t+\tau)} \tag{4.27}$$

and

$$H(\omega,\bar{x}+\bar{\xi},\bar{y}+\bar{\eta},t+\tau)H^{*}(\omega,\bar{x}+\bar{\xi},\bar{y},t)e^{j\phi'(\omega,\bar{x}+\bar{\xi},\bar{y}+\bar{\eta},t+\tau)} \quad . \tag{4.28}$$

The total phase of (4.27) is

$$\phi(\omega,\bar{x},\bar{y}+\bar{\eta},t+\tau) - \phi(\omega,\bar{x},\bar{y},t) + \phi'(\omega,\bar{x},\bar{y}+\bar{\eta},t+\tau). \tag{4.29}$$

The first two terms in (4.29) are random variables; the term $\phi'(\omega,\bar{x},\bar{y}+\bar{\eta},t+\tau)$ is the deterministic and yet unknown average phase

shift necessary for scanning. The quantity

$$\phi'(\omega,\bar{x},\bar{y}+\bar{\eta},t+\tau) - \phi'(\omega,\bar{x}+\bar{\xi},\bar{y}+\bar{\eta},t+\tau) \tag{4.30}$$

will be found to be the negative of the phase of the coherence function.

The transfer functions for the scan channels after cophasing for the beacon source are

$$\mathcal{H}_m(\omega) = H_m'(\omega)H_m^*(\omega) \tag{4.31}$$

and

$$\mathcal{H}_n(\omega) = H_n'(\omega)H_n^*(\omega) \tag{4.32}$$

where the subscripts m and n denote sensors at $\bar{x}$ and $\bar{x}+\bar{\xi}$, respectively, and the prime denotes the scan channels, i.e.

$$H_m(\omega) = H(\omega,\bar{x},\bar{y},t) = \sum_{k=1}^{K_m} A_{km} e^{-j\omega T_{km}} , \tag{4.33}$$

$$H_m'(\omega) = H(\omega,\bar{x},\bar{y}+\bar{\eta},t+\tau) = \sum_{k=1}^{K_m} A_{km}' e^{-j\omega T_{km}'} , \tag{4.34}$$

$$H_n(\omega) = H(\omega,\bar{x}+\bar{\xi},\bar{y},t) = \sum_{k=1}^{K_n} A_{kn} e^{-j\omega T_{kn}} , \tag{4.35}$$

$$H_n'(\omega) = H(\omega,\bar{x}+\bar{\xi},\bar{y}+\bar{\eta},t+\tau) = \sum_{k=1}^{K_n} A_{kn}' e^{-j\omega T_{kn}'} . \tag{4.36}$$

The MCF for scanning in space and time is now

$$\gamma_{Smn}(\omega) = \frac{\left\langle H_m(\omega) H_n^*(\omega) \right\rangle}{\left\langle |H_m(\omega)|^2 \right\rangle^{\frac{1}{2}} \left\langle |H_n(\omega)|^2 \right\rangle^{\frac{1}{2}}}$$

$$= \frac{\left\langle H_m'(\omega) H_m^*(\omega) H_n'^*(\omega) H_n(\omega) \right\rangle}{\left\langle |H_m'(\omega) H_m^*(\omega)|^2 \right\rangle^{\frac{1}{2}} \left\langle |H_n'^*(\omega) H_n(\omega)|^2 \right\rangle^{\frac{1}{2}}} \quad . \tag{4.37}$$

4.3.1 DISCUSSION OF SCANNING CHANNEL

The extension to scanning introduces the remaining type of acoustic fluctuation, that due to spatially varying multipath interference as discussed in Section 3.2.1.

In order to determine this effect on scanning, the following scan channel model will be postulated. The scanning geometry is depicted in Fig. 4.3, in which S is the linear horizontal scan distance from the beacon to a new source location. The components along the new source-receiver paths are designated x_m and x_n, and correspond to the changes in source range due to scanning. As postulated in Section 3.1, $S \ll \mathcal{L}_0$, the correlation distance of the large scale, long period environmental fluctuations. The deterministic multipath field in the absence of the smaller scale environmental fluctuations can then be considered as azimuthally isotropic for a given receiver. As prescribed in Section 3.2.1, the same rays are received throughout the scan area, and the requirement that each ray describes a plane wave with the same arrival angle throughout the scan area is satisfied if

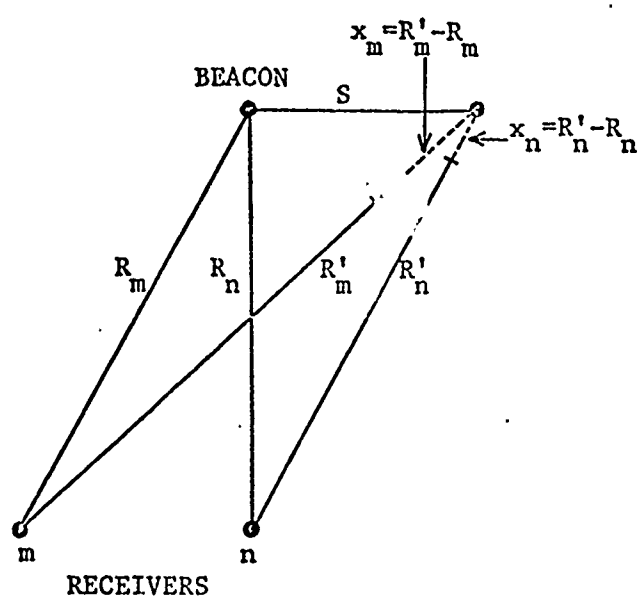

Fig. 4.3 Scanning geometry.

$$x_m << R_m \tag{4.38}$$

for each receiver. Also, the relative amplitudes of the rays do not vary with changes in source range due to scanning if the above condition is valid [11].

With this realistic model, then, the total ray travel time for each channel can be decomposed as follows (the subscript m or n is implied):

<u>beacon channel</u>

$$T_k = T_{k0} + t_{Wk} + t_T, \text{ ray } k \tag{4.39}$$

identified as

T_{k0} - nominal travel time defined in Section 4.2.

t_{Wk} - the fluctuation described in Section 4.2 which is independent and identically distributed among the rays of the beacon channel, and uncorrelated between receivers. It is now assumed that it is a zero-mean Gaussian random process with the following characteristics:

$$\left\langle t_{Wkm} t_{W\ell n} \right\rangle = 0, \; k \neq \ell \text{ or } m \neq n; \tag{4.40}$$

$$\left\langle t^2_{Wkm} \right\rangle = \Phi^2_m, \text{ for all } k, m. \tag{4.41}$$

t_T - the correlated fluctuation defined in Section 4.2.

<u>scan channel</u>

$$T'_{k'} = T'_{k'0} + t'_{Wk'} + t'_T \;,$$

$$T'_{k'0} = T_{k'0} + t'_{Sk'} \;, \text{ ray } k' \tag{4.42}$$

identified as

$T'_{k'0}$ - the nominal travel time in scan channel.

$T_{k'0}$ - the component of $T'_{k'0}$ which is the nominal travel time of ray k' in the beacon channel.

$t'_{Sk'}$ - the additional travel time in the scan channel due to a change, x, in the source range, defined in Section 3.2.1 as

$$t'_{sk'} = \frac{x}{c}\cos\theta_{k'} \quad . \tag{4.43}$$

The $\theta_{k'}$ were assumed to be independent random samples from the same distribution. An additional assumption is now made that the arrival angles are independent between receivers. This is reasonable, since widely spaced sensors receive entirely different multipath fields. The ray arrivals are not plane waves across the receivers, and the nominal travel times also differ due to the larger scale fluctuations (note that no restriction was made on receiver spacing with respect to the larger scale fluctuations; due to the large time scale, they are frozen for all time parameters of relevance in this problem, and can therefore be considered as deterministic, contributing only to the nominal travel times).

$t'_{Wk'}$ - the fluctuation described previously. However it may now be correlated with the fluctuation of ray k' in the beacon

channel of the same receiver if the scan distance is small. With the Gaussian assumption, its characteristics can be summarized in terms of rms values and its correlation coefficient as

$$\left\langle t'_{Wk'm} t'_{W\ell'n} \right\rangle = 0, \; k' \neq \ell' \text{ or } m \neq n; \tag{4.44}$$

$$\left\langle t'^{2}_{Wk'm} \right\rangle = \Phi'^{2}_{m}, \text{ for all } k', m. \tag{4.45}$$

$$\left\langle t'_{Wk'm} t_{W\ell n} \right\rangle = 0, \; k' \neq \ell \text{ or } m \neq n; \tag{4.46}$$

$$\left\langle t'_{Wk'm} t_{Wk'm} \right\rangle = \rho \Phi'_{m} \Phi_{m}, \text{ for all } k', m. \tag{4.47}$$

t'_T - the fluctuation which is correlated among rays of the scan channel. Since there may be a correlation between receivers, this implies that there may also be a correlation between the scan channel and beacon channel, since scan distance will generally be smaller than receiver separation.

4.3.2 DERIVATION OF THE COHERENCE FUNCTION

From (4.31), (4.32), and (4.37) the numerator of the MCF is

$$\left\langle H_m H^*_n \right\rangle = \left\langle H'_m H^*_m H'^*_n H_n \right\rangle \quad . \tag{4.48}$$

Substituting the transfer functions from (4.33) - (4.36) yields the expressions

$$H'_m H^*_m = \sum_{k}^{K_m} \sum_{k'}^{K_m} A_{km} A_{k'm} \exp -j\omega (T'_{k'm} - T_{km}) \quad , \tag{4.49}$$

$$H'^{*}_{n}H_{n} = \sum_{\ell}^{K_n}\sum_{\ell'}^{K_n} A_{\ell n}A_{\ell' n}\exp j\omega(T'_{\ell' n}-T_{\ell n}) \ . \tag{4.50}$$

The expected value in (4.48) will then be

$$\left\langle H_m H_n^* \right\rangle = \sum_{k}\sum_{k'}\sum_{\ell}\sum_{\ell'} A_{km}A_{k'm}A_{\ell n}A_{\ell' n}\left\langle \exp -j\omega[T'_{k'm}-T_{km}-T'_{\ell' n}+T_{\ell n}]\right\rangle \ . \tag{4.51}$$

Expanding the exponential into its components gives

$$\begin{aligned}
&\left\langle \exp -j\omega[T'_{k'm}-T_{km}-T'_{\ell' n}+T_{\ell n}]\right\rangle = \\
&\quad \exp -j\omega(T'_{km0}-T_{km0})\left\langle \exp -j\omega(t'_{Wk'm}-t_{Wkm})\right\rangle\left\langle \exp -j\omega\frac{x_m}{c}\cos\theta_{k'm}\right\rangle \ . \\
&\quad \exp j\omega(T_{\ell' n0}-T_{\ell n0})\left\langle \exp j\omega(t'_{W\ell' n}-t_{W\ell n})\right\rangle\left\langle \exp j\omega\frac{x_n}{c}\cos\theta_{\ell' n}\right\rangle \ . \\
&\quad \left\langle \exp -j\omega(t'_{Tm}-t_{Tm}-t'_{Tn}+t_{Tn})\right\rangle \ .
\end{aligned} \tag{4.52}$$

Denoting the three factors on the above lines by $\alpha_{k'km}$, $\alpha_{\ell'\ell n}$, α_{mn} then

$$\left\langle H_m H_n^* \right\rangle = \left(\sum_{k}\sum_{k'} A_{km}A_{k'm}\alpha_{kk'm}\right)\left(\sum_{\ell}\sum_{\ell'} A_{\ell n}A_{\ell' n}\alpha_{\ell\ell' n}\right)\alpha_{mn} \ . \tag{4.53}$$

The first component factor of $\alpha_{k'km}$ contains the phase due to the nominal travel times of channel m, the second due to uncorrelated ray fluctuations, and the last due to spatial variations in scanning; the same description applies to the factors of $\alpha_{\ell'\ell n}$ for

channel n. The factor γ_{Tmn}' contains the effect of fluctuations which are correlated between channels m and n, including the scan channels.

Consider now the expansion of (4.51) due to the first factor in (4.52),

$$\sum_{k'}\sum_{k} A_{km}A_{k'm}\exp-j\omega(T'_{k'0m}-T_{k0m})\left\langle \exp-j\omega(t'_{Wk'm}-t_{Wkm})\right\rangle\left\langle \exp-j\omega\frac{x_m}{c}\cos\theta_{k'm}\right\rangle . \tag{4.54}$$

The first expected value is

$$\left\langle \exp-j\omega(t'_{Wk'm}-t_{Wkm})\right\rangle = \exp-\frac{1}{2}\omega^2\left\langle (t'_{Wk'm}-t_{Wkm})^2\right\rangle$$

$$= \begin{cases} \exp-\frac{1}{2}\omega^2 D'_m(S,\tau)\ , & k'=k \\ \exp-\frac{1}{2}\omega^2(\Phi'^2_m+\Phi^2_m), & k'\neq k\ , \end{cases} \tag{4.55}$$

in which $D'_m(S,\tau)$ is the structure function of t_{Wkm} defined as

$$D'_m(S,\tau) = \Phi^2_m - 2\rho(S,\tau)\Phi_m\Phi'_m + \Phi'^2_m \tag{4.56}$$

where $\rho(S,\tau)$ is the correlation coefficient from (4.47). The characteristic functions are

$$c_{Sm}(\omega) = \left\langle \exp-j\omega\frac{x_m}{c}\cos\theta'_{km}\right\rangle \tag{4.57}$$

$$c_{Wm}(\omega) = \exp-\frac{1}{2}\omega^2\Phi^2_m \tag{4.58}$$

$$c'_{Wm}(\omega) = \exp-\frac{1}{2}\omega^2\Phi'^2_m \tag{4.59}$$

so that (4.54) becomes

$$c_{Sm}[\exp - \frac{1}{2}\omega^2 D'_m(S,\tau)]\sum_k A_{km}^2 + c_{Sm}c_{Wm}c'_{Wm}\sum_{k'}\sum_{\neq k} A_{km}A'_{k'm}\exp -j\omega(T'_{k'0m}-T_{k0m}). \tag{4.60}$$

An important simplification can be made if it can be assumed that scan distance and time are greater than the correlation distance and time of t_{Wk}, i.e., $S > L_0$ and $\tau > T_0$, so that $\rho(S,\tau) = 0$. In Chapter 5, t_{Wk} will be identified with internal wave fluctuations, for which $L_0 = 6.4$ km and $T_0 = 1.6$ hr [4]. Since the primary interest of this study is for scan distances and times greater than these values, it will be assumed that $\rho(S,\tau)=0$. (This point will be discussed further in Chapter 5.) With this simplification then

$$\exp - \frac{1}{2}\omega^2 D'_m(S,\tau) = \exp - \frac{1}{2}\omega^2(\phi'^2_m+\phi^2_m) = c_{Wm}c'_{Wm} \tag{4.61}$$

so that (4.60) becomes

$$c_{Sm}c_{Wm}c'_{Wm}(\sum_k A_{km})^2|H_{m0}|^2 = [c_W(\sum_k A_{km})|H_{m0}|][c_S c'_W(\sum_k A_{km}|H_{m0}|] \tag{4.62}$$

which has been factored into separate terms for the beacon and scan channels and where H_{m0} is the normalized transfer function of channel m in the absence of fluctuations, as defined in (4.12).

The result for the second factor of (4.52) is derived in an identical manner. The complete result for the numerator of the MCF is

$$\langle H_m H_n^* \rangle = [c_{Wm}(\sum_k A_{km})|H_{m0}|][c_{Sm}c'_{Wm}(\sum_k A_{km})|H_{m0}|] \cdot$$

$$[c_{Wn}(\sum_k A_{kn})|H_{n0}|][c^*_{Sn}c'_{Wn}(\sum_k A_{kn})|H_{n0}|]\gamma_{Tmn} \cdot \qquad (4.63)$$

The two factors of the denominator of the MCF likewise have identical derivations. The first factor is

$$\langle |H_m|^2 \rangle^{\frac{1}{2}} = \langle |H'_m H^*_m|^2 \rangle^{\frac{1}{2}} = \langle |H_m|^2 |H'_m|^2 \rangle^{\frac{1}{2}} \quad . \qquad (4.64)$$

With the assumption made above that $\rho(S,\tau) = 0$, the magnitudes of the transfer functions are independent between the beacon channel and scan channel, so that

$$\langle |H_m|^2 \rangle^{\frac{1}{2}} = \langle |H_m|^2 \rangle^{\frac{1}{2}} \langle |H'_m|^2 \rangle^{\frac{1}{2}} \quad . \qquad (4.65)$$

The square of the first factor of (4.65) is equation (4.13),

$$\langle |H_m|^2 \rangle = \sum_k A^2_{km} + [(\sum_k A_{km})^2 |H_{m0}|^2 - \sum_k A^2_{km}] c^2_{Wm} \quad , \qquad (4.13)$$

and a similar derivation for the scan channel yields

$$\langle |H'_m|^2 \rangle = \sum_{k'} A^2_{k'm} + [(\sum_{k'} A_{k'm})^2 |H_{m0}|^2 - \sum_{k'} A^2_{k'm}] |c_{Sm}|^2 c'^2_{Wm} \quad . \qquad (4.66)$$

The expressions for $\langle |H_n|^2 \rangle$ and $\langle |H'_n|^2 \rangle$ are analogous.

The final result can now be written as a composite of five factors,

$$\gamma_{Smn} = \gamma_m \gamma'_m \gamma^*_n \gamma'^*_n \gamma_{Tmn} \qquad (4.67)$$

in which the prime denotes the auto-coherence for the scan channel. As in (4.14), the substitution $K = (\sum A_k)^2/(\sum A_k^2)$ is made for each auto-coherence factor. Using the envelope approximation, the results are

$$\gamma_m = \left[\frac{K_m c_{Wm}^2}{1+(K_m-1)c_{Wm}^2}\right]^{\frac{1}{2}} \cdot |H_{m0}| = \gamma_{Wm} \cdot \gamma_{Mm} \quad ; \tag{4.68}$$

$$\gamma'_m = \left[\frac{K_m |c_{Sm}|^2 c'^2_{Wm}}{1+(K_m-1)|c_{Sm}|^2 c'^2_{Wm}}\right]^{\frac{1}{2}} e^{j\phi_{Sm}} \cdot |H_{m0}| = \gamma'_{W,Sm} \cdot \gamma'_{Mm} \quad ,$$

$$c_{Sm} = |c_{Sm}| e^{j\phi_{Sm}} \quad ; \tag{4.69}$$

$$\gamma^*_n = \left[\frac{K_n c_{Wn}^2}{1+(K_n-1)c_{Wn}^2}\right]^{\frac{1}{2}} \cdot |H^*_{n0}| = \gamma_{Wn} \cdot \gamma_{Mn} \quad ; \tag{4.70}$$

$$\gamma'^*_n = \left[\frac{K_n |c_{Sn}|^2 c'^2_{Wn}}{1+(K_n-1)|c_{Sn}|^2 c'^2_{Wn}}\right]^{\frac{1}{2}} e^{-j\phi_{Sn}} \cdot |H^*_{n0}| = \gamma'^*_{W,Sn} \cdot \gamma'_{Mn} \quad ,$$

$$c_{Sn} = |c_{Sn}| e^{j\phi_{Sn}} \quad ; \tag{4.71}$$

$$\gamma_{Tmn} = \left\langle \exp -j\omega(t'_{Tm} - t_{Tm} - t'_{Tn} + t_{Tn}) \right\rangle \quad . \tag{4.72}$$

The solution to an extremely complex problem has been reduced to a composite of strikingly simple factors, with no restrictive

assumptions or approximations. Equations (4.67)-(4.72) are the most important results of this work.

The first important feature of this solution is that it includes the MCF without scanning developed in Section 4.2 as a special case. That solution is obtained by setting all primed auto-coherences to unity, and omitting the primed fluctuations from γ_{Tmn}. (The resultant phase of the multipath transfer functions does not appear now since the beacon is used as a focus; also, the former solution cannot be found by letting $S \to 0$, since it was assumed that $S > L_0$, which makes the scan channel and beacon channel independent.)

The first auto-coherence factor, equation (4.68), is a composite of the effects of uncorrelated ray fluctuations and frequency selective fading in beacon channel m. Equation (4.69) is the auto-coherence for scan channel m. The additional effect of fluctuations due to spatially varying multipath interference now multiplies the effect of uncorrelated fluctuations. The phase of $\gamma'_{W,Sm}$, ϕ_{Sm}, is the average phase difference between the scan location and the beacon. It is the primary component of the phase shift for receiver m which will be required for scanning. The auto-coherence factor due to frequency selective fading is the same as that for the beacon channel, since it has been stipulated that the multipath field is azimuthally isotropic over small scan distances. The resulting effect is that the extension to scanning has squared the coherence due to frequency selective multipath interference. However, it will be seen in Chapter 5 that this has no degrading effect at coherent frequencies.

The auto-coherences for channel n have the same interpretation as above. The last factor of the MCF is the coherence due to fluctuations which have some correlation among the channels, and which will be developed in Chapter 5. The phase of this term is an additional phase difference between channels m and n required for scanning.

The convenient factorization of the MCF into eight auto-coherence functions and a coherence due to correlated fluctuations allows grouping of terms to determine relative effects of various combinations. To study the relative contribution of scanning to coherence, write

$$\gamma_{Smn} = (\gamma_m \gamma_n^*)(\gamma_m' \gamma_m'^*)\gamma_{Tmn}$$

$$= \gamma_{mn} \gamma_{mn}' \gamma_{Tmn} \quad , \tag{4.73}$$

and γ_{mn}' can be compared to γ_{mn}. The relative contribution of each receiver channel is similarly determined from

$$\gamma_{Smn} = (\gamma_m \gamma_m')(\gamma_n \gamma_n')^* \gamma_{Tmn}$$

$$= \gamma_m \gamma_n^* \gamma_{Tmn} \quad , \tag{4.74}$$

by comparing γ_m to γ_n. The most important simplification is the separation of the effect of random fluctuations from that of frequency selective multipath interference by writing

$$\gamma_{Smn} = (\gamma_{Wm}\gamma'_{W,Sm}\gamma_{Wn}\gamma'_{W,Sn}\gamma_{Tmn})(\gamma^2_{Mm}\gamma^2_{Mn})$$

$$= (\gamma_{W,S}\gamma_T)\gamma_M \quad . \tag{4.75}$$

The value of this factorization is that, since the effect of randomness forms an envelope of the MCF and is a monotonically decreasing function of frequency, it enables a prediction of maximum coherent frequencies without knowledge of the particular multipath structure or its frequency selective coherence function, $\gamma_M(\omega)$.

4.4 SUMMARY

This chapter is the most important, and the theory presented provides the basis for the rest of the dissertation. The theory of the multipath coherence function has been developed based upon a formulation of the spectral coherence function in terms of the random multipath channel transfer functions. This has shown that the MCF is independent of the signal source, and depends only on the characteristics of the channel. It therefore applies equally well for narrow band or broad band, random or deterministic signals, at each frequency in the source spectrum.

Due to the stochastic independence of channels, the MCF factors conveniently into two auto-coherences. The value of this factorization is that each channel can be analyzed independently, rather than computing non-separable coherences for all pairwise combinations of receivers.

The MCF has been formulated to consider the two types of environmental fluctuations: those which cause uncorrelated ray fluctuations and those which cause correlated fluctuations. The MCF has been generalized to include the latter type as a cause of acoustic fluctuations which may be partially correlated between receivers.

The next important development is the envelope approximation, whereby each auto-coherence factors into two coherence terms, one for the effects of random fluctuations alone, and the other for frequency selective multipath interference. This allows computation of maximum coherent frequency independent of the multipath configuration.

The generalization of the MCF to include the effects of scanning introduced another type of acoustic fluctuation, that due to spatially varying multipath interference. This fluctuation was accounted for by applying a stochastic model to the ray arrival angles. Due to the weak assumption that scan distance and time were larger than the corresponding correlations of environmental fluctuations, the MCF could again be factored into separate coherence functions for the scan channel and beacon channel. The resulting generalized MCF is a concise mathematical expression composed of simple factors which allow any single coherence term to be analyzed separately.

The remaining task to be performed in Chapter 5 is the

specification of the MCF parameters in terms of real oceanographic fluctuations. The parameters of environmentally caused fluctuations will be derived from the theory of internal waves and tides, and the effects of both spatial and frequency selective multipath interference will be determined from realistic models of the underwater channel. However it must be emphasized that the results of this chapter, the most important of which are equations (4.67) - (4.72), do not depend upon the presently known types of real oceanographic fluctuations and their actual stochastic parameters, but only require that they be classified as described in Section 4.3.1. Should future oceanographic developments provide an update of the present state of knowledge, the model will still be completely applicable.

REFERENCES

[1] P. W. Smith, Jr., "Spatial Coherence in Multipath or Multimodal Channels," J. Acoust. Soc. Am., Vol. 60, No. 2, August 1976.

[2] W. J. Jobst, "An Application of Poisson Process Models to Multipath Sound Propagation of Sinusoidal Signals," J. Acoust. Soc. Am., Vol. 57, No. 6, Part II, June 1975.

[3] R. F. Dashen, S. M. Flatte, W. H. Munk, and F. Zachariasen, "Limits on Coherent Processing Due to Internal Waves," JASON Report JSR-76-14, Stanford Research Institute, California, June 1977.

[4] R. F. Dashen, S. M. Flatte, W. H. Munk, and F. Zachariasen, "Sound Transmission Through a Fluctuating Ocean," JASON Report JSR-76-39, Stanford Research Institute, California, May 1977.

[5] W. H. Munk and F. Zachariasen, "Sound Propagation Through a Fluctuating Stratified Ocean: Theory and Observation," J. Acoust. Soc. Am., Vol. 59, No. 4, April 1976.

[6] M. J. Beran, J. J. McCoy, and B. B. Adams, "Effects of a Fluctuating Temperature Field on the Spatial Coherence of Acoustic Signals," NRL Report 7809, Washington, D. C., 1975.

[7] J. J. McCoy, "Beam Spreading and Loss of Spatial Coherence in an Inhomogeneous and Fluctuating Ocean," SACLANTCEN Conf. Proc. (La Spezia, Italy) 17,6,1975.

[8] S. L. Adams and J. W. Doubek, "Frequency Coherence and Time Coherence in Random Multipath Channels," J. Acoust. Soc. Am., Vol. 62, No. 2, August 1977.

[9] H. A. DeFerrari, "Time-Varying Multipath Interference of Broad-Band Signals Over a 7-NM Range in the Florida Straits," J. Acoust. Soc. Am., Vol. 53, No. 1, 1973.

[10] R. L. Veenkant, "Investigation of the Propagation Stability of a Doubly Spread Underwater Acoustic Channel," IEEE Trans. Acoust. Sp. Sig. Proc., Vol. ASSP-25, No. 2, April 1977.

[11] J. G. Clark, R. P. Flanagan, and N. L. Weinberg, "Multipath Acoustic Propagation with a Moving Source in a Bounded Deep Ocean Channel," J. Acoust. Soc. Am., Vol. 60, No. 6, December 1976.

CHAPTER 5

THE COHERENCE FUNCTION IN TERMS OF THE OCEANOGRAPHIC FLUCTUATIONS

5.1 INTRODUCTION

In Chapter 4 the general form of the MCF was derived for beamforming and scanning in multipath channels. The travel time fluctuations in the ray paths were defined in terms of their general stochastic characteristics, but their parameters were not specified in terms of environmental fluctuations.

Chapter 3 identified the four primary types of oceanographic fluctuations which affect coherence: spatial variations due to multipath interference, internal waves, internal tides, and frequency selective multipath interference. The first three types cause travel time fluctuations in the ray paths, and the stochastic parameters of these fluctuations were specified. It now remains to identify these fluctuations with those of the MCF developed in Chapter 4 in order to determine signal coherence in real ocean channels.

The travel time of a ray in the beacon channel was decomposed as

$$T_k = T_{k0} + t_{Wk} + t_T, \quad \text{ray } k \quad . \tag{4.39}$$

In terms of oceanographic fluctuations they are identified as

T_{k0} – nominal travel time affecting frequency selective multipath interference.

t_{Wk} - fluctuation due to internal waves.

t_T - fluctuation due to internal tides.

In the scan channel

$$T'_{k'} = T'_{k'0} + t'_{Wk'} + t'_T$$

$$T'_{k'0} = T_{k'0} + t'_{Sk'}, \qquad \text{ray } k' , \tag{4.42}$$

and there is an additional fluctuation,

$t'_{Sk'}$ - fluctuation in scanning causing spatial variations due to multipath interference.

The effect of each of these fluctuations on coherence will be determined in the following sections.

5.2 EFFECT ON COHERENCE OF OCEANOGRAPHIC FLUCTUATIONS

The system geometry for scanning away from a beacon using a two-receiver array was described in Section 4.3.1 and illustrated in Fig. 4.3. The purpose of this section is to determine the MCF

$$\gamma_{mn} = \gamma_{Wm}\gamma_{Mm}\gamma'_{W,Sm}\gamma'_{Mm}\gamma_{Wn}\gamma_{Mn}\gamma'^{*}_{W,Sn}\gamma'_{Mn}\gamma_{Tmn} \tag{5.1}$$

where the individual auto-coherence factors were defined in (4.68)-(4.72). In terms of oceanographic fluctuations they are now identified as

γ_{Wm} - effect of internal waves in channel from beacon to receiver m.

γ_{Mm} - effect of frequency selective multipath interference in

beacon channel to receiver m.

$\gamma'_{W,Sm}$ - effect of internal waves and spatial variations due to multipath interference in scan channel to receiver m.

γ_{Tmn} - effect of internal tides in beacon channels and scan channels to both receivers m and n.

The remaining factors in (5.1) have corresponding definitions for receiver n or for the scan channel (denoted by a prime). The contribution of each type of fluctuation to the MCF and its relative importance will now be determined in terms of its respective autocoherence factor.

5.2.1 INTERNAL WAVES

A basic premise of this work has been that the receivers are separated by such large distances that travel time fluctuations induced by internal waves are independent between them. In Section 4.3.2 it was further assumed that horizontal scan distance, S, and scan time, τ, are larger than the corresponding correlation distance and time of the fluctuations, so that the fluctuations in the scan channel are independent of those in the beacon channel. In Section 3.2.2 the correlation coefficient was given as

$$\rho(S,\tau) = 1 - \frac{1}{2}\left[\left(\frac{S}{6.4\ \text{km}}\right)^2 + \left(\frac{\tau}{1.6\ \text{hr}}\right)^2\right] \tag{3.12}$$

and is illustrated in Fig. 5.1. From this equation the scan distance S for which the beacon and scan channels are independent can

be determined for a given time τ from initial focus on the beacon.

The auto-coherence due to internal waves in each beacon channel is of the form

$$\gamma_W = \left[\frac{Kc_W^2}{1+(K-1)c_W^2}\right]^{\frac{1}{2}} . \tag{5.2}$$

In Section 4.3.2 the characteristic function was shown to be

$$c_W = \exp(-\frac{1}{2}\omega^2\phi^2) \tag{5.3}$$

as is shown in Fig. 5.2 as a function of $f\Phi$. The mean square travel time fluctuations were given as

$$\Phi^2 = (3.4\text{x}10^{-8}\text{sec}^2\text{km}^{-1})R, \text{ steep ray;} \tag{3.9}$$

$$\Phi^2 = (6.8\text{x}10^{-8}\text{sec}^2\text{km}^{-1})R, \text{ axis ray,} \tag{3.10}$$

and are shown in Fig. 5.3.

With these equations the auto-coherence due to internal waves for each channel can be computed as a function of acoustic frequency and the range to the beacon from each receiver. Fig. 5.4 illustrates a typical variation of γ_W with beacon range, and the attenuation with acoustic frequency is depicted in Fig. 5.5. Both computations assume steep rays using (3.10) and the ray parameter is K = 4.

5.2.2 SPATIAL VARIATIONS DUE TO MULTIPATH INTERFERENCE

The effect of spatial variations due to scanning for each channel

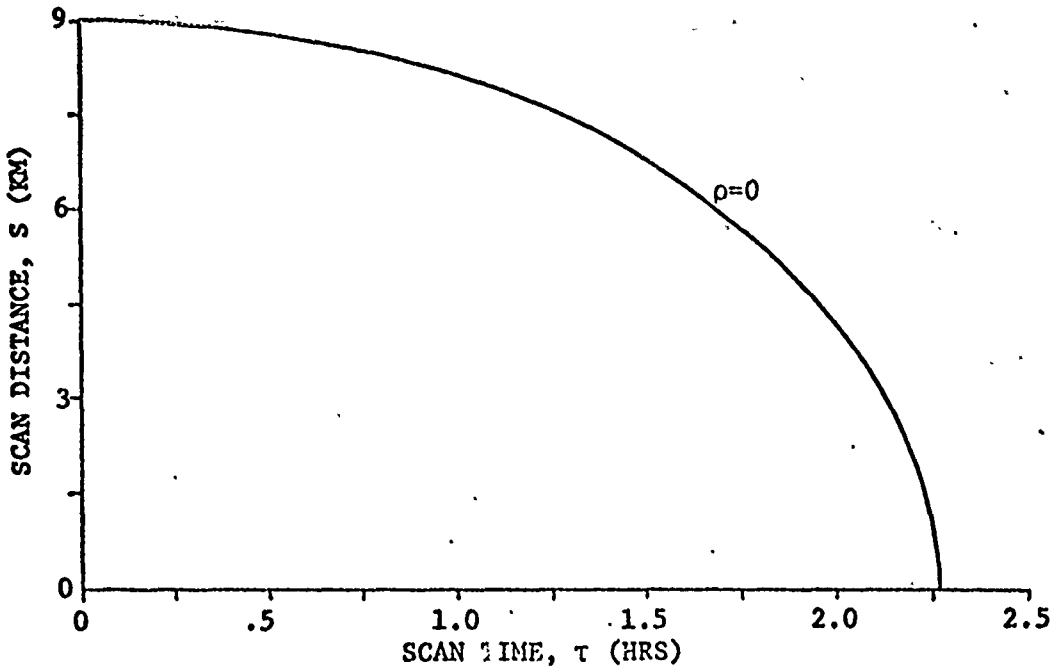

Fig. 5.1 Scan distance and scan time for uncorrelated internal wave fluctuations.

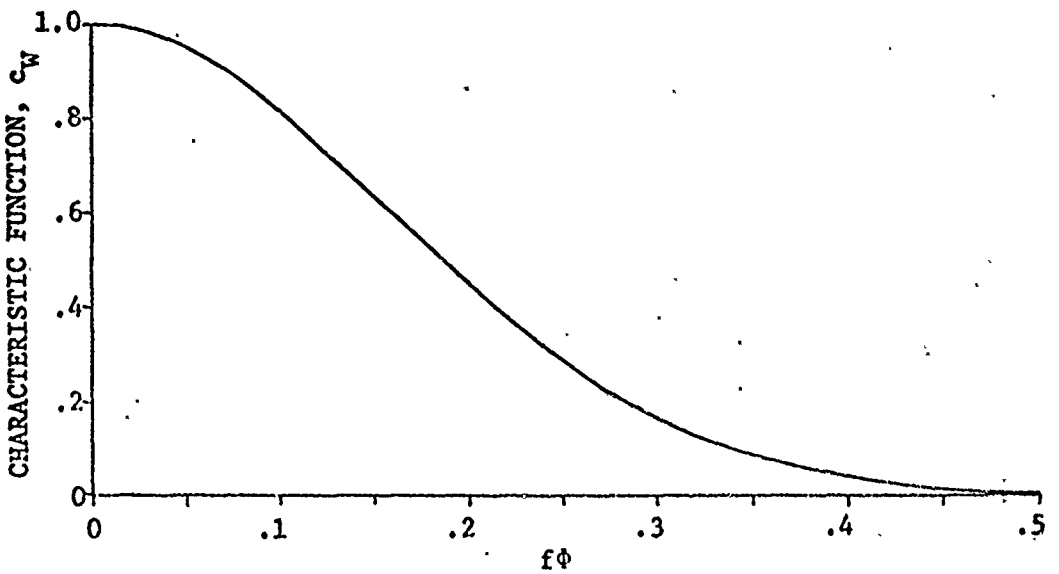

Fig. 5.2 Characteristic function for internal wave fluctuations.

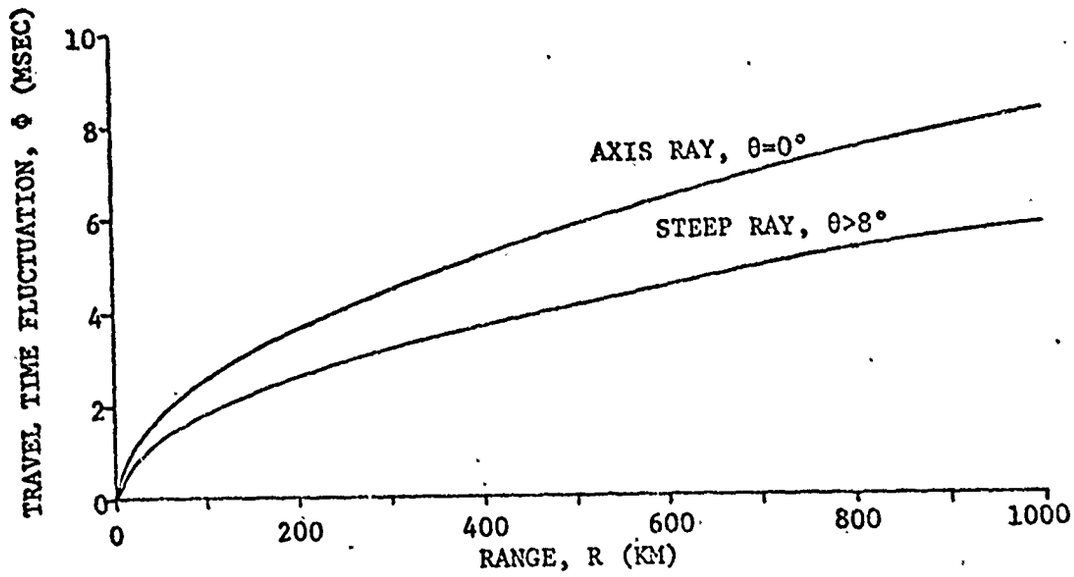

Fig. 5.3 RMS travel time fluctuation due to internal waves.

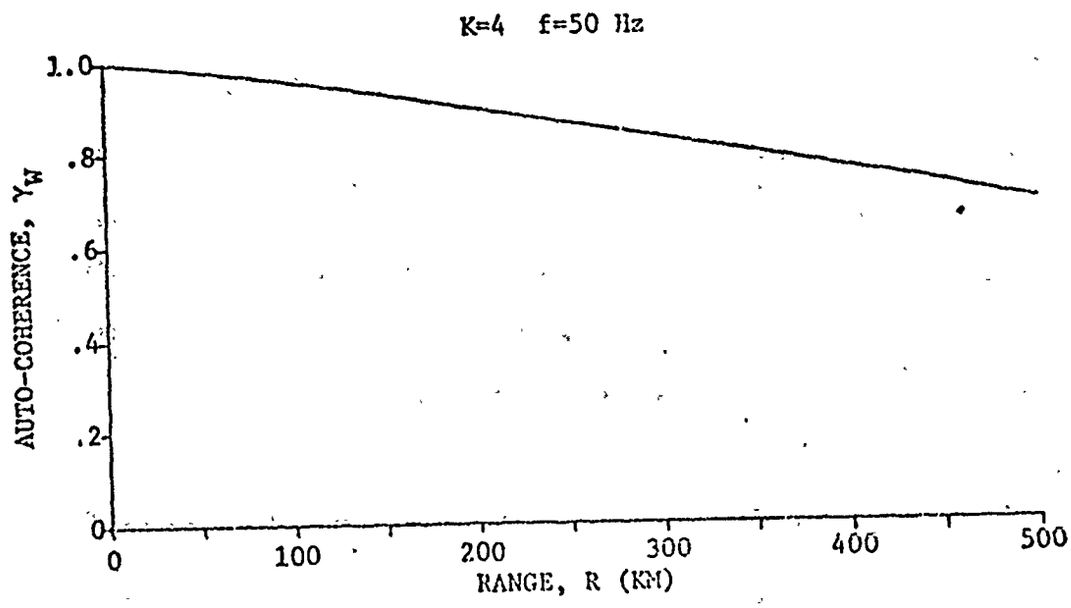

Fig. 5.4 Range variation of internal wave auto-coherence.

is determined from

$$\gamma'_{W,S} = \left[\frac{K|c_S|^2 c'^2_W}{1+(K-1)|c_S|^2 c'^2_W}\right]^{\frac{1}{2}} e^{j\phi_S} . \tag{5.4}$$

The characteristic function for the spatial variations,

$$c_S = |c_S| e^{j\phi_S} , \tag{5.5}$$

was developed in Section 3.2.1 and can be written in terms of the wavenumber, k_0, as

$$c_S = \left[1+(k_0 x\sigma^2)^2\right]^{-\frac{1}{4}} \exp j\left[-k_0 x + \frac{1}{2}\tan^{-1}(k_0 x\sigma^2)\right] . \tag{5.6}$$

The magnitude of c_S consists of the first factor. Fig. 5.6 shows the variation of $|c_S|$ with $|x|/\lambda$ for characteristic values of the ray spread, σ.

In Section 5.2.3 it is shown that internal tides have no effect on average signal phase. Therefore the term ϕ_S is the total average phase change for one receiver channel due to scanning away from the beacon. In (5.6) it is seen to consist of two terms. The first term is the linear component, $-k_0 x$. The second component is due to the ray spread. Note that $\phi_S(-x) = -\phi_S(x)$. The phase with the

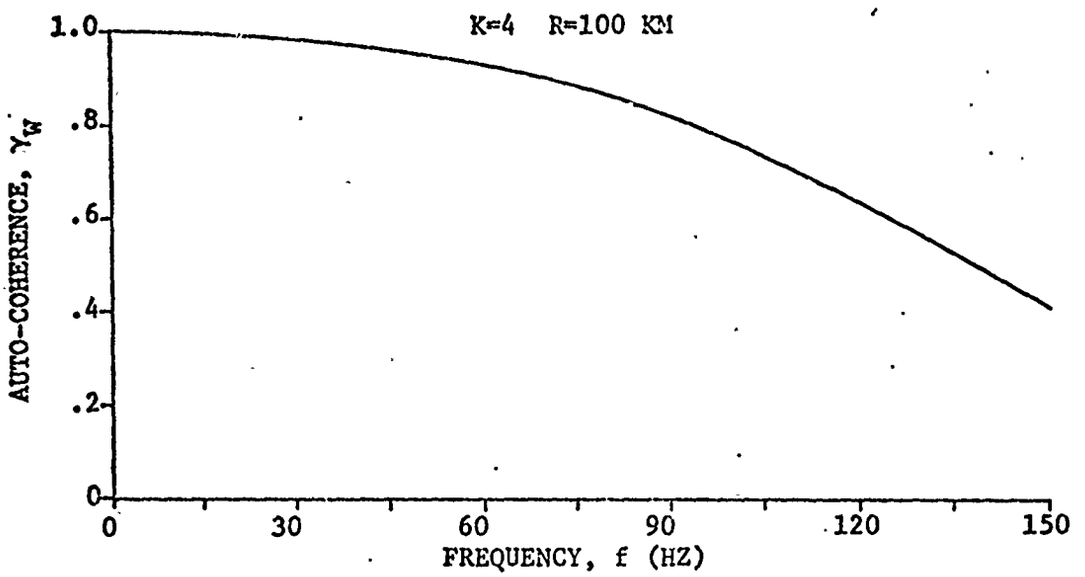

Fig. 5.5 Frequency variation of internal wave auto-coherence.

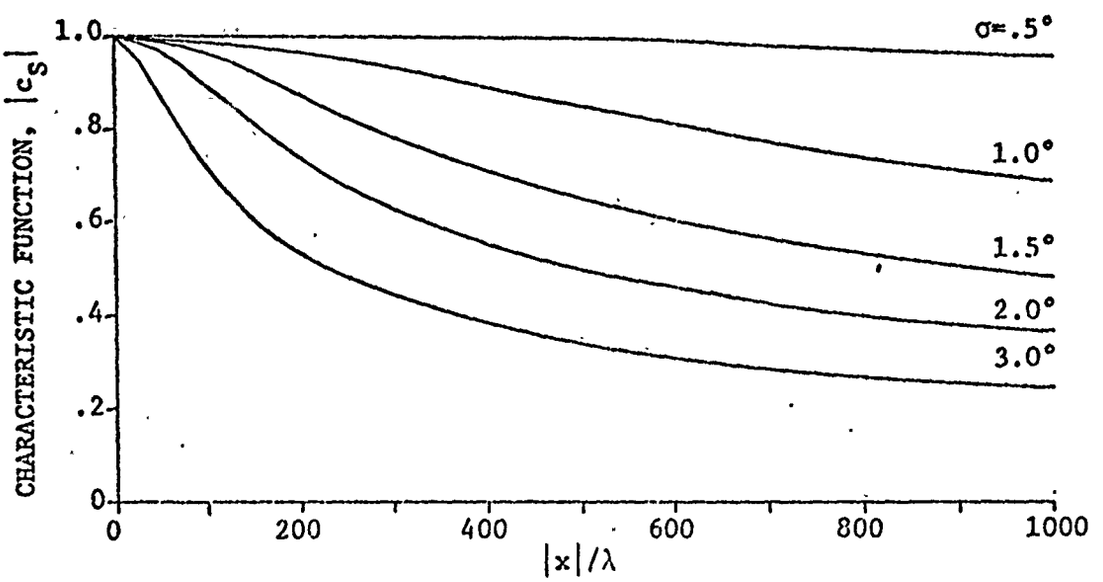

Fig. 5.6 Characteristic function for spatial multipath interference.

linear component removed is illustrated as a function of x/λ in Fig. 5.7 for characteristic ray spreads.

The coherence $\gamma'_{W,S}$ also includes the effect of internal waves in the scan channel. For the purpose of comparison with γ_W, the characteristic function c'_W is set equal to unity and

$$|\gamma'_S| = \left[\frac{K|c_S|^2}{1+(K-1)|c_S|^2}\right]^{\frac{1}{2}} \tag{5.7}$$

is computed. Assuming a ray spread $\sigma = 2°$, the variation of $|\gamma'_S|$ is illustrated in Fig. 5.8 as a function of $|x|$, and in Fig. 5.9 as a function of frequency. Note the larger rate of attenuation of $|\gamma_S|$ with range and frequency compared to that of γ_W in Figs. 5.4 and 5.5. This indicates that for a given increase in range due to scanning, the decrease in $|\gamma_S|$ is much more severe than the corresponding decrease in γ_W, and is the limiting factor in scanning ability. Since x is the change in range due to scanning, it can also be concluded that the maximum limitation on scanning is in the direction of the propagation path from beacon to receiver. In a direction perpendicular to this path the change in range is much less so that there is less limitation on scanning.

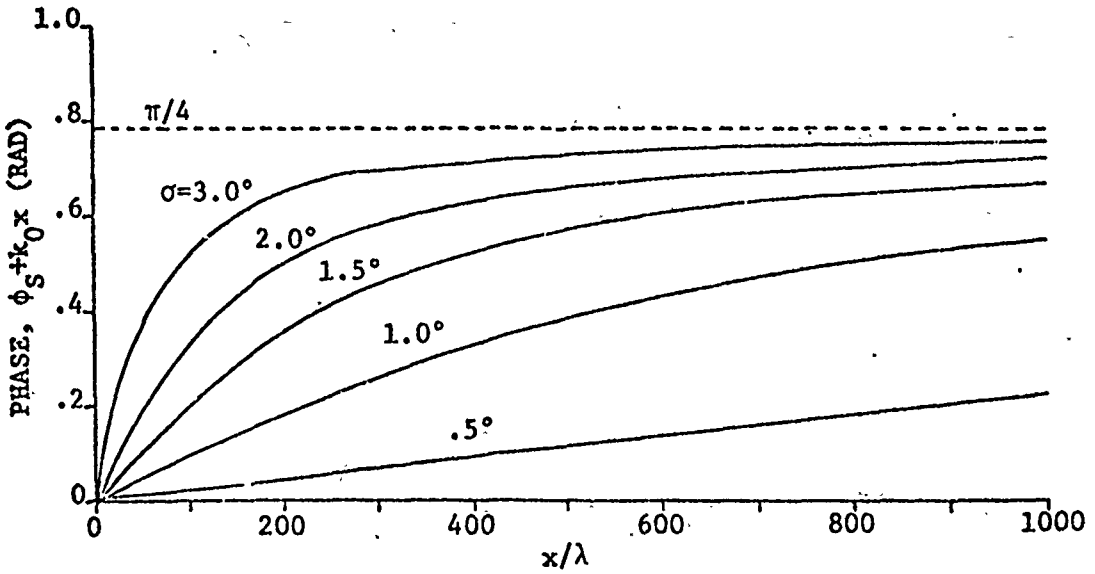

Fig. 5.7 Average phase variation due to spatial multipath interference.

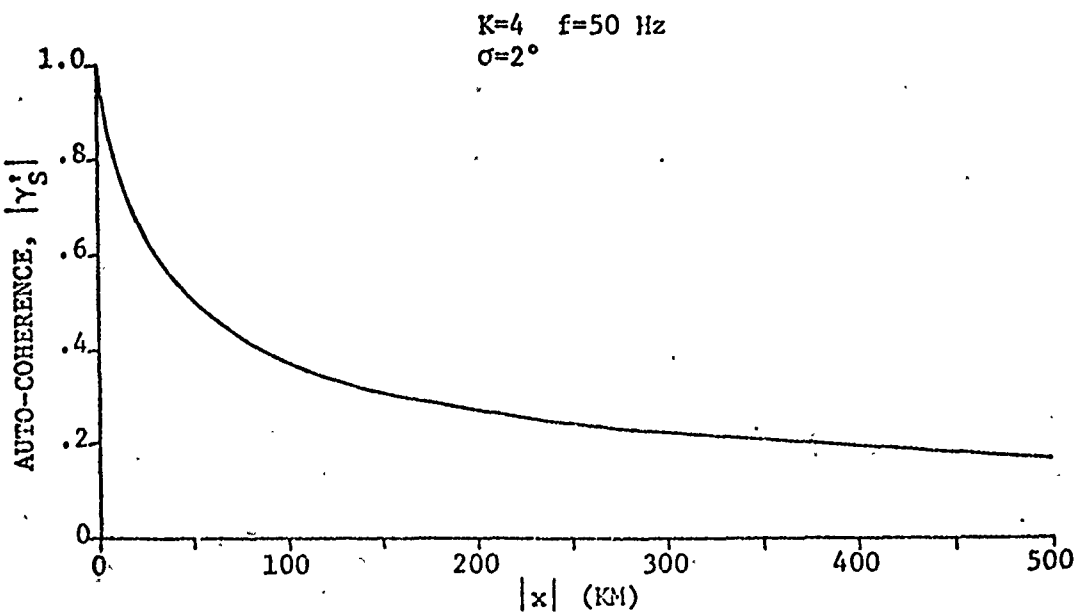

Fig. 5.8 Range variation of auto-coherence due to spatial multipath interference.

5.2.3 INTERNAL TIDES

The effect of internal tides on coherence is described by

$$\gamma_{Tmn} = \left\langle \exp -j\omega(t'_{Tm} - t_{Tm} - t'_{Tn} + t_{Tn}) \right\rangle$$
$$= \left\langle \exp -j\omega\Delta t_T \right\rangle \quad . \tag{5.8}$$

The travel time of an axis ray from source to receiver in the presence of internal tides was derived in Section 3.2.3 as

$$T = T_0\left[1 - \frac{2\Delta c_0}{c_0}\sin(\omega_T t - k_T R\cos\phi/2)\frac{\sin(k_T R\cos\phi/2)}{(k_T R\cos\phi/2)}\right] \tag{3.18}$$

where $T_0 = R/c_0$. The travel time fluctuation due to internal tides is the same for each ray [1] so that the results for an axis ray are used.

Consider the simplified source-receiver configuration shown in Fig. 5.10. Two sensors separated by a distance R_S are located on a baseline perpendicular to the direction of internal tide propagation (e.g., on a continental shelf). A beacon is located equidistant from the two receivers at a range R_0. At time t, the travel times to the two sensors are

$$T_m = T_{m0}\left[1 - \frac{2\Delta c_0}{c_0}\sin(\omega_T t - k_T R_m\cos\phi_m/2)\ \frac{\sin(k_T R_m\cos\phi_m/2)}{(k_T R_m\cos\phi_m/2)}\right]$$
$$= T_{m0}(1-\Delta_m) \tag{5.9}$$

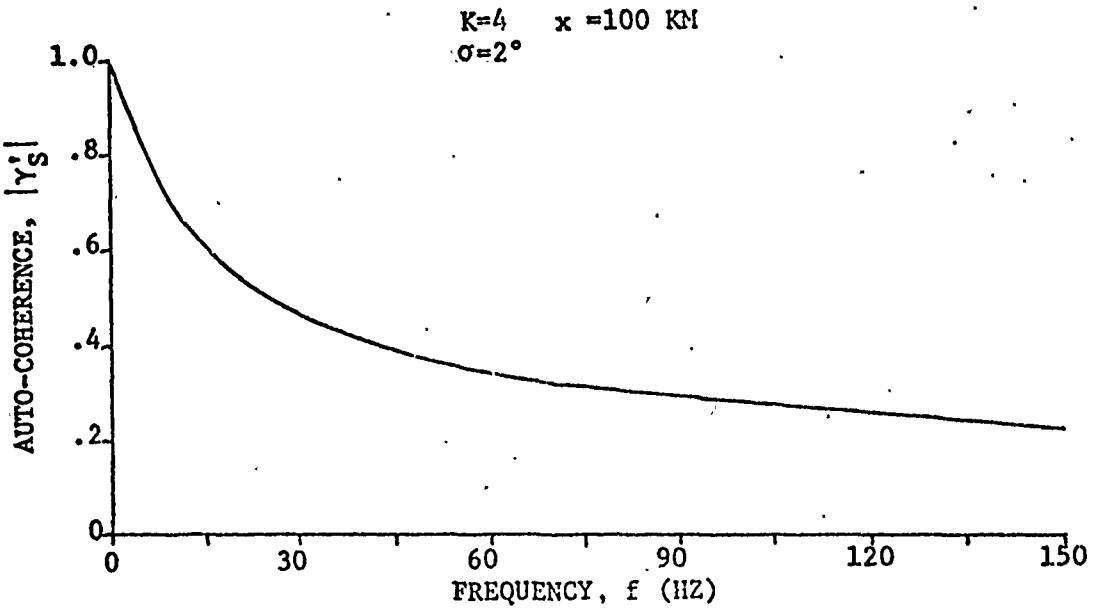

Fig. 5.9 Frequency variation of auto-coherence due to spatial multipath interference.

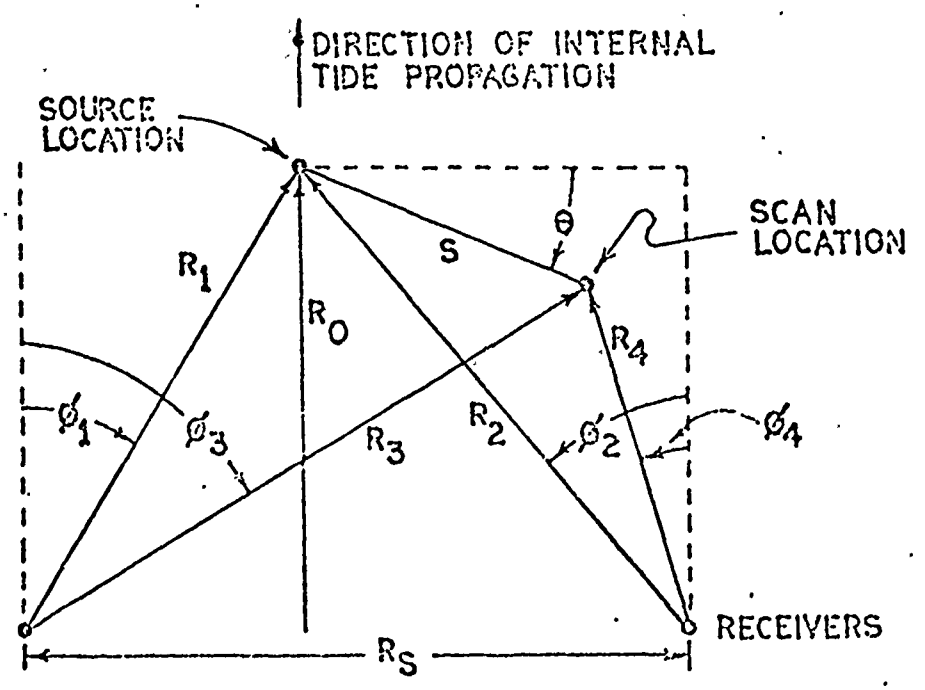

Fig. 5.10 Source-receiver configuration for internal tide fluctuations.

and

$$T_n = T_{n0}\left[1 - \frac{2\Delta c_0}{c_0}\sin(\omega_T t - k_T R_n \cos\phi_n/2)\,\frac{\sin(k_T R_n \cos\phi_n/2)}{(k_T R_n \cos\phi_n/2)}\right]$$

$$= T_{n0}(1-\Delta_n) \quad . \tag{5.10}$$

The travel times from the scan location at (S,θ), at some later time $t + \tau$ are

$$T'_m = T'_{m0}\left\{1 - \frac{2\Delta c_0}{c_0}\sin[\omega_T(t+\tau) - k_T R'_m \cos\phi'_m/2]\,\frac{\sin(k_T R'_m \cos\phi'_m/2)}{(k_T R'_m \cos\phi'_m/2)}\right\}$$

$$= T'_{m0}(1-\Delta'_m) \tag{5.11}$$

and

$$T'_n = T'_{n0}\left\{1 - \frac{2\Delta c_0}{c_0}\sin[\omega_T(t+\tau) - k_T R'_n \cos\phi'_n/2]\,\frac{\sin(k_T R'_n \cos\phi'_n/2)}{(k_T R'_n \cos\phi'_n/2)}\right\}$$

$$= T'_{n0}(1-\Delta'_n) \quad . \tag{5.12}$$

The travel time fluctuations due to the internal tide are

$$\begin{aligned} t_{Tm} &= -\frac{R_m}{c_0}\Delta_m \quad , \\ t_{Tn} &= -\frac{R_n}{c_0}\Delta_n \quad , \\ t'_{Tm} &= -\frac{R'_m}{c_0}\Delta'_m \quad , \\ t'_{Tn} &= -\frac{R'_n}{c_0}\Delta'_n \quad . \end{aligned} \tag{5.13}$$

But $t_{Tm} = t_{Tn}$, so that

$$\Delta t_T = t'_{Tm} - t'_{Tn} \quad . \tag{5.14}$$

It is also true that

$$R'_n \cos\phi'_n = R'_m \cos\phi'_m = R_0 + S\sin\theta$$

so

$$\Delta t_T = \left(\frac{\Delta R_{mn}}{c_0}\right)\left(\frac{2\Delta c_0}{c_0}\right)\sin[\omega_T(t+\tau) - k_T(R_0+S\sin\theta)]\ \frac{\sin[k_T(R_0+S\sin\theta)/2]}{[k_T(R_0+S\sin\theta)/2]} \quad . \tag{5.15}$$

Here the quantity ΔR_{mn} is the range difference

$$\Delta R_{mn} = R'_m - R'_n \tag{5.16}$$

$$= \sqrt{(R_0+S\sin\theta)^2 + (\frac{R_S}{2} + S\cos\theta)^2} - \sqrt{(R_0+S\sin\theta)^2 + (\frac{R_S}{2} - S\cos\theta)^2} \, .$$

the effect on coherence is given by the factor

$$\gamma_{Tmn} = \left\langle e^{-j\omega\Delta t_T} \right\rangle \tag{5.17}$$

which will denote an ensemble average over all time of initial focus on the beacon $0 \leq t \leq 2\pi/\omega_T$, i.e.

$$\left\langle e^{-j\omega\Delta t_T} \right\rangle \triangleq \frac{\omega_T}{2\pi} \int_0^{2\pi/\omega_T} e^{-j\omega\Delta t_T}\, dt \quad . \tag{5.18}$$

Writing the phase as

$$\omega\Delta t_T = \alpha\sin[\omega_T(t+\tau)-\psi \tag{5.19}$$

then

$$\left\langle e^{-j\omega\Delta t_T}\right\rangle = \frac{\omega_T}{2\pi}\int_0^{2\pi/\omega_T} e^{-j\alpha\sin[\omega_T(t+\tau)-\psi]}dt$$

$$= J_0(\alpha) \tag{5.20}$$

in which J_0 is the zero order Bessel function. The complete effect on coherence between channels m and n, due to internal tides, is therefore given by the expression

$$\gamma_{Tmn} = J_0\left\{\omega\left(\frac{2\Delta c_0}{c_0}\right)\left(\frac{\Delta R_{mn}}{c_0}\right)\frac{\sin[k_T(R_0+S\sin\theta)/2]}{[k_T(R_0+S\sin\theta)/2]}\right\}. \tag{5.21}$$

The only assumption which has been made in this derivation is that $\Delta c_0/c_0 << 1$ (a characteristic value for $\Delta c_0/c_0$ due to internal tides is 10^{-5}). Since γ_{Tmn} is real, it makes no contribution to the average phase difference between the signals.

It is important to analyze the physical significance of this result. For this purpose, assume that the scan distance $S << R_0$. It can then be shown that

$$\Delta R \approx \frac{2S\cos\theta}{\sqrt{4\left(\frac{R_0}{R_S}\right)^2 + 1}} \quad . \tag{5.22}$$

The coherence then becomes

$$\gamma_{Tmn} = J_0\left[\omega\left(\frac{2\Delta c_0}{c_0}\right)\left(\frac{2S\cos\theta}{c_0}\right)\frac{1}{\sqrt{4(R_0/R_S)^2 + 1}}\;\frac{\sin(k_T R_0/2)}{(k_T R_0/2)}\right] . \tag{5.23}$$

First, there is a noticeable absence of dependence on the time difference, τ. This is explained by the fact that the bulk time delays are equal for the first source location. If they were not chosen to be equal, the mathematics would become unwieldy, but it can be shown that, in general, the effect on coherence would be a dependence on a sinusoidal function of $\omega_T\tau$. This would cause the coherence to oscillate between unity and some minimum value determined by the other parameters. The configuration considered here corresponds to the minimum value.

The manner of dependence of γ_{Tmn} on the quantities ω and $(\Delta c_0/c_0)$ is obvious. The effect of the quantity $S\cos\theta$ is interesting: the coherence depends primarily on the component of scan distance perpendicular to the tide normal. This is consistent with the previous observation that the maximum effect on phase fluctuations is when ray propagation is perpendicular to the direction of the tide.

As the quantity R_0/R_S becomes large, the difference in travel time between the two sensor channels for a constant scan distance S becomes small, causing coherence to increase. Likewise, as R_0/λ_T increases, coherence increases. The explanation for this is the fact that, since R_0 is the component of the ray paths in the direction of the internal tide propagation, as R_0/λ_T becomes large the ray travels through a larger number of periods of the internal tide, and the positive and negative variations of the sound speed variations tend to average out to zero. Note that when the ray has travelled through an integer number of periods of the internal tide, the sound speed variations are completely cancelled out, and coherence becomes unity, i.e.,

$$\frac{\sin(k_T R_0/2)}{(k_T R_0/2)} = 0, \quad \text{for } \frac{R_0}{\lambda} = 1,\ 2,\ \ldots\ldots \quad . \tag{5.24}$$

This is, of course, exactly true only for axial rays as considered here; however it can be concluded that, in general, coherence is greater when acoustic propagation is in the direction of the internal tide.

The coherence, γ_{Tmn}, is plotted in Fig. 5.11 as a function of $\omega\delta T$ where

$$\delta T = \left(\frac{2\Delta c_0}{c_0}\right)\left(\frac{\Delta R_{mn}}{c_0}\right)\frac{\sin[k_T(R_0+S\sin\theta)/2]}{[k_T(R_0+S\sin\theta)/2]} \tag{5.25}$$

is the travel time variation due to the internal tide. In the deep

ocean it has been found that the 4m internal tide is predominant. For a typical sound speed profile with the sound axis at a depth of 1200m, reference [2] gives the sound speed variation as $\Delta c_0 = .06$m/sec for $c_0 = 1489.55$ m/sec., so that $\Delta c_0/c_0 = 4.03 \times 10^{-5}$. Fig. 5.12 shows the corresponding variation of δT with scan distance S, for $\theta = 0°$ and $R_S = 150$ km, and for selected values of range R_0. For other amplitudes of the internal tide, the appropriate value of $\Delta c_0/c_0$ should be substituted in (5.25).

Based on the results derived here, it will be shown in Section 5.3 that internal tides have a negligible effect on coherence compared to internal waves and spatial multipath interference.

5.2.4 FREQUENCY SELECTIVE MULTIPATH INTERFERENCE

The effect of frequency selective multipath interference on the MCF is given by

$$\gamma_M = \gamma_{Mm}\gamma'_{Mm}\gamma_{Mn}\gamma'_{Mn} \quad . \tag{5.26}$$

The individual auto-coherence has the form

$$\gamma_{Mm} = |H_{0m}(\omega)| \quad . \tag{5.27}$$

where $H_{0m}(\omega)$ is the normalized transfer function of the channel in the absence of random fluctuations. The effect of $\gamma_{Mn}(\omega)$ on the total coherence is best determined by assuming K rays which arrive with equal time spacings and equal amplitudes. Following [3], the rays arrive over an interval of time T_S which is the time spread of the

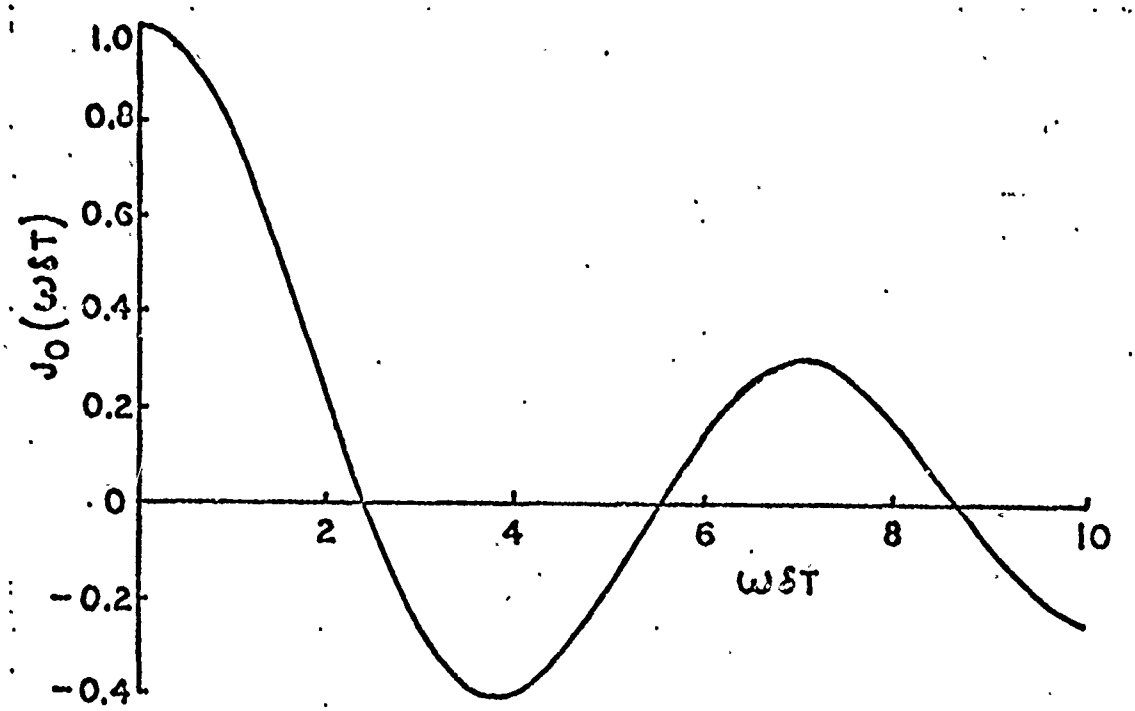

Fig. 5.11 Coherence due to internal tides.

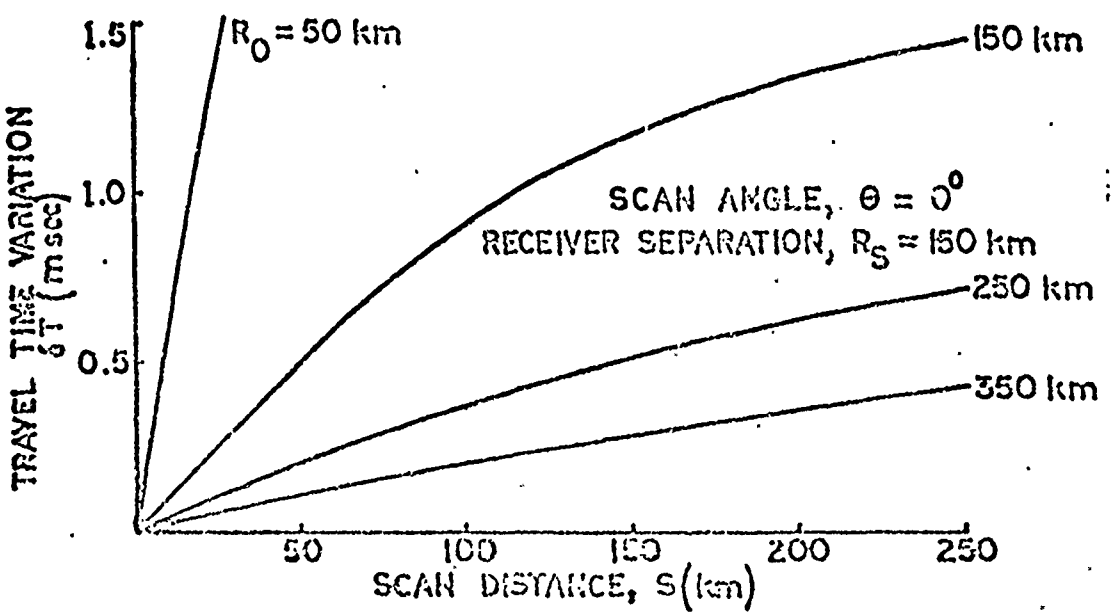

Fig. 5.12 Travel time fluctuation due to 4m amplitude internal tide.

channel, and T_0 is the bulk time delay of the channel as depicted in Fig. 5.13. The auto-coherence $\gamma_{Mm}(\omega)$ is easily found to be

$$\gamma_{Mm}(\omega) = \left| \frac{\sin(\omega T_S/2)}{K\sin(\omega T_S/2K)} \right| \quad . \tag{5.28}$$

The periodic lobe structure of this function determines the actual coherent frequencies, i.e., the frequencies of the primary maxima of the structure where

$$\omega_n T_S = 2n\pi K \ ,$$

$$f_n = \frac{nK}{T_S} \quad , \ n = 1, 2, \ldots \quad . \tag{5.29}$$

As the time spread of the channel increases for a given number of rays, there is an increasing number of coherent frequencies in a given bandwidth. This is the case for increasing source range. Also for a constant value of T_S, the spacing between coherent frequencies increases as K increases, as would occur upon entering a convergence zone. Also, if the time spread is proportional to the number of rays, the location of coherent frequencies does not change.

The coherence bandwidth centered on f_n is determined by

$$\Delta f = \frac{1}{T_S} \quad . \tag{5.30}$$

For long range propagation, T_S is on the order of seconds, so that

Δf is generally less than 1 Hz. Although exact only for ray arrivals which are equally spaced on the time axis, (5.29) and (5.30) are reasonable order of magnitude estimates for arbitrary multipath fields, given K and T_S (see footnote to (4.1)).

The effect of scanning is to square the auto-coherence factor for each channel so that

$$\gamma_{Mm}\gamma'_{Mm} = |H_{Om}(\omega)|^2 \quad . \tag{5.31}$$

The effect of squaring this factor is to narrow the peaks and widen the nulls of the interference pattern causing an effective decrease in the coherent bandwidth to

$$\Delta f = \frac{1}{2T_S} \quad . \tag{5.32}$$

However there is no effect exactly at the peaks of the pattern, and coherent frequencies will remain the same.

The total coherence is

$$\gamma_M = |H_{Om}(\omega)|^2 |H_{On}(\omega)|^2 \quad . \tag{5.33}$$

Since receivers spaced by large distances may receive entirely different multipath fields, the resulting coherent or partially coherent frequencies must be computed by multiplying the coherence factors for each receiver as indicated by (5.33). However if the sensors receive

identical multipath fields, the coherent frequencies remain the same, but the coherent bandwidth is reduced to

$$\Delta f = \frac{1}{4T_S} \quad . \tag{5.34}$$

An example of the variation of γ_M with frequency for identical multipath fields with K = 4 and T_S = 4 sec is illustrated in Fig. 5.14. For these parameters it is found that f_n = 1 Hz, 2 Hz, ..., and Δf = .0625 Hz.

5.3 THE COMPLETE MULTIPATH COHERENCE FUNCTION

The previous sections have presented the effects of the individual oceanographic fluctuations on their respective auto-coherence factors. It now remains to compare the various effects and to determine their combined effect on coherence. A summary is then given with respect to the application of these results to the computation of coherence.

5.3.1 COMBINED EFFECTS ON COHERENCE

In Section 4.3.2 the MCF was factored into an envelope due to travel time fluctuations and a coherence term due to frequency selective multipath interference which was written as

$$\gamma_{Smn} = (\gamma_{W,S}\gamma_T)\gamma_M \quad . \tag{4.75}$$

Since the first factors, due to random travel time fluctuations alone, decrease monotonically with frequency, it is appropriate that

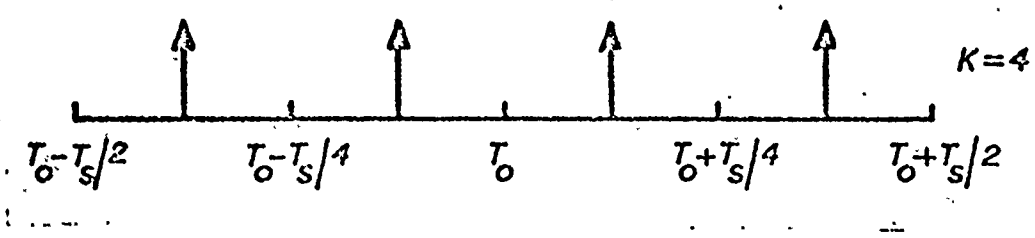

Fig. 5.13 Temporal multipath configuration for 4 ray arrivals.

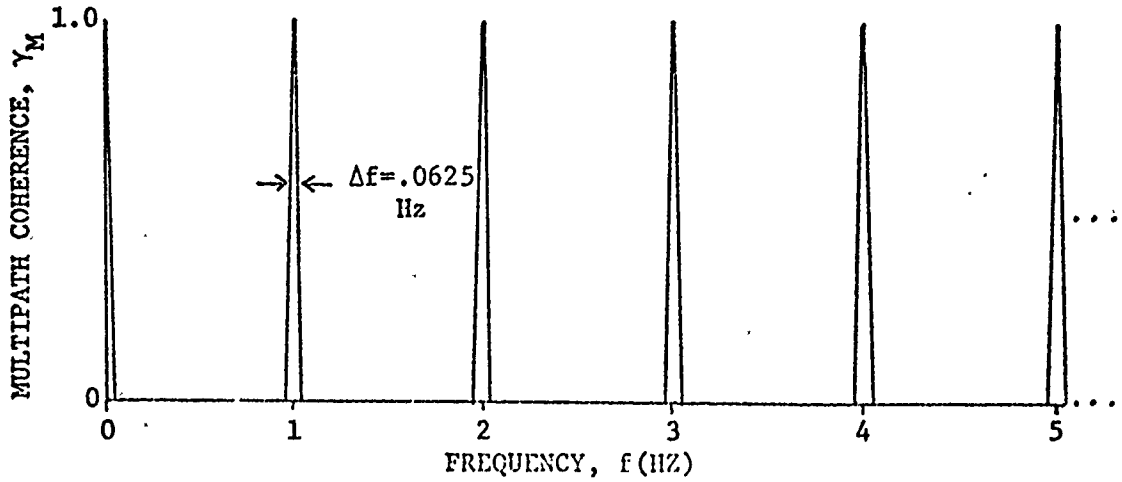

Fig. 5.14 Auto-coherence due to frequency selective multipath interference.

they be considered separately. The factor γ_M containing the frequency selective effects on coherence gives the coherent frequencies for which $\gamma_M = 1$.

The four components of the factor $\gamma_{W,S}$ all have the same functional form written as

$$\gamma(c) = \left[\frac{Kc^2}{1+(K-1)c^2}\right]^{\frac{1}{2}} , \tag{5.35}$$

and is shown in Fig. 5.15 for various values of K.

There is a subtle dependence on the ray parameter K (equal to the number of rays when they have equal amplitudes). Since this form was obtained from the envelope approximation in Section 4.3.2, each corresponding auto-coherence has a companion factor due to frequency selective multipath interference. Consider a coherent frequency of this factor obtained from the equal time spacing formulation, say f_n, and keep it constant while increasing K so that the corresponding factor of γ_M equals unity. Since K satisfies

$$K = \frac{f_n T_S}{n} , \tag{5.36}$$

this can be accomplished by allowing K to increase by increasing T_S. From (5.35) it can be seen that the auto-coherence then increases as K increases. The explanation for this is that coherence is primarily determined by the variations of the resultant phase of a single frequency component of each multipath signal. For a given

phase variation in the individual rays; as the number of independent rays increases, the variation in the resultant phase decreases. This phenomenon has actually been observed in convergence zones, i.e., where many ray paths converge in a focal zone [4].

The above effect must be carefully considered in analyzing the effects of spatial variations due to multipath interference. Although $\gamma'_{W,S}$ will increase with K when the other parameters are held constant, the ray spread σ may also increase due to the increase in the number of rays, and this will cause a decrease in $\gamma'_{W,S}$. The relationship between K and σ should therefore be considered in computations of $\gamma'_{W,S}$.

For the purpose of comparing the various effects on coherence, the simplified geometry of Fig. 5.10 will be used. Each auto-coherence term in (5.1) due to random travel time fluctuations was computed as a function of scan distance for $\theta = 0$ (perpendicular to R_0) and $\theta = \pm 90°$ (parallel to R_0), which are the approximate directions of extrema of the variations due to internal tides and spatial multipath interference. The ranges used are $R_0 = 250$ km and $R_S = 150$ km, the multipath parameters are $K = 16$ and $\sigma = 2°$, and the acoustic frequency is $f = 50$ Hz. Figs. 5.16-5.18 show the results for scan distances up to 50 km.

Fig. 5.17 illustrates the results for $\theta = 0$, which is the direction of the maximum effect of internal tides, and the approximate minimum of spatial fluctuations. The solid lines are the approximate region of validity of the assumption of independence between scan

channel and beacon channel. The dashed lines are extrapolated to give the proper coherence of unity at S = 0.

The highest coherence factor is γ_{Tmn} which remains at unity throughout the entire scan distance. It was shown that the effect of internal tides decreases with increasing range R_0, while all other effects increase. The conclusion is that internal tides have a negligible effect on coherence for long range propagation and for scan distances of this magnitude, and henceforth they may be ignored. This result removes any restrictions on the system configuration or its orientation with respect to the direction of internal tide propagation as in Section 5.2.3. Furthermore it was shown in Section 5.2.3 that internal tides have no effect on coherence phase.

Next in value are the auto-coherences due to internal waves in the beacon channels, which are equal due to system geometry and do not vary with scan distance.

The auto-coherences $\gamma'_{W,Sm}$ and $\gamma'_{W,Sn}$ due to the combined effect of internal waves and spatial multipath interference in the scan channels have the largest effect on coherence. However $\theta = 0°$ is the direction of the approximate minimum effect of the spatial variations, due to smaller changes in range, so that total coherence should be higher in this direction. The difference in the values of $\gamma'_{W,Sm}$ and $\gamma'_{W,Sn}$ is due to differences in scanning ranges. The composite MCF, γ_{Smn} is largest in the direction $\theta \approx 0°$ so that this is the direction of largest scan distance for a constant coherence.

Fig. 5.16 demonstrates coherence for $\theta = +90°$. The coherence factors γ_{Tmn}, γ_{Wm} and γ_{Wn} are the same as in Fig. 5.17. The increase in range for a given scan distance is the greatest in this direction. The effects of both the spatial variations and internal waves therefore are greater than in any other direction and the auto-coherences $\gamma'_{W,Sm}$ and $\gamma'_{W,Sn}$ (equal by symmetry) attain their absolute minimum values. The MCF γ_{Smn} is minimum in the direction $\theta = +90°$ and scanning ability is consequently the most limited.

Fig. 5.18 shows the effect of scanning in the direction $\theta = -90°$. The effect of spatial variations is approximately the same as $\theta = +90°$ for a given S, but since range from the receivers to the scan location is decreasing, the effect of internal waves is somewhat less than $\theta = +90°$. This accounts for the slightly higher values of $\gamma_{W,Sm}$ and $\gamma_{W,Sn}$ causing a slight increase in the MCF, γ_{Smn}. However for scan distances of the magnitude considered here, the difference in the MCF between $\theta = +90°$ and $\theta = -90°$ is minimal and scanning ability is approximately the same in these directions.

The average signal phase for each receiver channel varies as a function of scan distance according to the change in source range. Negative values of phase correspond to increases in source-receiver range relative to the beacon, and positive values indicate decreases in range. The primary component of the phase is the linear variation k_0x. It can be seen from (5.6) that for large values of $k_0|x|\sigma^2$, the magnitude of the phase is approximately $|\phi_S| = k_0|x| - \frac{\pi}{4}$. The decrease in $\mathrm{Re}\gamma_{Smn}$ when scanning with the plane wave phase k_0x rather than ϕ_S is as large as $1-\cos\frac{\pi}{4} = .293$.

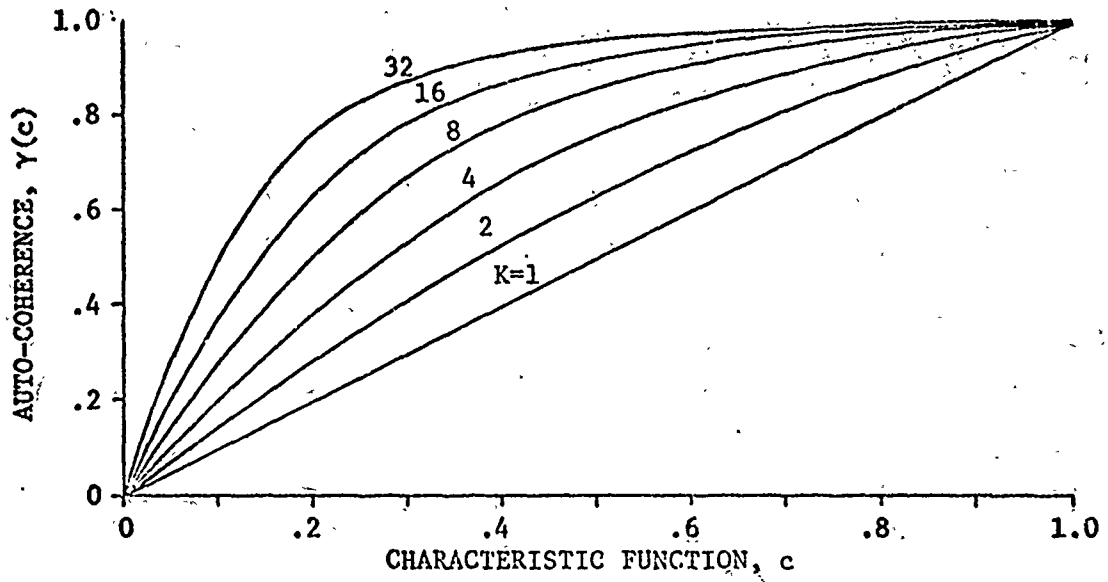

Fig. 5.15 General form of auto-coherence.

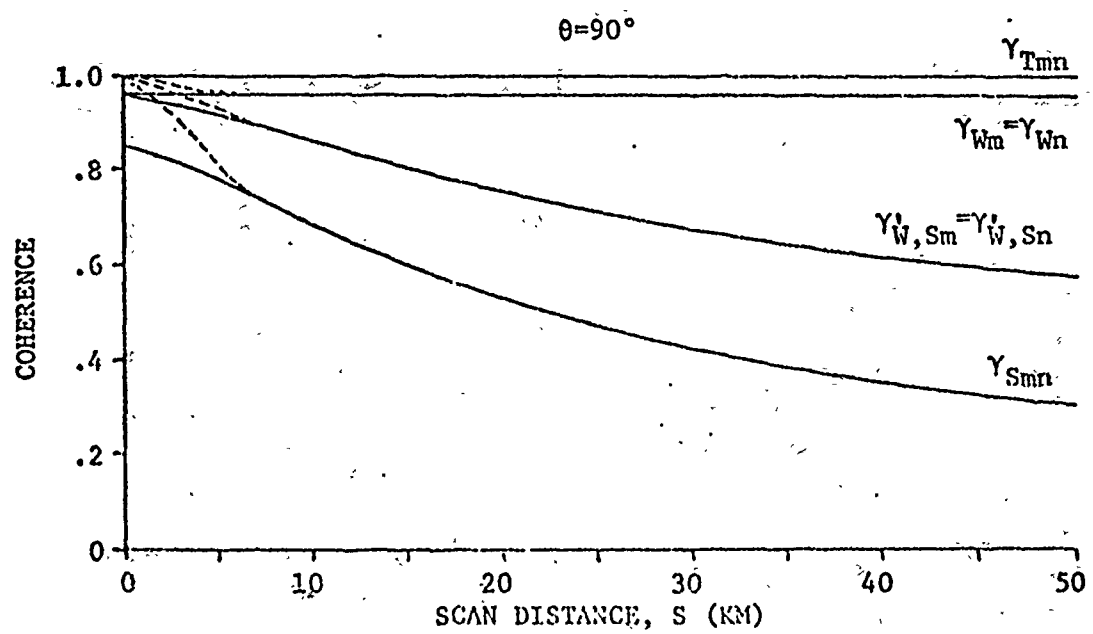

Fig. 5.16 Comparison of auto-coherences--θ=+90°.

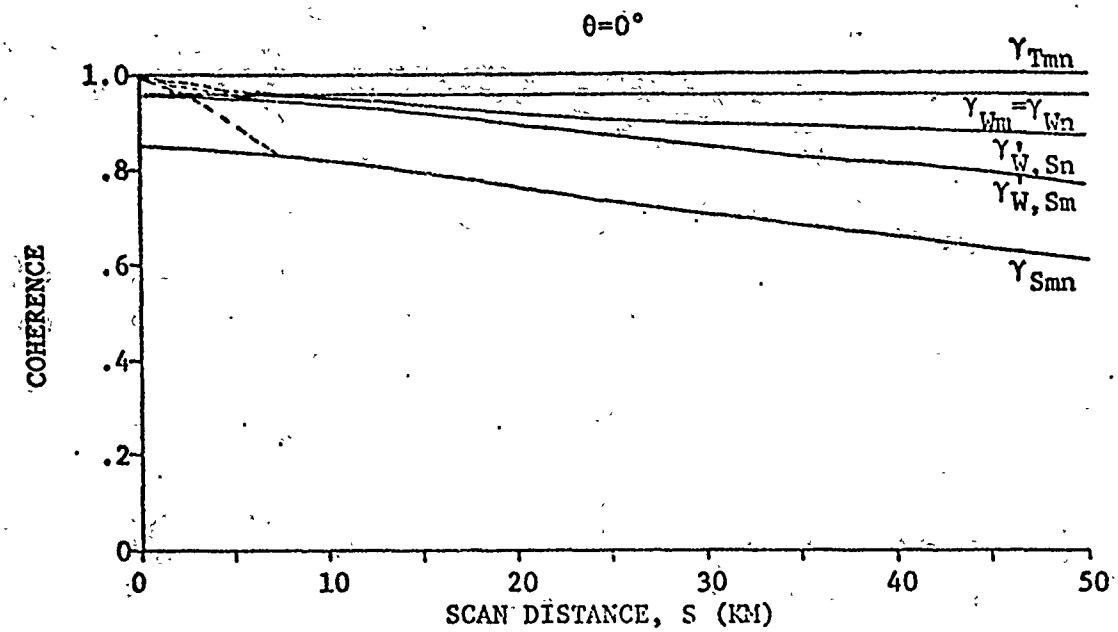

Fig. 5.17 Comparison of auto-coherences--θ=0°.

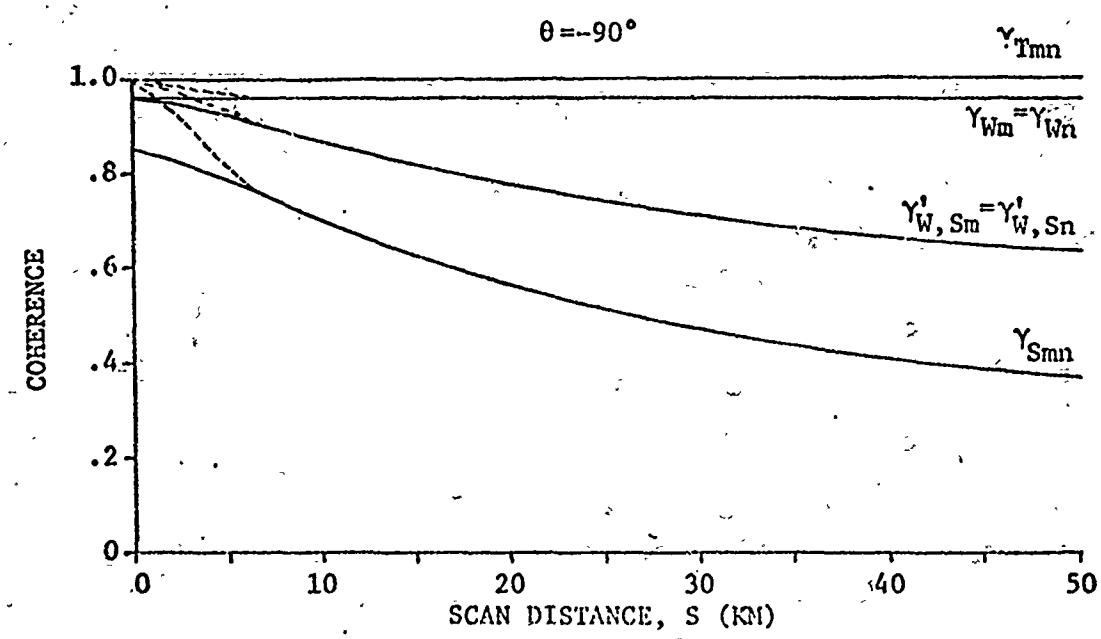

Fig. 5.18 Comparison of auto-coherences--θ=-90°.

5.3.2 COMPUTATION OF THE COHERENCE FUNCTION

The purpose of this section is to summarize the procedure for computation of the MCF. It has been emphasized that the MCF can be computed for all receiver pairs by the computation of only the auto-coherence for each receiver. The following outline gives the procedure for computation of receiver auto-coherence, and the MCF for each receiver pair is computed by multiplying their auto-coherences.

Procedure

1. For a given sound speed profile, beacon depth, receiver depth, range R to beacon, and frequency f, compute the number of ray arrivals K', relative pressure amplitudes, A_k, travel times, T_{k0}, and arrival angles, θ_k (usually from a ray tracing program).

2. Compute the ray parameter

$$K = \left(\sum_{k=1}^{K'} A_k\right)^2 \Bigg/ \left(\sum_{k=1}^{K'} A_k^2\right) \tag{5.37}$$

and estimate the rms ray arrival angle from

$$\sigma = \left[\frac{1}{K'} \sum_{k=1}^{K'} \theta_k^{\,2}\right]^{\frac{1}{2}} . \tag{5.38}$$

3. For given scan location determine new range to receiver, R', and compute x = R'-R.

4. Determine $\Phi = \Phi(R)$ and $\Phi' = \Phi(R')$ from Fig. 5.3 or from (3.9) and (3.10) for characteristic ray type in channel.

Find $c_W = c_W(f\Phi)$ and $c_W' = c_W(f\Phi')$ from Fig. 5.2 or from (5.3).

5. Determine $|c_S| = |c_S(x/\lambda,\sigma)|$ from Fig. 5.6 or from (5.6).

6. From Fig. 5.15 or from (5.35) compute $\gamma(c_W)$ and $\gamma(c_W'|c_S|)$ for the value of K found in (5.37).

7. Determine the phase $\phi_S = \phi_S(x/\lambda,\sigma)$ from Fig. 5.7 or from (5.6).

8. If f is a coherent frequency ($\gamma_M = 1$), the complete auto-coherence is

$$\gamma(c_W)\gamma(c_W'|c_S|)e^{j\phi_S} .$$

Coherent frequencies are determined from

$$|H_0(\omega)| = \left|\sum_{k=1}^{K'} A_k e^{-j\omega T_{k0}}\right| \Big/ \sum_{k=1}^{K'} A_k = 1. \qquad (5.39)$$

The above procedure is performed for each receiver-channel. In terms of these auto-coherences for N receivers, γ_m, m = 1,2, ... N, the MCF for each pair of receivers is

$$\gamma_{Smn} = \gamma_m \gamma_n^*, \; m, n = 1,2, \ldots. N, \; m \neq n. \qquad (5.40)$$

5.4 SUMMARY

This chapter has presented the MCF in terms of real oceanographic fluctuations, and has compared the effect of each type of fluctuation.

The condition for which the scan channels are independent for

internal wave fluctuations was shown to depend upon scan distance, S, and scan time, τ. For $\tau = 0$, $\rho(S,\tau) = .5$ for $S = 6.4$ km, so by restricting the analysis to $S > 6.4$ km the channels can be considered to be independent, and the time dependence can also be ignored. The coherence due to internal wave fluctuations was shown to decrease with both range and frequency and to increase with the number of rays.

Spatial fluctuations due to multipath interference were shown to have the most severe effect on scanning, and their effect is combined with that of internal waves in the scan channel. Their effect on coherence depends upon a difference in range to the receiver between the beacon and the scan location. This implies that the maximum scanning ability is generally perpendicular to the direction from receiver to beacon. Scanning is much more limited in the parallel direction. The coherence decreases with increasing angular ray spread, frequency, and scan distance; it increases with an increasing number of rays within the same spread of arrival angles. The total average signal phase to the scan location is determined by the spatial fluctuations and each receiver uses this as an average phase shift for scanning.

The coherence due to internal tides decreases with increasing scan distance and frequency, but increases with range. However, the effect of internal tides is negligible compared to the other effects for the scan distances, ranges, and frequencies of interest here. Internal tides also have no effect on average signal phase.

The above effects form a monotonically decreasing coherence envelope of the effects of frequency selective multipath interference. This latter effect depends upon the constructive and destructive interference of the rays as frequency varies. It can be stated in general that the spacing between coherent frequencies decreases with increasing time spread and decreasing number of rays, and that the coherence bandwidth (about a coherent frequency) decreases with increasing time spread. However, the exact interference pattern must be computed from the ray amplitudes and travel times. The dependence of the auto-coherence on γ_M is determined by the location of the coherent frequencies. Rather than compute γ_M for an arbitrary frequency (since γ_M may be low due to destructive interference), the approach taken has been to assume location at a coherent frequency so that $\gamma_M = 1$. Since there generally will be small spacings between coherent frequencies, the preferred approach is to determine coherent frequencies from the exact multipath summation, and to assume that the signal bandwidth is large enough to include at least one coherent frequency. This frequency is then used for computation of the coherence envelope. This subject will be discussed further in Chapter 6.

The complete auto-coherence can be computed simply from the equations and figures given in this chapter. With the aid of a ray tracing computer program or other data, the procedure of Section 5.3.2 can be used to predict the MCF.

REFERENCES

[1] N. L. Weinberg, J. G. Clark, and R. P. Flanagan, "Internal Tidal Influence on Deep-Ocean Acoustic-Ray Propagation," J. Acoust. Soc. Am., Vol. 56, No. 2, August, 1974.

[2] C. N. K. Mooers, "Sound Speed Perturbations Due to Internal Tides," J. Acoust. Soc. Am., Vol. 53, p. 333(A), 1973.

[3] S. L. Adams and J. W. Doubek, "Frequency Coherence and Time Coherence in Random Multipath Channels," J. Acoust. Soc. Am., Vol.62, No. 2, August 1977.

[4] R. J. Urick and G. R. Lund, "Coherence of Convergence Zone Sound," J. Acoust. Soc. Am., Vol. 43, No. 4, 1968.

CHAPTER 6

APPLICATION TO A SUPERARRAY SYSTEM DESIGN

6.1 SYSTEM DESIGN APPROACH

Array processing was discussed in Chapter 2 and the VLA was compared with a conventional array. In particular, a VLA of conventional subarrays was discussed, and its advantages with respect to gain and beam pattern were emphasized. In Chapter 5 the final formulation of the MCF was presented in terms of known oceanographic fluctuations. The purpose of this chapter is to apply the results derived from the MCF to a VLA of subarrays.

Consider a system of N_V widely spaced conventional subarrays, each of which has N_S sensors and beamwidth $\Delta\theta_S$. A beacon is placed at B at the range R_0, and the beam of each subarray is scanned to this location as shown in Fig. 6.1(a). The beacon radiates a waveform which enables each receiver to measure the impulse response of the channel. With this information each receiver then focuses on the beacon as described in Section 4.3. The pattern of the system then changes from the independent patterns of the subarrays to the near field pattern of a VLA with a high resolution, coherent focus on the beacon as shown in Fig. 6.1(b). Any ambiguities in the VLA pattern are limited to the original area of intersection of the subarray beams.

At the beacon the coherence is unity for all subarray pairs, so

that the VLA gain attains its maximum value, $G_V = N_V$. The goal is to scan the superarray focus away from the beacon in search of an unknown signal source while maintaining an acceptable value of gain. First each subarray scans its beam to the location S as shown in Fig. 6.1(c). To focus the superarray at S, the phase shift determined from (5.6) is applied to the output of each subarray and the outputs are summed as depicted in Fig. 6.1(d). The VLA gain at S is determined by the degradation of coherence due to the random fluctuations, as predicted by the MCF. The superarray continues to scan away from the beacon until pairwise coherence decreases to such a value that there is no appreciable gain.

Since it may be desirable to cover a larger area, it is necessary to place other beacons to insure continuous coverage. Each beacon has its own area of coverage, and the beacon locations are determined by the size of these areas so that coverage is continuous. The procedure outlined above is then repeated for each beacon.

It is, of course, necessary that the required density of beacons is practical for the given system specifications. One of the primary purposes of this work is to provide a procedure for determining the feasibility of a VLA system design for given acoustic parameters and system geometry, within the limitations of the oceanographic fluctuations considered here. It should be remembered that geographic anomalies have not been included as sources of fluctuations and will be a source of further performance degradation.

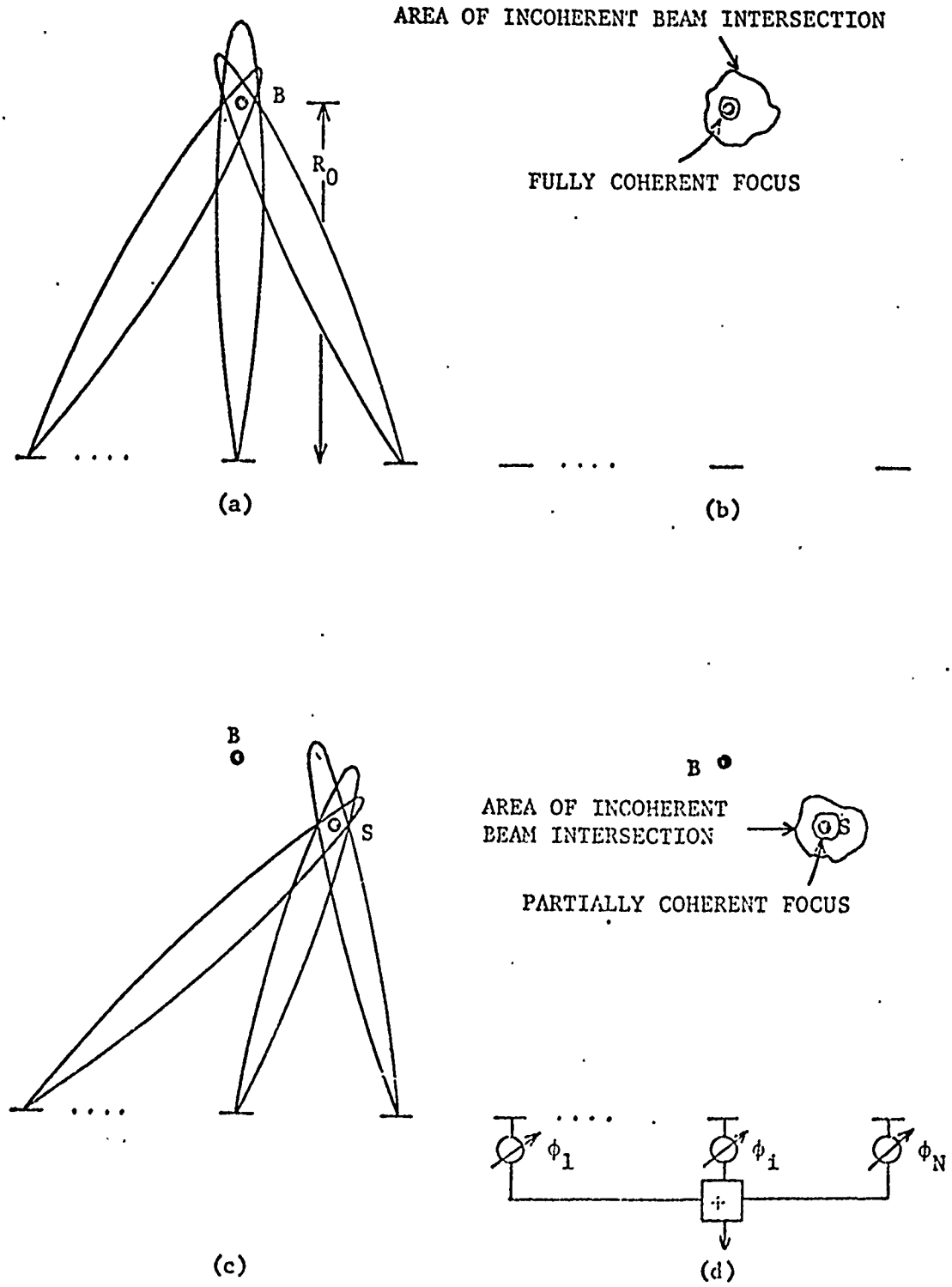

Fig. 6.1 VLA beamforming and scanning.

6.2 SYSTEM DESIGN PROCEDURE

The primary considerations in the design of a VLA of subarrays are the performance specifications of detection ability and localization ability. Detection ability is measured by the system gain and is determined by the MCF. Localization ability is determined primarily by the system configuration.

The primary system requirements related to the gain are the number and density of beacons required for coverage of a desired area, given the system configuration and the acoustic parameters for the ocean area of interest. Fig. 6.2 gives the value of the MCF required to achieve certain values of VLA gain, G_V, as a function of the number of subarrays, N_V, from (2.63). When the required value of γ_S has been determined, the area of coverage with one beacon, A_B, can be found from the contour of constant coherence using the results of Chapter 5. It was shown that the directions of extrema of scanning ability are approximately parallel and perpendicular to the VLA baseline. By computing these coherence distances, S_x and S_y, respectively, for the outermost pair of receivers, the area A_B can be approximated as a rectangle,

$$A_B = S_x S_y \quad . \tag{6.1}$$

Within this area the gain will exceed the minimum required value since the outermost pair of receivers has the lowest coherence. Assume that each beacon in the area of interest has approximately the same coherence contour with the same area A_B. Then the required spacing between

beacons is S_x in the direction parallel to the VLA baseline, and S_y in the perpendicular direction. For a desired total area of coverage, A_T, the required number of beacons is

$$N_B = \frac{A_T}{A_B} \quad . \tag{6.2}$$

Another design consideration is the required refocusing time for each beacon. In Section 3.1 the scanning time was limited to $\tau \ll T_0$, where T_0 is a characteristic time of the large scale environmental fluctuations, which is on the order of days. In addition there was shown to be no dependence on scan time due to internal waves and tides. For internal waves, the scan time determines the minimum distance for which the channels are independent; thus, for scan distances larger than this, there is no dependence on τ. Since internal tides were shown to have a negligible effect on coherence, their dependence on scan time can be ignored. The limiting factor on scanning time therefore is the characteristic time T_0.

Assume that an upper limit, τ_S, is placed on scan time so that $\tau_S \ll T_0$. A value of τ_S = 12 hr may be reasonable, but due to the limited knowledge of large scale fluctuations it should be determined by experiment. If a beacon has a lifetime T_B, and if $T_B > \tau_S$, then each subarray must refo us on the beacon at intervals of τ_S. However, if $T_B < \tau_S$ it will be necessary to replace each beacon at intervals of T_B. This is an important consideration for system design implementation and requires further study.

The localization ability of the VLA is determined primarily by the subarray beamwidths and the range to the source. If each subarray has a length L_S, then the beamwidth is

$$\Delta\theta_S = \frac{\lambda}{L_S} \quad . \tag{6.3}$$

When the separation between subarrays is large the area of intersection of the beams at a range R is then approximately

$$\begin{aligned} \sigma_S &= (R\Delta\theta_S)^2 \\ &= \lambda^2 \left(\frac{R}{L_S}\right)^2 \quad . \end{aligned} \tag{6.4}$$

The desired resolution determines limits on the relationships between frequency, range, and subarray length. The number of resolution cells per beacon is

$$N_R = \frac{A_B}{\sigma_S} \quad . \tag{6.5}$$

A requirement for feasibility is that $\sigma_S << A_B$ so that N_R is large.

The resolution cell of the VLA focus can be determined from (2.55) and (2.57) as

$$\begin{aligned} \sigma_V &= \Delta\rho_B \Delta S_B \\ &= \lambda^2 \left(\frac{R}{L_V}\right)^3 \end{aligned} \tag{6.6}$$

where L_V is the VLA length. If the subarray beamwidths are small enough it may be possible to have only the main focus of the VLA within σ_S, with all ambiguities outside.* The increase in resolution would be

$$\frac{\sigma_S}{\sigma_V} = \frac{RL_S^2}{L_V^3} . \tag{6.7}$$

For $R \sim L_V$ and $L_V = 100\ L_S$, $\sigma_S/\sigma_V = 10^4$, indicating that this is a subject well worth further study.

As a simple design example consider the VLA configuration shown in Fig. 6.3. There are $N_V = 7$ linear subarrays distributed along a baseline of $L_V = 150$ km. Each subarray has $N_S = 40$ sensors spaced one half wavelength apart at f = 50 Hz ($\lambda = 30$ m), so the subarray length is $L_S = 585$ m. If the noise is incoherent between individual sensors in a subarray, then the subarray gain is $G_S = 16$ dB from (2.62).

It is desired to form a VLA which will increase the system gain by a minimum of $G_V = 6$ dB at f = 50 Hz. The desired area of coverage is $A_T = 75000\ km^2$ centered about an initial beacon range of $R_0 = 250$ km as shown in Fig. 6.4. From Fig. 6.2 the required value of the MCF is found to be $\gamma_S = 0.5$.

Assume that the multipath parameters are K = 16 and $\sigma = 2°$. To determine the scan distances S_x and S_y, the outer pair of receivers is used for the computation since they will have the lowest coherence.

---

* Based on calculations using random array theory.

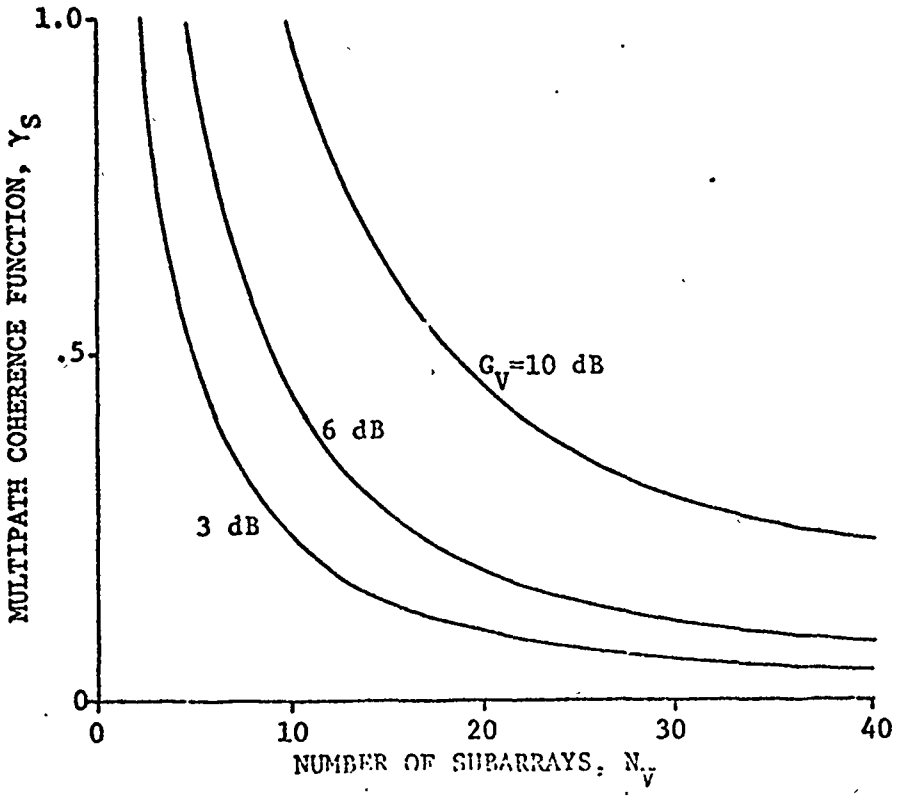

Fig. 6.2 Required value of MCF for specified VLA gain.

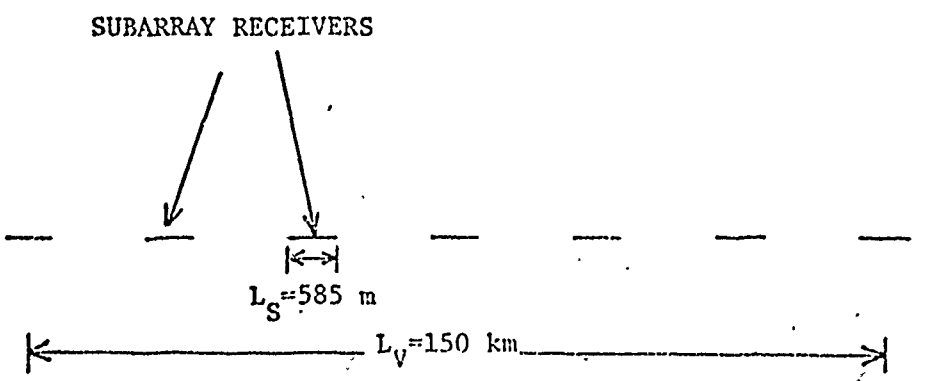

Fig. 6.3 VLA configuration for design example.

This insures that the gain will be greater than 6 dB throughout the scan area, A_B. At and near the beacon the gain will be $10\log_{10}7 = 8.5$ dB. Thus the average gain within the $\gamma = 0.5$ contour is in excess of 7 dB and the maximum gain is 8.5 dB. Using the MCF computation procedure of Section 5.3.2, it is found that $S_x = 165$ km and $S_y = 50$ km, giving a total coverage area of $A_B = 8250$ km^2 with a beacon at R_0. Assuming that the area of coverage for each beacon is the same, the total number of beacons required is $N_B = 9$, from (6.2). The beacon configuration and coverage areas are illustrated in Fig. 6.5.

The subarray beamwidth is found to be $\Delta\theta_S = .051$ rad. At $R_0 = 250$ km the resolution cell from (6.4) therefore is $\sigma_S = 164$ km^2, and the number of resolution cells per beacon is $N_R = 50$, from (6.5). From (6.6) the resolution size of the VLA focus is found to be $\sigma_V = 4000$ m^2. The beacon coverage area and resolution cell, σ_S, is illustrated in Fig. 6.6.

In summary, this VLA will increase system gain by more than 6 dB, covering an area of 75000 km^2 with 9 beacons spaced by 50 km in the perpendicular direction and 165 km in the parallel direction. The size of the resolution cell is 164 km^2 for a total of 50 resolution cells per beacon and 450 resolution cells over the entire coverage area.

6.3 CONSIDERATIONS IN SYSTEM IMPLEMENTATION

This work has been primarily concerned with the most important VLA system design consideration, that of signal coherence between widely spaced receivers. The derived multipath coherence function provides the

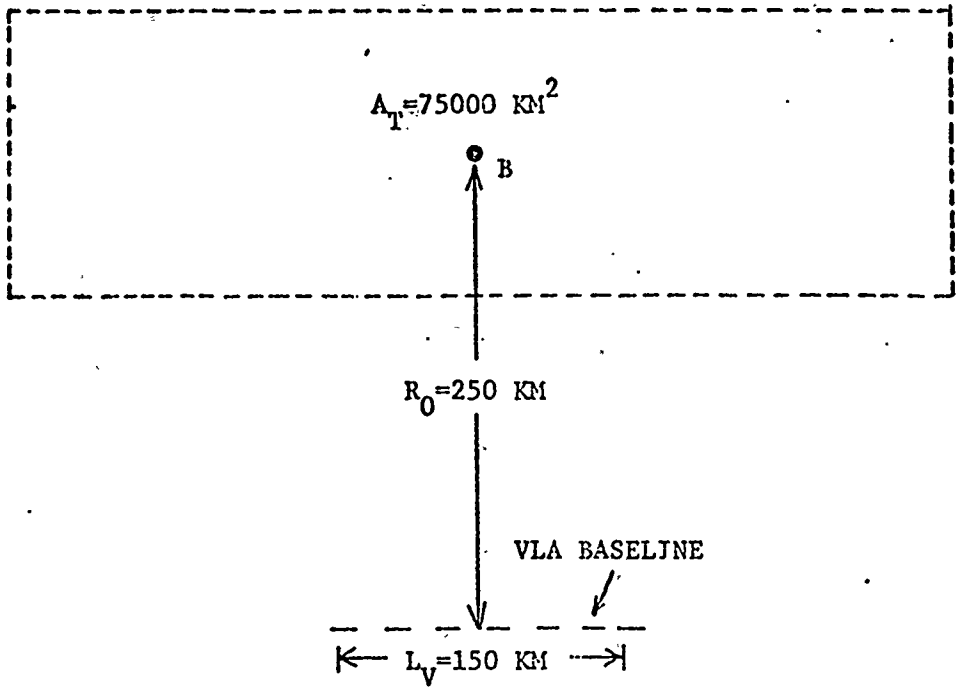

Fig. 6.4 VLA coverage area for design example.

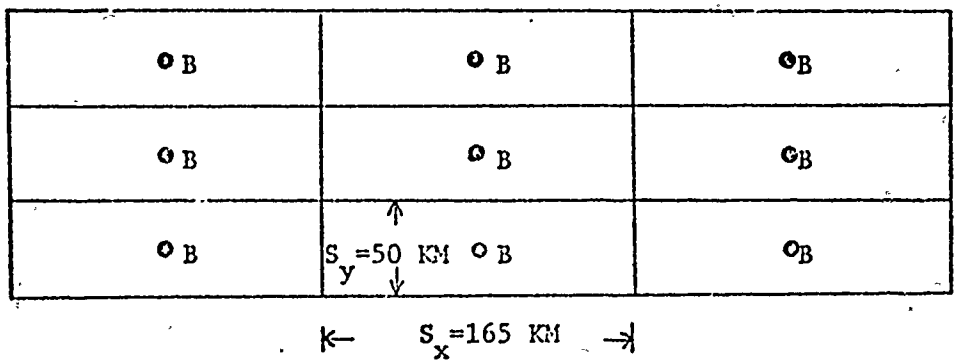

Fig. 6.5 Beacon configuration and coverage areas for design example.

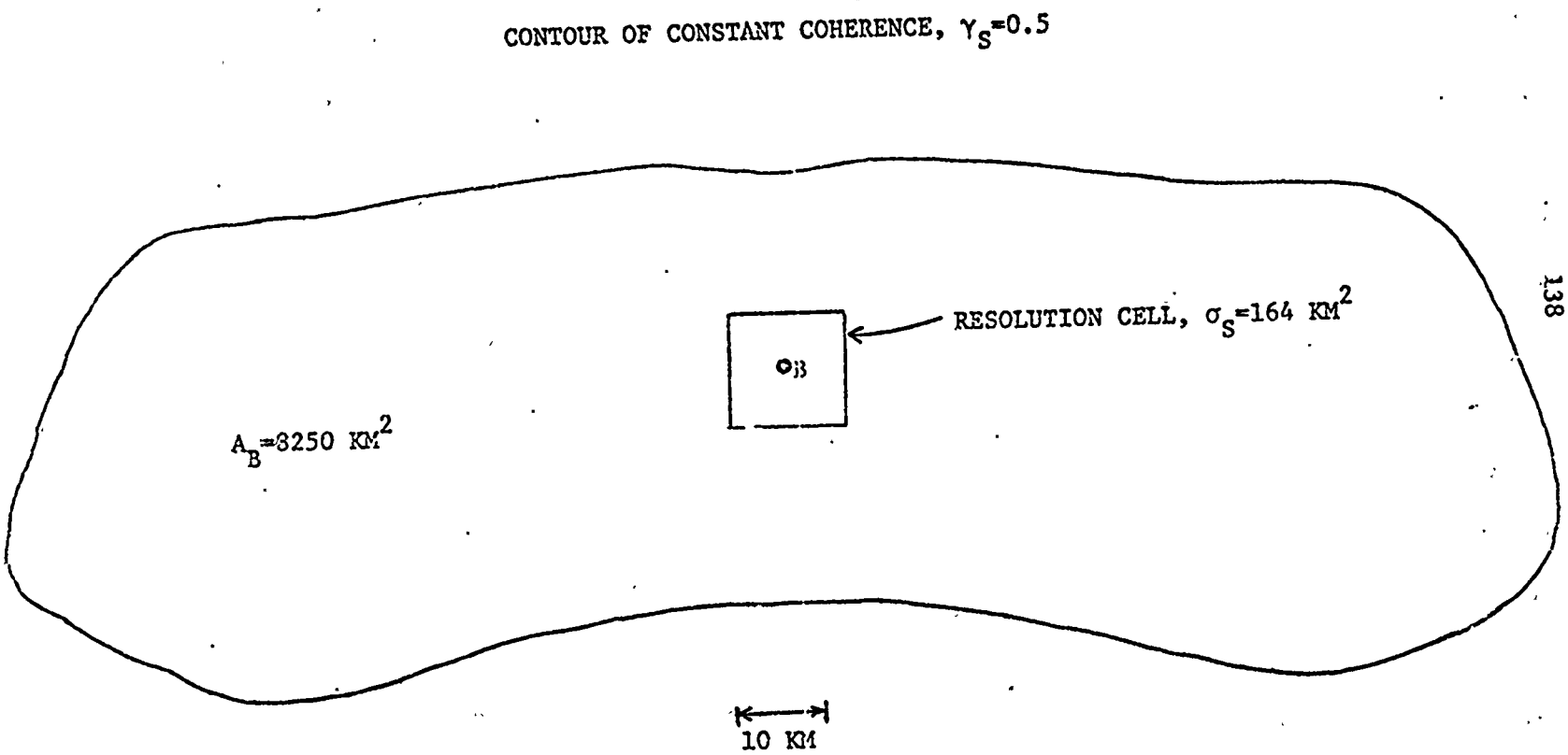

Fig. 6.6 Exact beacon coverage area and resolution cell for design example.

beacon spacings required to maintain a desired coherence and VLA gain. There are other considerations for a complete system design implementation which will determine system feasibility. A detailed discussion of these factors is beyond the scope of this work. However, this section enumerates the most important of them, with practical suggestions as a basis for further study.

Beacon placement

For a practical VLA system design the method of placement of beacons is an important consideration. Permanent beacon installations would be expensive with a lack of flexibility in location and a high probability of discovery. However, temporary beacons with a limited lifetime would avoid these problems. The controlling factors in determining the feasibility of temporary beacon installations would be the method of placement and the beacon lifetime, T_B. Since the use of temporary beacons implies a beacon replacement if the desired scan time about a beacon, τ_S, is greater than its lifetime, T_B, the method of beacon placement should be expedient. One method that warrants consideration is dropping beacons from an aircraft. The technology in this area is well developed and the method offers the obvious advantages of flexibility in beacon location, accuracy of location by navigational methods, and ease of immediate beacon replacement.

Another possibility is the use of beacons of opportunity such as surface shipping [1]. The advantages are availability at no expense, and concealment. There will be difficulties in phase measurement due to spatial variations, and a lack of reliability and flexibility in location.

However, due to the abundance of shipping traffic in areas where beacon placement would be difficult or impossible, it should be explored as a possibility.

Beacon waveforms

The most important requirement for a beacon waveform is that it enables accurate measurement of the channel impulse response in the presence of noise. The waveforms of all beacons must be known at all receiver sites and they must be distinguishable. In addition, the beacon signals should be undetectable to all others.

Measurements of the impulse response of underwater channels and acoustic phase detection have been investigated theoretically [2], [3], [4] and experimentally [5] - [10]. It appears that pseudo-noise (PN) sequences [11] satisfy the requirements stated above and should be considered in a superarray system design.

Some of the characteristics which the PN code should possess will be dictated by the channel characteristics. The time length of the code must be greater than the time spread of the channel to insure unambiguous measurement of the multipath arrivals. The sequences must be distinguishable between beacons, thus a different code should be used for each beacon. Each pair of sequences should have good cross-correlation properties so that only the desired beacon waveform is detected. Another consideration is the time required for each receiver to synchronize with the beacon PN sequence.

Source localization

The VLA localization accuracy is primarily determined by the accuracy of location of the beacons and subarrays, and by the number of ambiguous VLA focal areas within the area of intersection of the subarray beams. If there are VLA ambiguities within σ_S, then σ_S is the minimum resolution cell. The linear dimension of σ_S is typically on the order of tens of kilometers. The beacon locations and the locations and orientations of the subarrays will be known to at least navigational accuracy, whose error is much less than this value. Therefore, it can be assumed that there is little effect on the localization accuracy determined by the resolution cell σ_S.

It was shown in the previous section that if there are no VLA ambiguities within σ_S, then the size of the resolution cell will be decreased to σ_V, which is on the order of λ^2. However, the location of σ_V is highly sensitive to the location accuracy of the system components. Even if the subarray and beacon locations could be known within fractions of a wavelength, the location of σ_V would still be in error due to the randomness of the medium. However, due to the potential increase by orders of magnitude in localization ability, this subject should receive further study.

Source motion

An application of a VLA system to the detection of moving sources presents additional complications. In Section 2.4 it was shown that travel time fluctuations must vary slowly compared to signal duration time, so that the channel transfer functions will be time invariant.

However, this may not be valid for a moving source, because the spatial fluctuations due to multipath interference will vary with time. The seriousness of this effect will depend upon integration time and source velocity. A related problem is the ability to track the source by maintaining the VLA focus on its changing location. The source motion also causes a complicated Doppler effect due to a different frequency shift in each ray. However, this effect can be minimized by properly shifting the center frequency of the receiver filters.

Post-detection focusing and tracking

After initial detection of a signal source with the VLA, it may be possible to further increase the signal to noise ratio by enhancing the partially coherent VLA focus. Each subarray would measure the relative signal phase or coherence of the signal waveforms. Using this information a refocused, high resolution spot is placed on the source by self-cohering or adaptive beamforming techniques. The focus is then scanned in the vicinity of the source for the purpose of tracking.

Geographic fluctuations

In Chapter 3 geographic fluctuations such as currents and eddies were discussed. The theoretical developments in this work were limited to those which are not geographic in nature. However, due to the prevalence of geographic anomalies, they must be considered in a VLA system design.

Due to the variability and unpredictability of some of these fluctuations it is difficult to determine their effect on coherence. The

best approach would be to evaluate the effect of geographic fluctuations by experiment in the ocean area of interest for a VLA system. The geographic areas of prevalence of some of these fluctuations might be considered in the geographic location of a VLA.

Determination of actual phase for VLA scanning

The development of the MCF in Chapter 4 theoretically predicted the average phase shift required for each subarray in order to scan the VLA with partial coherence. However, this result depends on an accurate knowledge of the multipath structure which may not be available. It is important to know the correct average phase for each individual situation. If the average phase shift is inaccurate then another random variable is introduced which will further degrade coherence.

This suggests the desirability of experimentally measuring phase as a function of scan distance. This measurement will show a phase trend [12] with fluctuations about the trend due to the variations considered in this work. This procedure of surveying the scan area is performed only once, and the phase trend measured is then used as the average phase shift for future VLA scanning. The true phase will vary causing a degradation of coherence, but the trend should remain constant.

Coherent noise sources

In Section 2.3 noise was limited to random broadband ambient noise which is incoherent between VLA subarrays. However there is a possibility of discrete shipping interference which may be coherent between subarrays. Experimental [13] and theoretical [14] results can be used

to predict this shipping density for the North Atlantic. A method of near field adaptive nulling of coherent noise with a VLA of subarrays was developed in [14] based upon the concept of null steering [15].

Practical implementation of this technique would involve an initial localization of interfering shipping by airborne radar detection or other means, and a null tracking system in each subarray so that individual nulls in the subarray patterns can follow the shipping traffic. The near field pattern of the VLA can then be visualized as having "holes" which follow the ships as they move throughout the area.

Subarray location

Some additional system flexibility can be acquired if the subarrays can be placed in arbitrary locations. A possible VLA system might consist of several floating random arrays [16] which could be deployed by an aircraft in any desired locations*. Combined with the use of air dropped beacons, the VLA system would then have the advantage of complete mobility. The disadvantage would be a further degradation of system gain due to the larger spacings between sensors in a random floating array.

6.4 SUMMARY

This chapter has presented an application of the MCF to the design of a VLA of widely separated subarrays. The general system design

*This idea was suggested by Professor F. Haber, Moore School of Electrical Engineering, University of Pennsylvania.

approach was outlined. A procedure was then developed for determining beacon spacings required for a given VLA configuration to maintain a specified gain over a desired coverage area. VLA refocusing times were shown to be dependent on the large scale oceanographic fluctuations. Localization ability was discussed in terms of the subarray beamwidths and the size of the focal area of the VLA.

A design example was presented for some realistic system parameters. This example showed that coherent combination of 7 subarrays could increase system gain by an average of more than 7 dB over an area of 75000 km^2 with the use of only 9 beacons.

Finally, some important considerations in system implementation were discussed, and proposals were made for practical solutions. Specifically mentioned were the possibilities of beacon placement by aircraft, and PN sequences for beacon waveforms. The idea of floating subarrays also deployed from an aircraft was discussed as a method of making an entire VLA mobile.

REFERENCES

[1] T. L. Lim, "Beacons of Opportunity," Valley Forge Research Center QPR No. 22, Art. 3, August 1977.

[2] T. Kailath, "Measurements on Time-Variant Communication Channels," IRE Trans. Inform. Theory, Vol. IT-8, September 1962.

[3] P. A. Bello, "Measurement of Random Time-Variant Linear Channels," IEEE Trans. Inform. Theory, Vol. IT-15, July 1969.

[4] H. L. Van Trees, Detection, Estimation and Modulation Theory, Part III, Wiley, New York, 1971.

[5] R. L. Veenkant, "Investigation of the Propagation Stability of a Doubly Spread Underwater Acoustic Channel," IEEE Trans. Acoust. Sp. Sig. Proc., Vol. ASSP-25, No. 2, April 1977.

[6] J. C. Steinberg and T. G. Birdsall, "Underwater Sound Propagation in the Straits of Florida," J. Acoust. Soc. Am., Vol. 39, 301-315, 1966.

[7] J. C. Steinberg, J. G. Clark, H. A. DeFerrari, M. Kronengold, and K. Yacoub, "Fixed-System Studies of Underwater Acoustic Propagation," J. Acoust. Soc. Am., Vol. 52, No. 5 (Pt.2), 1972.

[8] H. A. DeFerrari, "Time-Varying Multipath Interference of Broad-Band Signals Over a 7-NM Range in the Florida Straits," J. Acoust. Soc. Am., Vol. 53, No. 1, 1973.

[9] T. G. Birdsall, G. E. J. Bold, and K. A. Winick, "The PANOIC77 Sequence Signal," PANOIC77 Report 013376-5-T, Part I, Cooley Electronics Laboratory, Michigan, March 1978.

[10] G. N. Cederquist, "The Use of Computer-Generated Pictures to Extract Information From Underwater Acoustic Transfer Function Data," Ph.D. Dissertation, University of Michigan, 1975.

[11] AGARD Lecture Series No. 58, "Spread Spectrum Communications," NATO, July 1973.

[12] J. G. Clark, R. P. Flanagan, and N. L. Weinberg, "Multipath Acoustic Propagation with a Moving Source in a Bounded Deep Ocean Channel," J. Acoust. Soc. Am., Vol. 60, No. 6, December 1976.

[13] I. Dyer, "Statistics of Distant Shipping Noise," J. Acoust. Soc. Am., Vol. 53, pp. 564-570, 1973.

[14] W. J. Graham, "A Large Underwater Aperture of Coherently Combined Subarrays," Valley Forge Research Center QPR No. 22, Art. 3, August 1977.

[15] D. E. N. Davies,"Independent Angular Steering of Each Zero of the Directional Pattern for a Linear Array," IEEE Trans. Antennas Propag., Vol. AP-15, March 1967.

[16] F. Haber, "Floating Acoustic Array," Valley Forge Research Center QPR No. 22, Art. 3, August 1977.

CHAPTER 7

SUMMARY AND RECOMMENDATIONS FOR FURTHER STUDY

7.1 SUMMARY OF RESULTS

In order to view the results of this work in the proper perspective, it is helpful to review the line of reasoning that led to their development. The motivation for this work was the idea of coherently combining widely spaced subarrays in a random multipath underwater medium. The purpose of forming this very large array is to increase the potential signal to noise ratio and the localization ability. The enhancement of detection ability is measured by the array gain, defined in terms of the signal coherences between all pairs of subarrays. The foremost problem, then, was to develop a solution for this coherence in terms of the environmental and acoustic characteristics of the ocean.

This led to the development of a new measure of coherence, called the multipath coherence function, defined in terms of ensemble averages of the random transfer functions of the multipath channels. Since the receivers are widely spaced the channels are stochastically independent. This important simplification demonstrated the existence of coherence without correlation between channels; it also enabled the MCF to be factored into separate auto-coherences, making the final solution mathematically feasible. Another important simplification was the

envelope approximation for the auto-coherence, which factored the effects of random fluctuations from those of frequency selective multipath interference. The MCF was then formulated as a function of source range and scanning distance, for general oceanographic fluctuations.

It then remained to specify the stochastic parameters of the MCF for real oceanographic fluctuations. This required original analyses of the effects of spatial variations due to multipath interference, and of internal tides, on coherence. The stochastic parameters of internal wave fluctuations were obtained from the literature. A comparison of these effects then showed that spatial variations were predominant in scanning, while internal tides were a negligible influence.

The remaining step was to apply these results to the initial objective of predicting VLA performance in terms of signal to noise gain for given system configurations. The system design approach was to use self-cohering techniques whereby the VLA initially focuses on a known beacon source in the near field, and then scans in the vicinity of the beacon in search of an unknown signal. Thus the quantities of interest were the number and spacing of beacons required to maintain a specified gain while scanning the VLA between beacons. A design example for some realistic parameters then showed the existence of significant coherence over large ocean areas. The conclusion is that a VLA design might be possible and practical.

In summary, there are three primary results from this research. The first is a general solution for signal coherence in uncorrelated multipath channels. The second is a specific application of this

multipath coherence function to the design of a VLA composed of widely spaced subarrays. Finally, numerical results showed that such a VLA design is feasible for certain system configurations and multipath characteristics.

7.2 ANALYSIS OF RESULTS

The following sections outline the important conclusions to be made from the results of this work, and an explanation of its limitations. The points considered are limited to the areas of the three primary results of this work stated in Section 7.1. Further information and detail can be obtained from the summaries at the end of relevant chapters.

7.2.1 CONCLUSIONS

The most important conclusion to be made from the development of the Multipath Coherence Function (MCF) is that it demonstrates the existence of coherence without correlation between random channels. The MCF demonstrates the importance of the size of fluctuations compared to their correlation. The existence of partial coherence implies a non-zero mean signal field for fluctuations which are small enough. It was also shown that the MCF is independent of the signal source and depends only on the properties of the medium.

The importance of frequency domain processing is readily observed by comparing the coherence function with the normalized cross-correlation function. A broad band signal waveform in a multipath medium may have only one or two discrete frequencies at which coherence is high. The

(Insert over.)

cont

cross-correlation function, however, considers the entire signal waveform and will have a much smaller value than the maximum value of the coherence function.

The relevance of the MCF is in its relation to array gain. The magnitude of the MCF gives the signal power gain achieved by combining the outputs of a pair of receivers. Its phase is the average phase difference between the received signals which is required to combine them with partial coherence.

The mathematical solution for coherence led to a convenient factorization into nine auto-coherence terms. The stochastic independence of the receiver channels permits an auto-coherence to be computed for each channel independent of the others resulting in a large computational savings. The envelope approximation further factored the effects of random fluctuations from those of frequency selective multipath interference. This allows the prediction of maximum coherent frequencies independent of the actual multipath ray configuration. The extension of the MCF to VLA scanning led to a further factorization of the MCF into an auto-coherence due to the effects of spatial variations in the multipath interference. The advantages of these factorizations are computational simplicity and the ability to compare various effects on coherence readily.

The MCF formulation is a simple, concise mathematical expression, and does not depend on present knowledge of oceanographic fluctuations. The solution is adaptable to future developments in the causes of these fluctuations.

A

The complete value of the MCF is determined by multiplying the eight auto-coherence factors for a given channel, system geometry, and acoustic frequency. It has been shown that, for a constant value of σ, and for a coherent frequency ($\gamma_M = 1$), the MCF increases as the number of rays, K, increases. However, if an increase in the number of ray arrivals causes a corresponding increase in the ray spread, σ, the coherence may decrease. This fact is an important consideration in the choice of receiver location. For example, it may be wise to place the receivers at depths where there is a large number of ray arrivals within a small angular spread, rather than to choose a location having only one ray with the hope of avoiding spatial variations due to multipath interference entirely.

The identification of the auto-coherence with specific oceanographic fluctuations allowed the relative effect of each type of fluctuation to be determined. For each receiver there is an auto-coherence due to internal waves in the beacon channel, γ_W; an auto-coherence due to internal waves and spatial multipath interference in the scan channel, $\gamma'_{W,S}$; and an auto-coherence due to frequency selective multipath interference, γ_M. There is also the effect of internal tides on the coherence between receivers, γ_T.

The factor γ_W depends upon the typical angle at which rays cross the sound channel axis and has a higher value for steeper rays. It decreases with the source range, R, and with the acoustic frequency, f.

$\gamma'_{W,S}$ contains the effect of internal waves in the scan channel plus the effect of spatial variations due to multipath interference in

scanning. The effect of spatial variations depends upon the change in source range, x, in scanning away from the beacon. Thus, the effect is most severe when scanning in a direction perpendicular to the baseline of a VLA. The parameter which affects the spatial variations is the angular ray spread at the receiver, σ, and it was found that coherence decreases as σ increases. For a given value of σ the coherence decreases in scanning as a function of $|x|/\lambda$.

The effect on coherence due to frequency selective multipath interference, γ_M, was found to depend on the nominal time configurations of the multipath arrivals for each receiver channel. The coherence γ_M is specified primarily in terms of coherent frequencies, i.e., frequencies at which the rays interfere constructively, and the coherent bandwidths centered on these frequencies. For a simplified equal time spacing formulation of the ray arrivals, it was found that coherent frequencies occur at harmonics. The fundamental coherent frequency increases as the number of rays, K, increases, and as the time spread, T_S, decreases. The coherence bandwidths are inversely proportional to T_S.

It was found that internal tides had a negligible effect on coherence in scanning compared to the effect of spatial multipath interference. Consequently γ_T has a value of unity for all scan distances of practical interest. However, the coherence due to frequency selective multipath interference is also a consideration, since the spacing between coherent frequencies increases as K increases. All of these factors should be taken into account for an optimum system design.

The argument of the MCF is the average phase difference between signals necessary to combine them with partial coherence. The only contribution to this phase is due to the spatial multipath interference. It was found that the phase has an expected linear variation, k_0x, and a contribution due to the ray spread, σ. It was found that the deviation of the average phase from the linear trend is less than $\pi/4$ radians.

The actual design of a superarray system requires the use of beacons with known locations and known waveforms for the purpose of initially focusing the VLA due to the unknown state of the medium. Scanning the VLA is performed by first scanning the subarray beams to the desired location and then applying the required phase shifts to the subarray outputs. These phase shifts are nominal or average values which are either predicted from a ray tracing program or experimentally measured. The MCF then predicts the defocusing of the VLA due to the fluctuations about the average phase. The localization accuracy of the VLA is determined primarily by the area of intersection of the subarray beams because of ambiguities in the VLA pattern.

The MCF predicts the contours of constant coherence giving the area of coverage with one beacon for a desired array gain. This determines the number of beacons and their geometric configuration for a required total area of coverage.

Numerical results for a specific multipath configuration and a VLA of 7 subarrays predicted an average gain in excess of 6 dB over an area of 75000 km^2 with the use of only 9 beacons.

7.2.2 LIMITATIONS

The restrictions of the foregoing theory are few, and are simply stated. There are some limitations, however, which may be important considerations in a VLA system design, and are itemized below.

- Geometrical optics - the theory of fluctuations has been limited to the geometrical optics regime (small fluctuations), with associated limits on frequency and range. However, since the fluctuations are uncorrelated, the MCF depends only on their size. Consequently, coherence would be very small for fluctuations larger than those of the geometrical optics region, so it is unnecessary to consider the other regions of fluctuations.
- Small scale size of fluctuations - the limitation to fluctuations of small correlation distance and time (internal waves) places restrictions on scan distance and scan time. But since coherence is low for larger scan distances due to the fluctuations considered here, there is no need to consider larger scale size fluctuations.
- Non-geographic fluctuations - the theory here does not consider geographic anomalies such as currents and eddies. These fluctuations should be seriously considered in a VLA system design, either by measuring their effect for the area of interest, or by avoiding them entirely in locating the VLA.
- Source motion - a restriction imposed early in this work was that signal duration time be much less than the characteristic time of all fluctuations. Source motion implies the existence of spatial variations of multipath interference in the signal duration time.

There is therefore a requirement that the source motion is minimal for the time that it takes the signal processor to compute the power spectral densities. The effect of Doppler can be accounted for by simply shifting the center frequency of the signal processor filter. This subject requires further study.

- Horizontal scanning - although no restriction was placed on receiver location due to the use of a beacon for initial cophasing, scanning was limited to a horizontal plane at the beacon depth. It is assumed that there are no great variations in depth for typical signal sources. The vertical coherence distance therefore can be presumed to be large enough to detect all sources of interest with beacons at only one or two depths.
- Accuracy of beacon and receiver locations - the VLA localization ability is determined by the area of intersection of the subarray beams, which may be on the order of tens of square kilometers. Since receiver and beacon locations will be known within areas much less than this, there will be essentially no effect on localization ability of the VLA.
- Incoherent noise - if the noise is incoherent between receivers there will be no effect on VLA gain due to ambiguities in the receiving pattern. Coherent noise sources, such as shipping traffic, will cause a decrease in gain if located at one of the ambiguous focal points of the VLA. The procedure of near field adaptive nulling discussed in Chapter 6 may avoid this problem.

- Isotropic multipath field - it was assumed that the number of rays, the nominal travel times, and the angles of arrival, are invariant throughout the scan area for each beacon. The source ranges and scan areas for which this condition is fulfilled must be predicted from a ray tracing program. This is a further consideration in beacon and receiver location.

7.3 RECOMMENDATIONS FOR FURTHER STUDY

Section 6.3 has discussed other considerations in a VLA system design implementation, and Section 7.2.2 has stated limitations of the theory and its applications. The topics mentioned warrant further study and are summarized here with further recommendations concerning experimental verification of results.

1 - An experimental test of the theory of the MCF using beacons.

2 - An experimental test of application to a VLA system design.

3 - A study of beacon waveforms such as PN sequences.

4 - Evaluation of methods of beacon placement such as beacons of opportunity and air-dropped beacons.

5 - An experimental test of source localization ability.

6 - A study of the effects of source motion.

7 - A study of the effects of geographic fluctuations such as currents and eddies.

8 - Evaluate the effects of coherent noise sources.

9 - A study of post-detection focusing and tracking.

10 - Consideration of methods of subarray location such as the use of floating random arrays.

11 - Study of the use of sources of opportunity instead of beacons.

APPENDIX

THE ENVELOPE APPROXIMATION

It is desired to approximate the envelope of the function

$$\gamma^2(\omega) = \frac{Kc^2(\omega)|H_0(\omega)|^2}{1+[K|H_0(\omega)|^2-1]c^2(\omega)} \quad . \qquad (A.1)$$

In the above equation $|H_0(\omega)|^2$ is the square of the normalized multipath transfer function exhibiting frequency selective fading. It is shown in Section 5.2.4 that coherent frequencies located at the primary maxima of the pattern have typical spacings on the order of 1 Hz, and that the nulls adjacent to each coherent frequency are separated by fractions of 1 Hz. Between coherent frequencies there are a number of secondary maxima which have generally the same spacings between their adjacent nulls. The function $c^2(\omega)$ is the squared characteristic function of random fluctuations and is a monotonically decreasing function of frequency. The typical characteristic functions considered, that of internal waves in (5.3) and of spatial variations in (5.6), vary slowly compared to $|H_0(\omega)|^2$, and can be considered constant between any two nulls.

At the nulls of $|H_0(\omega)|^2$, $\gamma^2(\omega) = 0$ when $c^2(\omega) < 1$, so the local maxima of $\gamma^2(\omega)$ also occur between the nulls. Consider a primary maximum of $|H_0(\omega)|^2$ located at $\omega = \omega_0$ so $|H_0(\omega_0)|^2 = 1$. Then in the region between the adjacent nulls

$$\gamma^2(\omega) = \frac{Kc^2(\omega_0)|H_0(\omega)|^2}{1+[K|H_0(\omega)|^2-1]c^2(\omega_0)} \quad . \tag{A.2}$$

Since $\gamma^2(\omega)$ increases monotonically with $|H_0(\omega)|^2$ when $c^2(\omega_0) < 1$, its maximum value in the region between the nulls about ω_0 is

$$\max \gamma^2(\omega) = \frac{Kc^2(\omega_0)}{1+(K-1)c^2(\omega_0)} \quad : \tag{A.3}$$

This is true for each primary maximum, so the envelope of $\gamma^2(\omega)$ for all ω is

$$\text{env } \gamma^2(\omega) \equiv \gamma_E^2(\omega) = \frac{Kc^2(\omega)}{1+(K-1)c^2(\omega)} \quad . \tag{A.4}$$

Since the primary maxima and zeroes of $\gamma^2(\omega)$ coincide with those of $|H_0(\omega)|^2$, the approximation to $\gamma^2(\omega)$ is now written as

$$\gamma_A^2(\omega) = \gamma_E^2(\omega)\gamma_M^2(\omega) \tag{A.5}$$

where

$$\gamma_M^2(\omega) = |H_0(\omega)|^2 \quad . \tag{A.6}$$

The fractional error in this approximation is

$$\varepsilon = \frac{\gamma^2-\gamma_A^2}{\gamma^2} \quad . \tag{A.7}$$

Equation (A.1) can be rewritten as

$$\gamma^2 = \gamma_A^2 \left[\frac{1}{1-(1-\gamma_M^2)\gamma_E^2} \right] . \tag{A.8}$$

Then

$$\varepsilon = (1-\gamma_M^2)\gamma_E^2 . \tag{A.9}$$

At the primary maxima, $\gamma_M^2 = 1$, so there is no error. These are the regions of main interest since they are the locations of coherent frequencies. The error in the approximation is greater at secondary maxima. For example, consider a secondary maximum where $\gamma_M^2 = \frac{1}{2}$. Assume that $\gamma_E^2 = \frac{1}{2}$. Then $\gamma_A^2 = \frac{1}{4}$, but $\gamma^2 = \frac{1}{3}$, so $\varepsilon = 25\%$. The fractional error continues to increase as γ_M^2 decreases.

It should be noted that the envelope approximation is not valid when there are no random fluctuations, i.e., when $c^2(\omega) = 1$ for all ω, since, from (A.1), $\gamma^2(\omega) = 1$ for all ω.

INDEX

Adaptive nulling, 144,155
Ambiguities, 3,4,35,38,42,43,46,128,134,141,153,155
Array
  gain, 1,5,7,9-11,31,34,38,39,42-46,66,67,70,128,129,131,134-136, 139,144,145,147,148,150,153,155
  processing, 1,8,9,11,33-46
Auto-coherence, 70,72,87-91,95-97,99-103,105,111,113-126,147,148, 150,151

Beacon, 4,5,7,14,50,74,75,77-82,85,86,88,91,94-97,102,104,107,119, 120,123,125,128-134,136-141,144,145,148,151,152,153,155-157
Beamforming, 7,8,11,34,94,128-130,142
Beamwidth, 3,38,41,42,128,133,134,136,145
Bendat, 9
Beran, 8,67
Bulk time delay, 20,60,109,113

Clark, 53
Coherence
  coherent combination, 1,3,4,5,9,14,32,33,43,45,46,66,68,147
  multipath coherence function, 6,13,63,66-92,94-96,115-124,126,128, 131,134,135,143,144,147-151,153,154,156
Conventional array, 3,11,35-44,128
Correlation, 1,3,4,8-11,23,25,27,32,33,37,39,49,51,58,63,66,67,70,71, 78,80,82,84,85,89,91,96,98,140,147-150,154

Doppler, 51-53,142,155

Eikonal equation, 17,18
Envelope approximation, 72,87,90,91,115,117,148,150,158-160.

Far-field, 3,37
Floating subarrays, 144,145,157
Focus, 1,4,5,7,11,50,74,88,107,128-130,132-134,136,141,142,145,148, 153,155,156
Frequency selective fading, 22,47,52,62,63,66,88,89,91,92,94,95,111, 113-117,126,148,150-152

Geometrical optics, 23,26,29,57,154

Haber, 144
HF, 8

Impulse response, 6,29,68,128,140
Internal tides, 2,6,7,14,23,49,51,52,57,59-64,70,92,94-96,100,104-112, 118,119,125,132,148,151,152

INDEX (continued)

Internal waves, 2,6,10,23,25,26,47,49,51,56-59,63,64,67,70,85,92,94-99,101,102,111,119,120,125,132,148,151,154

Jenkins, 9
Jobst, 10,67

Koopmans, 9

Localization, 3,4,14,43,46,131,133,141,145,147,153,155,156

Mandel, 9
McCoy, 67
Multipath, 6,9,10,13,14,20,22,24,26,47,50,53,54,59,66-68,74,78,81,88,90,94,126,134,140,143,147-150,152,153,156
Multipath interference, 2,6,9,13,22,52-55,62,66,67,73,78,88,89,91,92,94-97,103,105,111,113-119,125,126,142,148,150-154
Munk, 10,67

Near-field, 3,39,128,144,148,155
Noise, 2,3,11,28,30,34-36,39,42,134,140,143,155,156

Optics, 8

Parrent, 8
Pattern, 11,35,37,38,41,128,144,153,155
Piersol, 9
Pressure, 17,18,20,22,123
Propagation, 1,2,5,6,8,11,13,17,20,47,50,52,53,57,59-62,67,102,104,109,110,113,119

Random channel, 4,5,6,8,9,66,68,90,149
Ray solution, 11,17
Ray tracing, 6,18,20,53,54,123,153,156
Receiver spacing, 1,3,7,10,32,36,39,42,43,49,50,66,67,81,82,96,114,133,136,144,147,149
Resolution, 3,11,128,133,134,136,138,141,142
Roth, 9
Rytov solution, 26,29

Scanning, 3,4,7,8,11,13,14,50,54,63,74-91,94-96,98,100,102,106,108-112,118-125,131,132,134,136,143,148,150,152-156
Self-cohering, 7,8,142,148
Ship traffic, 2,139,140,143,144,155
Sidelobe, 35
Signal to noise ratio, 31,142,147,148
Smith, 9,66

INDEX (continued)

Sound speed, 2,11,17-20,23,27,36,51,57,59,60,62,64,110,111,123
Spatial variations, 1,2,6,47,52-54,63,64,67,78,83,88,91,92,94-97,100, 118-120,125,139,142,148,150-154

Temperature, 18,23,52
Temporal variations, 1,2,4,47,48
Time spread, 22,111,113,126,140,152
Transfer function, 66,68,69,71,72,74,77,82,85,86,88,90,111,141,147
Travel time, 4,20,25,26,28,32,47,53,55,58-60,62,68,70,71,80,81,83,94, 97,104,106,110,115,118,123,126,141,156

Valley Forge Research Center, 8
Very large array, 1,3,8,11,13,14,35,39-46,50,54,63,70,74,128-137,139, 141-145,147-150,152-156

Watts, 9
Wave equation, 11,17,23,26
Wavelength, 1,3,18,23,36,39,42,59,134,141
Weinberg, 59
Wiener, 9
Wolf, 9

Zabalgogeazcoa, 10

BIBLIOGRAPHY

Active and Adaptive Antennas, Special issue on, IEEE Trans. Antennas Prop., Vol. AP-12, No. 2, March 1964.

Adams, S. L., and J. W. Doubek, "Frequency Coherence and Time Coherence in Random Multipath Channels," J. Acoust. Soc. Am., Vol. 62, No. 2, August 1977.

Adaptive Optics, Special issue on, J. Opt. Soc. Am., Vol. 67, No. 3, March 1977.

Agard Lecture Series No. 58, "Spread Spectrum Communications," NATO, July 1973.

Bello, P. A., "Measurement of Random Time-Variant Linear Channels," IEEE Trans. Inform. Theory, Vol. IT-15, July 1969.

Bendat, J. S., and A. G. Piersol, Measurement and Analysis of Random Data, John Wiley and Sons, New York, 1966.

Beran, M. J.. and G. B. Parrent, Jr., Theory of Partial Coherence, Prentice-Hall, Inc., Englewood Cliffs, N. J., 1964.

Beran, M. J., J. J. McCoy, and B. B. Adams, "Effects of a Fluctuating Temperature Field on the Spatial Coherence of Acoustic Signals," NRL Report 780, Washington, D. C., 1975.

Birdsall, T. G., G. E. J. Bold, and K. A. Winick, "The PANOIC 77 Sequence Signal," PANOIC 77 Report 013376-5-T, Part I, Cooley Electronics Laboratory, Michigan, March 1978.

Carter, G. C., C. H. Knapp, "Coherence and its Estimation via the Partitioned Modified Chirp-Z Transform," IEEE Trans. Acous., Speech, Sig. Proc., Vol. ASSP-23, No. 3, June 1975.

Cederquist, G. N., "The Use of Computer-Generated Pictures to Extract Information From Underwater Acoustic Transfer Function Data," Ph.D. Dissertation, University of Michigan, 1975.

Clark, J. G., R. P. Flanagam. and N. L. Weinberg, "Multipath Acoustic Propagation with a Moving Source in a Bounded Deep Ocean Channel," J. Acoust. Soc. Am., Vol. 60, No. 6, December 1976.

BIBLIOGRAPHY
(Continued)

Dashen, R. F., S. M. Flatte, W. H. Munk, and F. Zachariasen, "Limits on Coherent Processing Due to Internal Waves," JASON Report JSR-76-14, Stanford Research Institute, California, June 1977.

Dashen, R. F., S. M. Flatte, W. H. Munk, and F. Zachariasen, "Sound Transmission Through a Fluctuating Ocean," JASON Report JSR-76-39, Stanford Research Institute, California, May 1977.

Davies, D. E. N.,"Independent Angular Steering of Each Zero of the Directional Pattern for a Linear Array," IEEE Trans. Antennas Propag., Vol. AP-15, March 1967.

DeFerrari, H. A., "Time-Varying Multipath Interference of Broad-Band Signals Over a 7-NM Range in the Florida Straits," J. Acoust. Soc. Am., Vol. 53, No. 1, 1973.

Dyer, I., "Statistics of Distant Shipping Noise," J. Acoust. Soc. Am., Vol. 53, pp. 564-570, 1973.

Dyson, F., W. Munk, and B. Zetler, "Interpretation of Multipath Scintillations Eleuthera to Bermuda in Terms of Internal Waves and Tides," J. Acoust. Soc. Am., Vol. 59, No. 5, May 1976.

Edelbluthe, D.J., J. M. Fisk, and G. L. Kinnison, "Criteria for Optimum-Signal-Detection Theory for Arrays," J. Acoust. Soc. Am., Vol. 41, No. 1, January 1967.

Flatte, S. M., and F. D. Tappert, "Calculation of the Effect of Internal Waves on Oceanic Sound Transmission," J. Acoust. Soc. Am., Vol. 58, No. 6, December 1975.

Graham, W. J., "A Large Underwater Aperture of Coherently Combined Subarrays," Valley Forge Research Center QPR No. 22, Article 3, August 1977.

Haber, F., "Floating Acoustic Array," Valley Forge Research Center QPR No. 22, Art. 3, August 1977.

Jenkins, G. M., D. G. Watts, Spectral Analysis and its Applications, Holden-Day, San Francisco, California, 1968.

Jobst, W. J., "An Application of Poisson Process Models to Multipath Sound Propagation of Sinusoidal Signals," J. Acoust. Soc. Am., Vol. 57, No. 6, Part 11, June 1975.

BIBLIOGRAPHY
(Continued)

Jobst, W., and L. Dominijanni, "Measurements of the Temporal, Spatial, and Frequency Stability of an Underwater Acoustic Channel," J. Acoust. Soc. Am., Vol. 65, No. 1, January 1979.

Jobst, W., and X. Zabalogogeazcoa, "Coherence Estimates for Signals Propagated Through Acoustic Channels with Multiple Paths," J. Acoust. Soc. Am., Vol. 65, No. 3, March 1979.

Kailath, T., "Measurements on Time-Variant Communication Channels," IRE Trans. Inform. Theory, Vol. IT-8, September 1962.

Koopmans, L. H., The Spectral Analysis of Time Series, Academic Press, New York, 1974.

Lim, T. L., "Beacons of Opportunity," Valley Forge Research Center QPR No. 22, Art. 3, August 1977.

Mandel, L., E. Wolf, "Spectral Coherence and the Concept of Cross-Spectral Purity," J. Opt. Soc. Am., Vol. 66, No. 6. June 1976.

McCoy, J. J., "Beam Spreading and Loss of Spatial Coherence in an Inhomogeneous and Fluctuating Ocean," SACLANTCEN Conf. Proc. (La Spezia, Italy) 17,6,1975.

Mooers, C. N. K., "Sound Speed Perturbations Due to Internal Tides," J. Acoust Soc. Am., Vol. 53, p. 333(A), 1973.

Munk, W. H., and F. Zachariasen, "Sound Propagation Through a Fluctuating Stratified Ocean: Theory and Observation," J. Acoust. Soc. Am., Vol. 59, No. 4, April 1976.

Roth, P. R., "Effective Measurements Using Digital Signal Analysis," IEEE Spectrum, April 1971.

Schultheiss, P. M., S. Chow, "Signal Processing for Very Large Arrays," Final Report, Yale University, Dept. of Engineering and Applied Science, June 1976.

Smith, P. W., Jr., "Spatial Coherence in Multipath or Multimodal Channels," J. Acoust. Soc. Am., Vol. 60, No. 2, August 1976.

Steinberg, B. D., Principles of Aperture and Array System Design, John Wiley and Sons, New York, 1976.

BIBLIOGRAPHY
(Continued)

Steinberg, J. C., J. G. Clark, H. A. DeFerrari, M. Kronengold, and K. Yacoub, "Fixed-System Studies of Underwater Acoustic Propagation," J. Acoust. Soc. Am., Vol. 52, No. 5 (Pt. 2), 1972.

Steinberg, J. C. and T. G. Birdsall, "Underwater Sound Propagation in the Straits of Florida," J. Acoust. Soc. Am., Vol. 39, 301-315, 1966.

Sykes, A. O., "Environmental and Acoustic Fluctuations in the Sea," ONR, Arlington, Virginia, June 1977.

Tatarskii, V. I., Wave Propagation in a Turbulent Medium (Translated from the Russian), McGraw-Hill, New York, 1961.

Urick, R. J., and G. R. Lund, "Coherence of Convergence Zone Sound," J. Acoust. Soc. Am., Vol. 43, No. 4, 1968.

Urick, R. J., Principles of Underwater Sound, McGraw-Hill, New York, 1975.

Valley Forge Research Center Quarterly Progress Reports Nos. 1-29, May 1972 to May 1979, Moore School of Electrical Engineering, University of Pennsylvania, Philadelphia, Pennsylvania.

Van Trees, H. L., Detection, Estimation and Modulation Theory, Part III, Wiley, New York, 1971.

Veenkant, R. L., "Investigation of the Propagation Stability of a Doubly Spread Underwater Acoustic Channel," IEEE Trans. Acoust. Sp. Sig. Proc., Vol. ASSP-25, No. 2, April 1977.

Vural, A. M., "An Overview of Adaptive Array Processing for Sonar Applications," Proceedings Eascon '75.

Weinberg, N. L., J. G. Clark, and R. P. Flanagan, "Internal Tidal Influence on Deep-Ocean Acoustic-Ray Propagation," J. Acoust. Soc. Am., Vol. 56, No. 2, August 1974.

Wiener, N., "Generalized Harmonic Analysis." Acta Math, 55, reprinted in Selected Papers of Norbert Wiener, MIT Press, Cambridge, Mass., 1964.